Jet Propulsion Laboratory
California Institute of Technology

# The Fluid Mechanical Particle Barrier (FMPB) for the Prevention of Sample Contamination on the Mars 2020 Mission

## External Aerobiology Review

Ioannis Mikellides
Douglas Bernard
Adam Steltzner

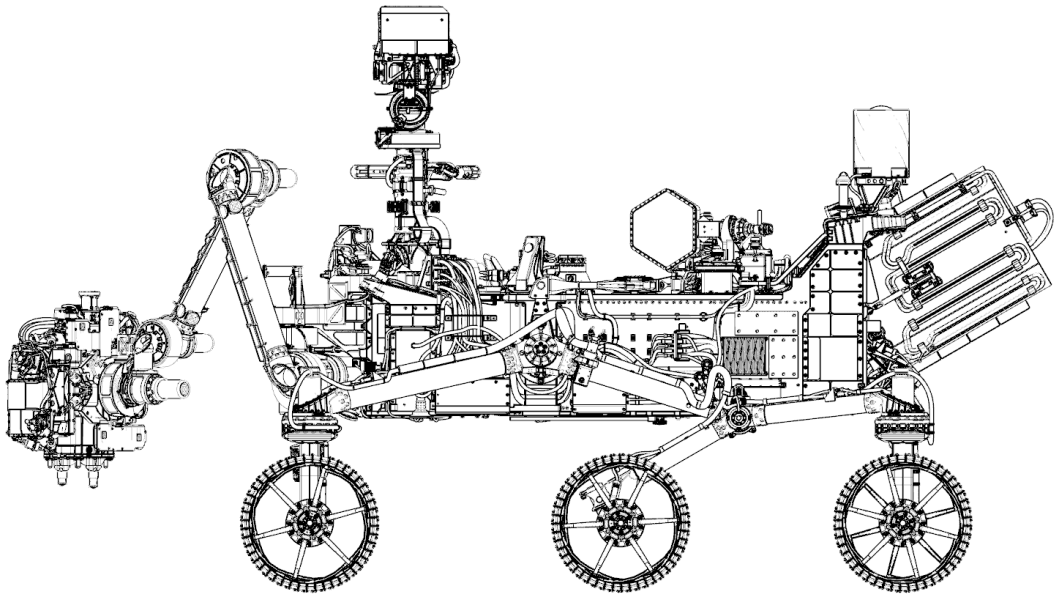

May 14, 2018

© 2018 California Institute of Technology. Government sponsorship acknowledged.

# Agenda

Jet Propulsion Laboratory
California Institute of Technology

- **10:30-11:00 AM: Arrive at NASA Headquarters for visitor badging.**
  - Reviewers will be escorted to meeting room and lunches will be ordered.
- **11:00-11:30 AM: Introductions and charge.**
  - Lisa Pratt will lead.
- **11:30-12:30 PM: Background on FMPB.**
  - Mars 2020 team will give a 40 min. presentation followed by 20 minutes for questions and discussion with reviewers.
- **12:30-12:45 PM: Break.**
  - Food and beverages will be distributed for a working lunch.
- **12:45 -1:30 PM: Biological particle-size distribution and size-dependent motion.**
  - Each reviewer will give a 5 minute technical comment followed by questions and discussion with all participants.
- **1:30-2:30 PM: FMPB verification analyses and tests**.
  - Mars 2020 team will give a 20 min presentation followed by 40 minutes for questions and comments from reviewers.
- **2:30-2:45 PM: Break.**
  - Snacks and beverages will be delivered.
- **2:45-3:30 PM: Risk for contamination of Mars Samples.**
  - Each reviewer will give a 5 minute technical comment followed by questions and discussion with all participants
- **3:30-4:15 PM: Reviewer discussion and selection of panel chair**.
  - Reviewers will meeting separately from other participants to identify a chair and outline preliminary findings.
- **4:15-5:15 PM: Presentation of preliminary panel findings.**
  - Panel chair will give a 15 minute overview of reviewer findings followed by 45 minutes of discussion with all participants on potential approaches to risk mitigation.

# 11:30-12:30 PM

# Background & Discussions

# Mars 2020 Mission Objectives

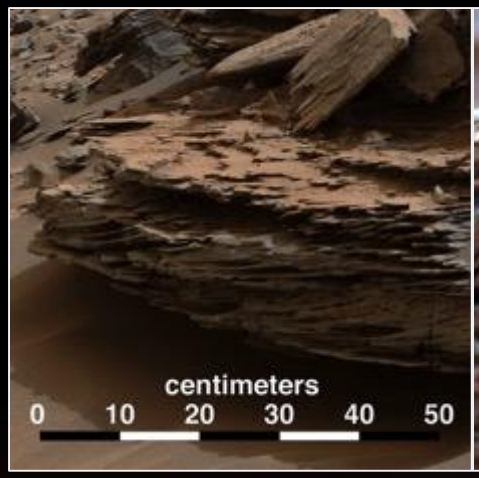


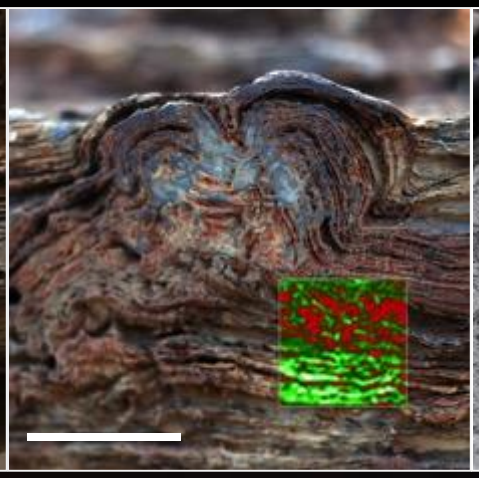

## GEOLOGIC EXPLORATION

- Explore an ancient environment on Mars
- Understand processes of formation and alteration

## HABITABILITY AND BIOSIGNATURES

- Assess habitability of ancient environment
- Seek evidence of past life
- Select sampling locations with high biosignature preservation potential

## PREPARE A RETURNABLE CACHE

- Capability to collect ~40 samples and blanks, 20 in prime mission
- Include geologic diversity
- Deposit samples on the surface for possible return

## PREPARE FOR HUMAN EXPLORATION

- Measure temperature, humidity, wind, and dust environment
- Demonstrate In Situ Resource Utilization by converting atmospheric $CO_2$ to $O_2$

# Mission Overview

Jet Propulsion Laboratory
California Institute of Technology

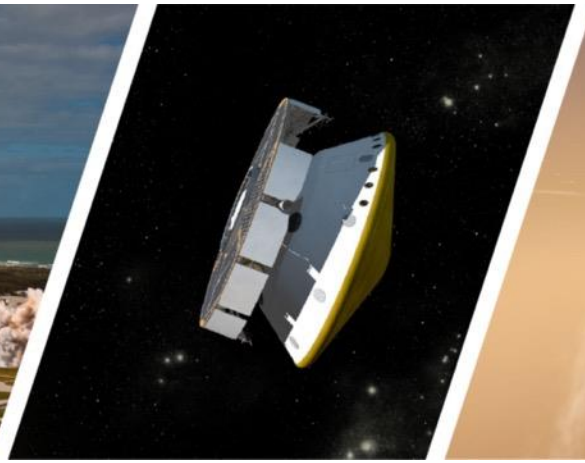

## LAUNCH

- Atlas V 541 vehicle
- Launch Readiness Date: July 2020
- Launch period: July/August 2020

## CRUISE/APPROACH

- ~7 month cruise
- Arrive Feb 2021

## ENTRY, DESCENT & LANDING

- MSL EDL system (+ Range Trigger and Terrain Relative Navigation): guided entry and powered descent / Sky Crane
- 16 x 14 km landing ellipse (range trigger baselined)
- Access to landing sites ±30° latitude, ≤ -0.5 km elevation
- Curiosity-class Rover

## SURFACE MISSION

- 20 km traverse distance capability
- Enhanced surface productivity
- Qualified to 1.5 Martian year lifetime
- Seeking signs of past life
- Returnable cache of samples
- Prepare for human exploration of Mars

# Sampling and Caching Subsystem Overview

Jet Propulsion Laboratory
California Institute of Technology

**Sample Tube Storage**
- Storage structure
- Sample tubes (43)
- FMPB gloves (43)

**Seal Dispenser**
- Dispensing mechanisms (7)
- Hermetic seals (49)
- FMPB covers (7)

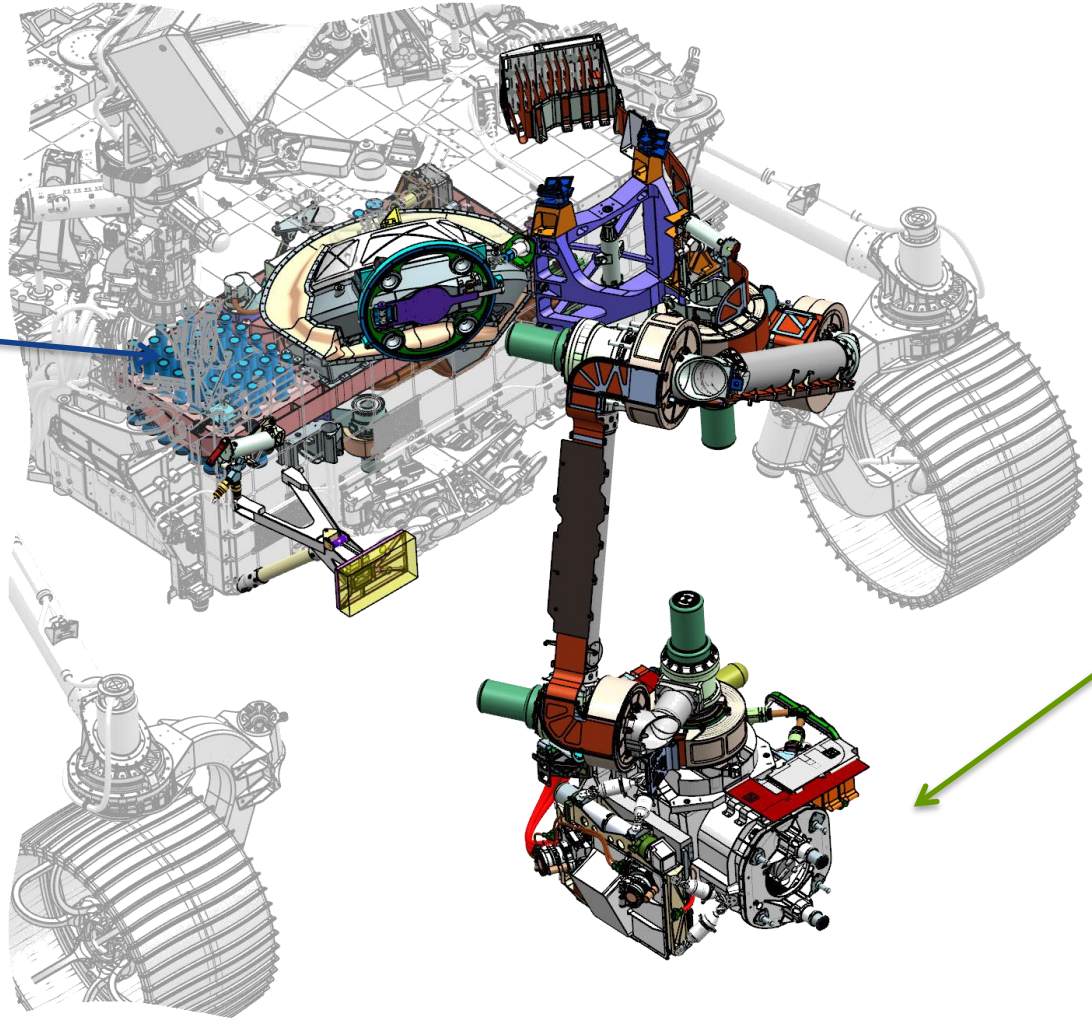

**Coring Drill on Turret at end of Robotic Arm**
- Drill body
- Feed / turret structure
- Stabilizers

# Adaptive Caching Assembly (ACA)



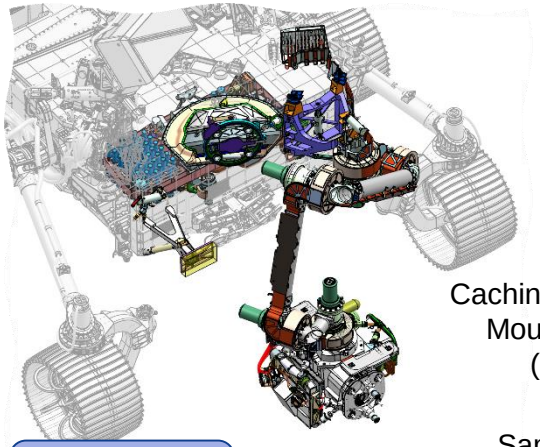

- Store Bits
- Manipulate Tubes
- Assess Sample
- Seal Sample
- Store Sample
- Drop-off Sample

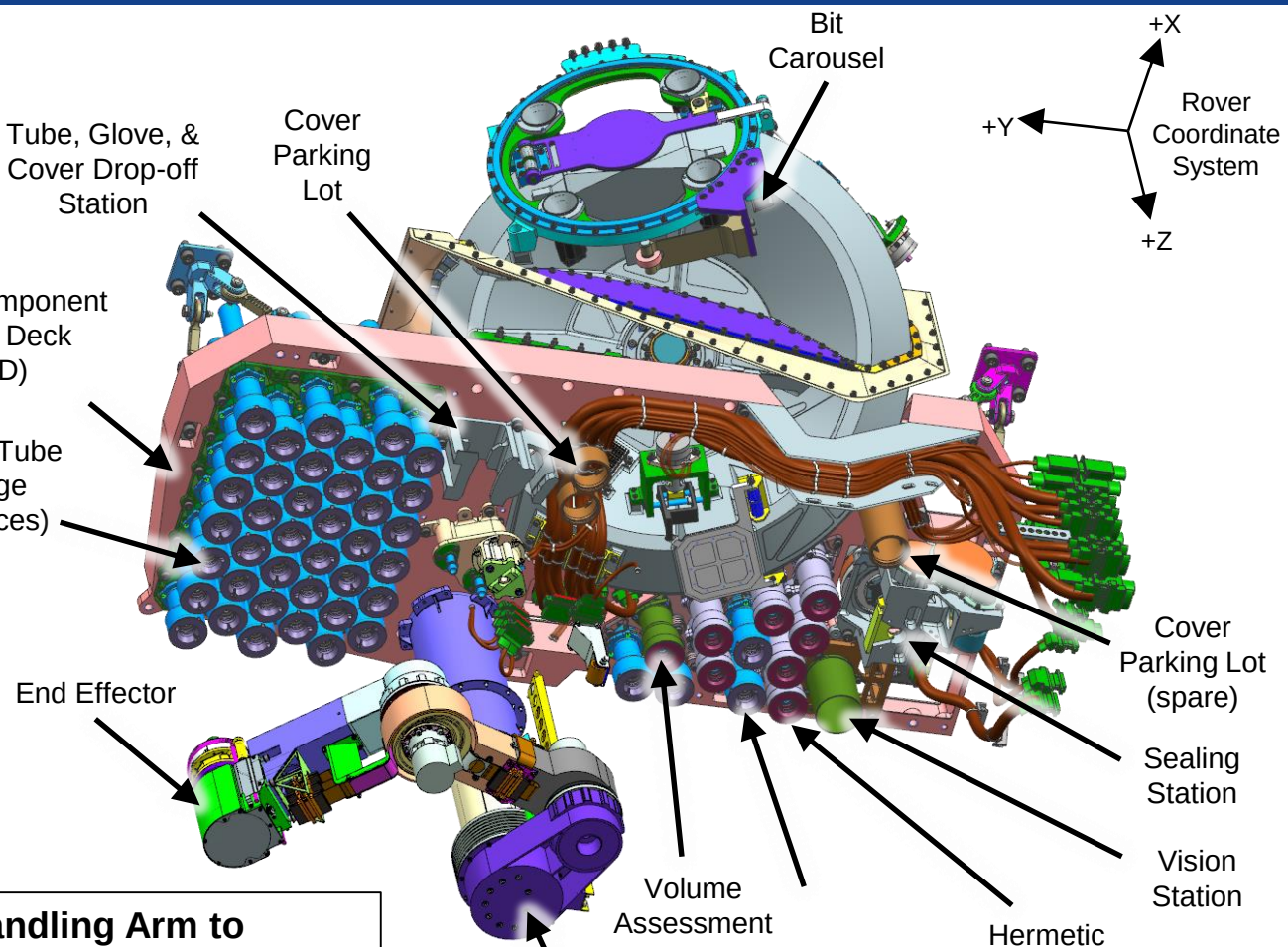


**Single Sample Handling Arm to access individual stations:**

**Bit carousel, tube storage, hermetic seal dispensers, vision assessment, volume assessment, cover parking lot, sealing, passive drop-off**

# ACA Hardware Details

Jet Propulsion Laboratory
California Institute of Technology

**"Sample Intimate Hardware"**
*Hardware that comes into direct contact with the samples*

- Sample Tubes
- Hermetic Seals
- Volume Probe
- Bits

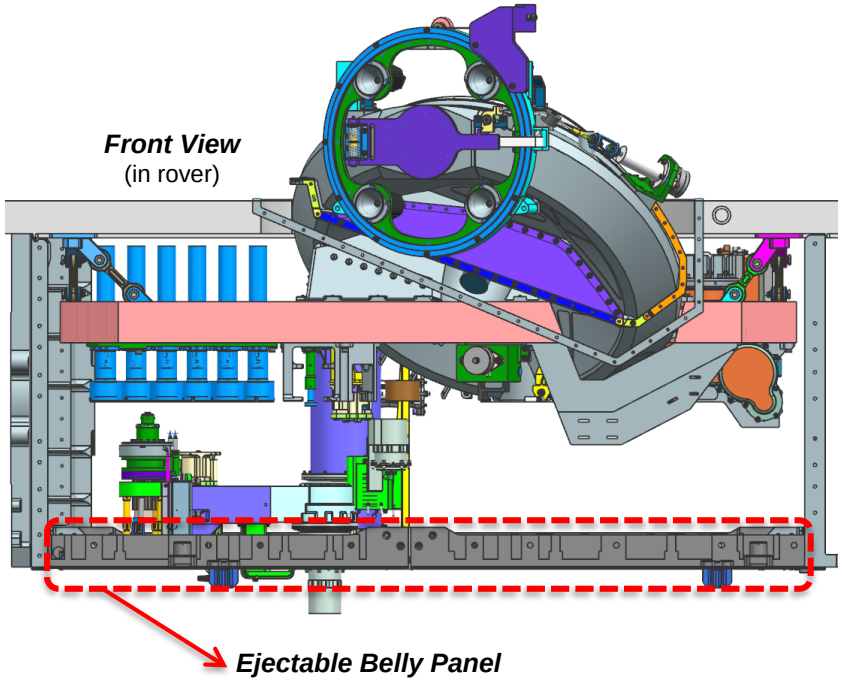


**"Sample Handling Hardware"**
*Hardware that comes into close proximity to sample or SIH*

- Tube Sheath
- Gloves/Covers
- Dispenser
- Volume Housing
- Vision Station Baffle & illuminator
- Bit Carousel
- Bit assembly (sleeve)
- Hermetic seal assembly (non-seal cup)

# Contamination Requirements

Jet Propulsion Laboratory
California Institute of Technology

## Viable Organism Requirements

| Topic | Text |
|---|---|
| Probability of viable Earth organism in returned sample | The Mars 2020 Project shall be capable of encapsulating samples for return such that each sample in the returned sample set has more than a 99.9% probability of being free of any viable Earth-sourced organisms. |

## Organic Carbon Requirements

| Topic | Text |
|---|---|
| Organic Carbon | The Mars 2020 landed system shall be capable of encapsulating samples for return such that the organic contamination levels in each sample in the returned sample set are less than:<br>• Any Tier 1 compound (organic compounds deemed as essential analytes for mission success): 1 ppb<br>• Any Tier 2 compound (organic compounds not categorized as Tier 1): 10 ppb<br>• Total Organic Carbon: 10 ppb Baseline, 40 ppb Threshold |

# Operational Principle of the Fluid Mechanical Particle Barrier (FMPB)

Jet Propulsion Laboratory
California Institute of Technology

- **Particle Penetration Prevention Mechanism #1: Flow Through Orifice-1 (O1)**
  - Fluid viscosity slows down the flow speed through a thin annular orifice at the entrance to the FMPB
  - Reduces the aerodynamic force on particles that may have entered it
- **Particle Penetration Prevention Mechanism #2: Flow Into Cavity-1 (C1)**
  - Flow speed reduced further due to expansion into large area.
- **Particle Penetration Prevention Mechanism #3: Finite filling time**
  - Pressure in the FMPB closed volume rises as mass flux enters it thereby reducing the pressure difference across all paths to the interior. Consequently the flow speed and aerodynamic force on particles are also reduced.

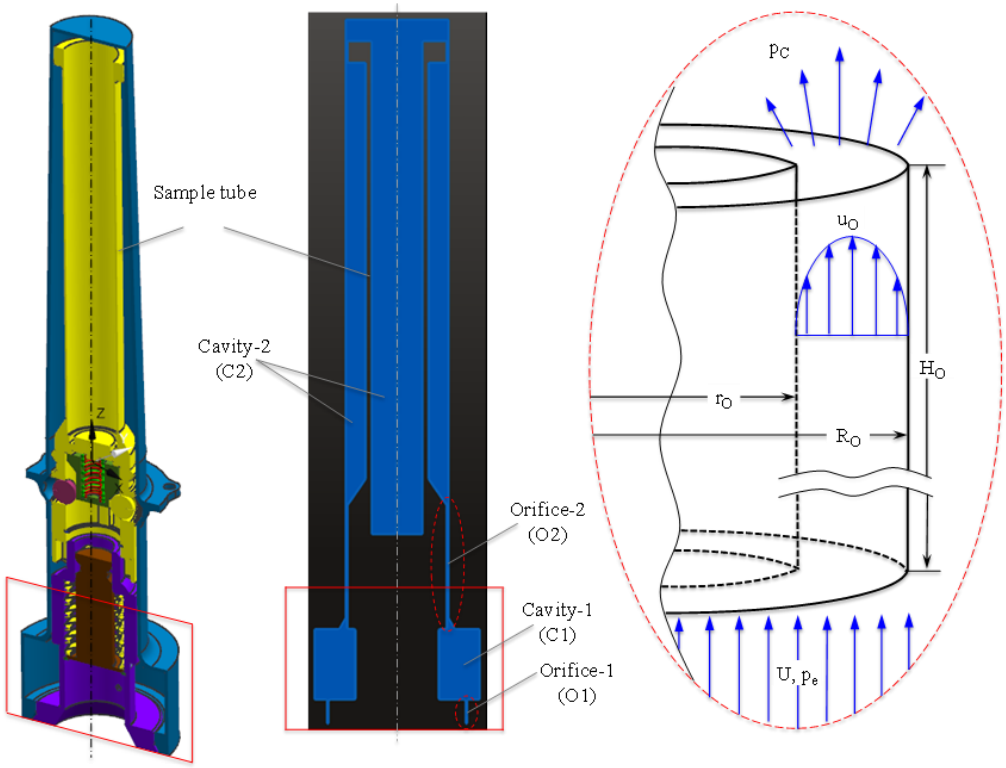

# A Combination of First-principles Models, Numerical Simulations and Flow Tests Employed to Verify the FMPB

Jet Propulsion Laboratory
California Institute of Technology

**First-principles analytical modeling of flow & particle dynamics (1D, time-dep)**

- Isolates driving physics in a tractable model that can be used to easily guide the design
- Processes captured: pressurization and sustained-wind events ($\Delta p \neq 0$)

**Numerical simulation (2D & 3D, time-dep) of flow and particle dynamics**

- Validates analytical model
- Assesses scenarios/conditions that cannot be addressed by 1D model
- Processes captured: pressurization and sustained-wind events ($\Delta p \neq 0$)

**Mars-similar flow experiments (3D, time-dep)**

- Validates theoretical models
- Assesses scenarios/conditions that are challenging, even in CFD sims
- Processes captured: flow penetration allowed by flow non-uniformities, in pressure eq. ($\overline{\Delta p} = 0$)

$$\mathbf{p}_C(t) = \begin{pmatrix} p_{C1} \\ p_{C2} \end{pmatrix} = \frac{p_0}{2\Lambda} \begin{pmatrix} \frac{e^{\lambda_1 t}}{2}(\Theta^+ - 1)(\Theta^- + 1) - \frac{e^{\lambda_2 t}}{2}(\Theta^+ + 1)(\Theta^- - 1) \\ e^{\lambda_2 t}(\Theta^+ + 1) - e^{\lambda_1 t}(\Theta^- + 1) \end{pmatrix} + \frac{2p_e\bar{k}}{\Lambda} \begin{pmatrix} \frac{1-e^{\lambda_1 t}}{2}\frac{1-\Theta^-}{1+\Theta^-} - \frac{1-e^{\lambda_2 t}}{2}\frac{1-\Theta^+}{1+\Theta^+} \\ \frac{1-e^{\lambda_2 t}}{1+\Theta^-} - \frac{1-e^{\lambda_1 t}}{1+\Theta^+} \end{pmatrix}$$

$$z_p = z_{p0} + \left(u_{O1} - \frac{g}{k_p}\right)t + \left(\dot{z}_{p0} - u_{O1} + \frac{g}{k_p}\right)\frac{1 - e^{-k_p t}}{k_p}$$

$$\mathrm{k_p} \equiv \frac{g}{\mathrm{u}_{T\mathrm{p}}} \qquad \mathrm{u}_{T\mathrm{p}} \equiv (\rho_\mathrm{p} - \rho_\infty)\frac{g d_p^2}{18\mu_\infty C_\mathrm{Kn}} \approx \frac{\rho_\mathrm{p} g d_p^2}{18\mu_\infty C_\mathrm{Kn}}$$

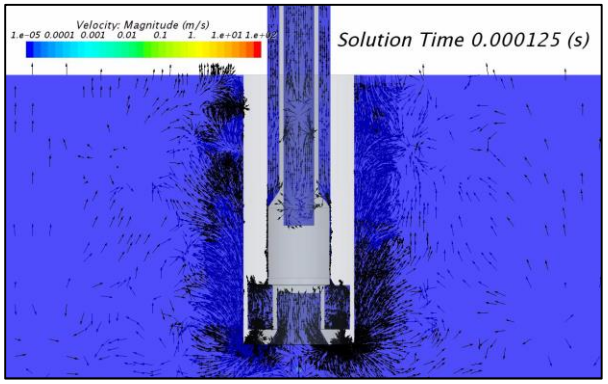


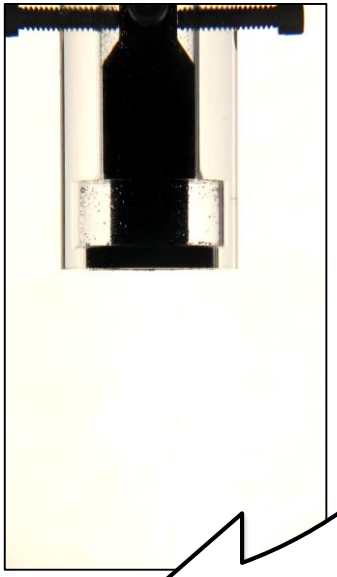

**Demonstration of FMPB's Effectiveness to Prevent Particle Penetration into Sample Tubes**

# First-principles model of the viscous flow in the FMPB

Jet Propulsion Laboratory
California Institute of Technology

- Flow into the FMPB orifice is fully-developed (also known as Poiseuille flow)
  - By design, orifice height H >> annular gap size ($r_2$-$r_1$)
  - Entrance flow Mach number << 1 → incompressible viscous flow
- Fully-developed flow $\frac{\partial u_z}{\partial z} = 0$ in an annular cavity has a well-known analytical solution
  - $\frac{\Delta p}{H} = -\frac{\partial p}{\partial z}, \quad \Delta p = p_o - p_i$
  - $u(r) = \frac{1}{4\mu}\left(-\frac{\partial p}{\partial z}\right)\left[\frac{\ln\left(\frac{r}{r_1}\right)}{\ln\left(\frac{r_2}{r_1}\right)}(r_2^2 - r_1^2) - (r^2 - r_1^2)\right]$
  - $u_{max} = u(R)$ where $R = \sqrt{\frac{r_2^2 - r_1^2}{2\ln(r_2/r_1)}}$

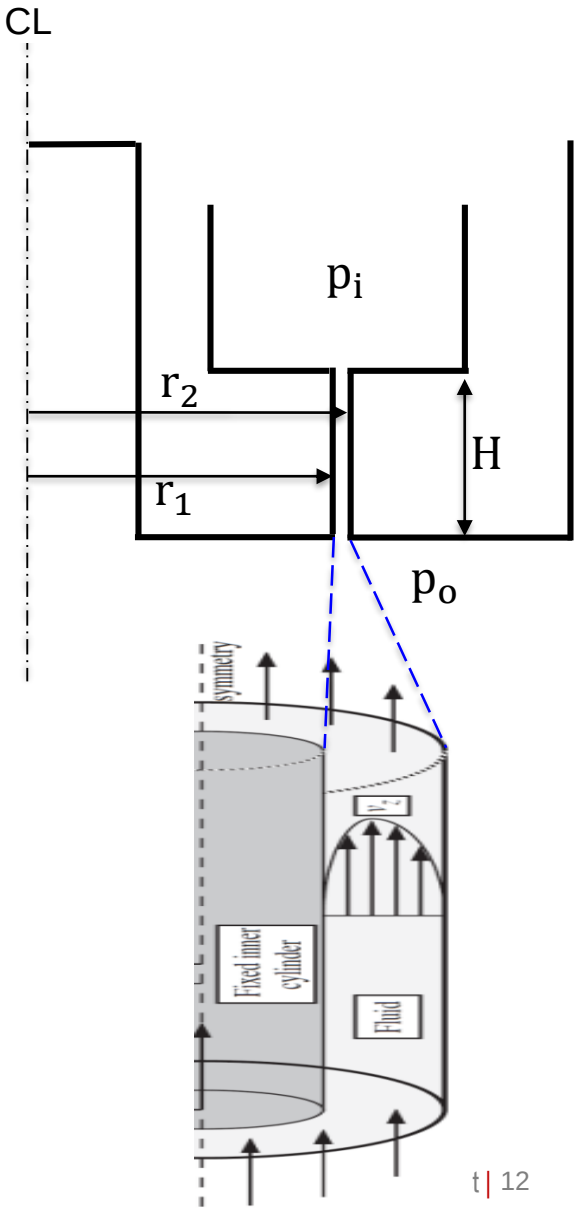

# First-principles model of the single particle aerodynamics



- Once flow velocity known, particle trajectory determined from Newton's second law
  - Aerodynamic force given by Stokes' drag, corrected for particle Reynolds number and slip (Knudsen number ≳0.1) effects (next chart)
- Particle dynamics dominated by gravity ($F_g$) vs. drag ($F_D$) as other forces* found to be negligible

$$m_p \frac{d\dot{\mathbf{z}}_p}{dt} = \mathbf{F}_D + \mathbf{F}_P + \mathbf{F}_M + \mathbf{F}_B + \mathbf{F}_g$$

($\mathbf{F}_P \sim 0$, $\mathbf{F}_M \sim 0$, $\mathbf{F}_B \sim 0$)

Solution with drag force and gravity in the z and –z directions, respectively.

$$\ddot{z}_p = k_p\left(V_z - \dot{z}_p\right) - g$$

$$\dot{z}_p = V_z - \frac{g}{k_p} + \left(\dot{z}_{p0} - V_z - \frac{g}{k_p}\right) e^{-k_p t}$$

$$z_p = z_{p0} + \left(V_z - \frac{g}{k_p}\right) t + \left(\dot{z}_{p0} - V_z + \frac{g}{k_p}\right) \frac{1 - e^{-k_p t}}{k_p}$$

$$\mathrm{k_p} \equiv \frac{g}{\mathrm{u}_{T\mathrm{p}}} \qquad \mathrm{u}_{T\mathrm{p}} \equiv \left(\rho_\mathrm{p} - \rho_\infty\right) \frac{g d_p^2}{18 \mu_\infty C_{\mathrm{Kn}}} \approx \frac{\rho_\mathrm{p} g d_p^2}{18 \mu_\infty C_{\mathrm{Kn}}}$$

Plot of Particle Terminal Velocity as a function of particle diameter

*inertial force due to virtual mass ($F_M$), Basset force ($F_B$), & pressure gradient, or Froude-Krylov force ($F_P$)

# First-principles model of the single particle aerodynamics, continued.



- Creeping flow: For particle Reynolds number $Re_p$<<1, the total drag force exerted on a spherical particle of diameter $d_p$, by a fluid of density $\rho_\infty$ and kinematic viscosity $\mu_\infty$, moving with speed $V_\infty$ is given by:

Drag force on a particle: $$F_D = F_{D_S} \frac{C_{Re}}{C_{Kn}}$$

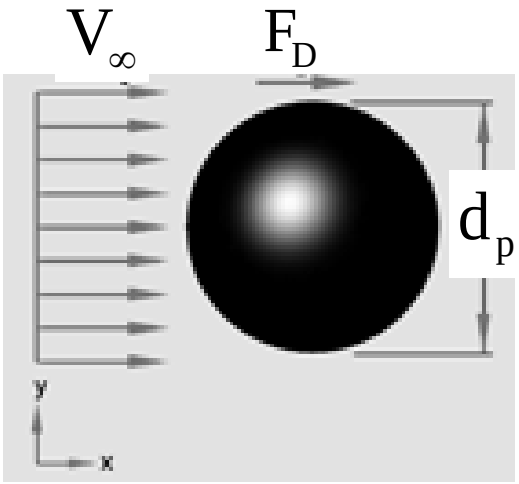


Stokes force: $$F_{D_S} = 3\pi\mu_\infty d_p V_\infty$$

$$Re_p = \frac{\rho_\infty d_p V_\infty}{\mu_\infty} \sim \frac{\text{inertia forces}}{\text{viscous forces}}$$

$C_{Re}$ & $C_{Kn}$ are corrections to Stokes formula accounting for Reynolds no. and slip effects

# Combining models for viscous flow and particle aerodynamics in the (2-cavity) FMPB



- A detailed mathematical model of the FMPB's first-principles of operation has been developed and validated [1]. Captures coupled dynamics of the viscous flow and particles inside the FMPB.

Pressure in FMPB cavities:

$$\mathbf{p}_C(t)=\begin{pmatrix} p_{C1} \\ p_{C2} \end{pmatrix}=\frac{p_0}{2\Lambda}\begin{pmatrix} \frac{e^{\lambda_1 t}}{2}\left(\Theta^+-1\right)\left(\Theta^-+1\right)-\frac{e^{\lambda_2 t}}{2}\left(\Theta^++1\right)\left(\Theta^--1\right) \\ e^{\lambda_2 t}\left(\Theta^++1\right)-e^{\lambda_1 t}\left(\Theta^-+1\right) \end{pmatrix}+\frac{2p_e\bar{k}}{\Lambda}\begin{pmatrix} \frac{1-e^{\lambda_2 t}}{2}\frac{1-\Theta^-}{1+\Theta^-}-\frac{1-e^{\lambda_1 t}}{2}\frac{1-\Theta^+}{1+\Theta^+} \\ \frac{1-e^{\lambda_2 t}}{1+\Theta^-}-\frac{1-e^{\lambda_1 t}}{1+\Theta^+} \end{pmatrix}$$

Flow speed in O1:

$$u_{O1}(t)=\frac{G_{O1}}{S_{O1}}\left[p_e-p_{C1}(t)\right]$$

$$z_p=z_{p0}+\left(u_{O1}-\frac{g}{k_p}\right)t+\left(\dot{z}_{p0}-u_{O1}+\frac{g}{k_p}\right)\frac{1-e^{-k_p t}}{k_p}$$

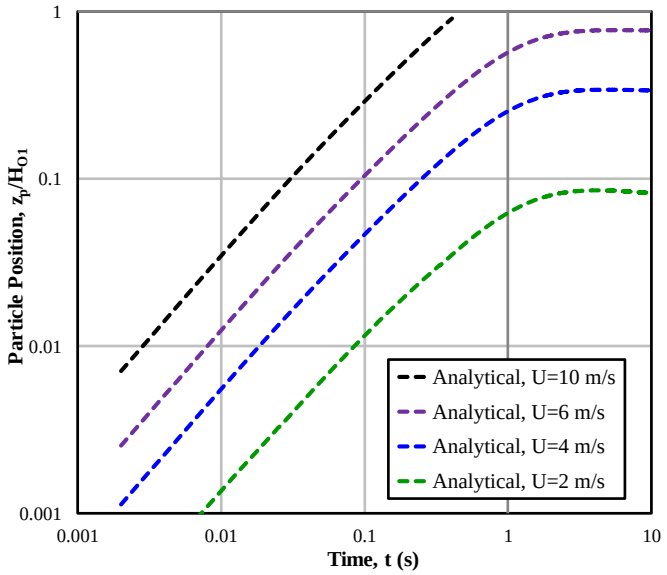


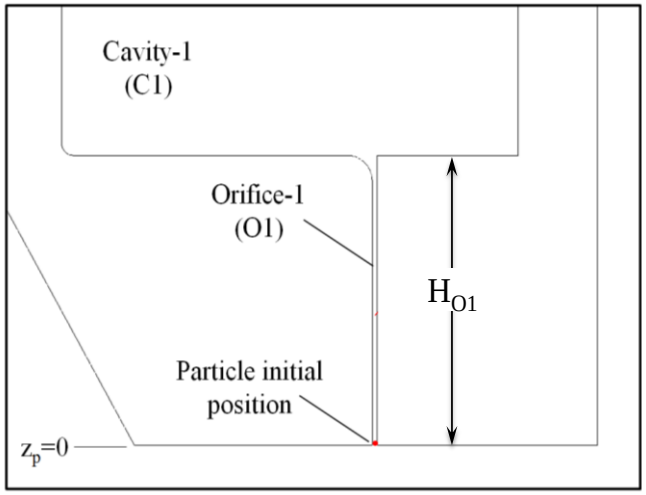


[1] Mikellides, I. G., Steltzner, A. D., Blakkolb, B. K., Matthews, R. C., Kipp, K. A., Bernard, D. E., Stricker, M., Benardini, J. N., Shah, P., Robinson, A., "The Viscous Fluid Mechanical Particle Barrier for the Prevention of Sample Contamination on the Mars 2020 Mission," *Planetary and Space Sciences,* PSS4337, 2017.

# Mission Timeline

Jet Propulsion Laboratory
California Institute of Technology

Earth: ATLO | Launch | Cruise | Mars EDL | Mars Surface: Commissioning | Mars Surface: Operations, Non-Sampling | Mars Surface: Operations, Sampling | Mars Surface: Future Missions

**Cruise**
- 7 month cruise, vacuum environment
- ACA volume is closed out, preferred flow path via HEPA filters
- Protections in place to protect sensitive hardware from contamination

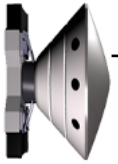

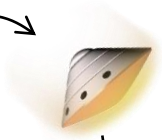

**Entry, Descent, and Landing (EDL)**
- Transient event, repressurization
- ACA volume is closed out, preferred flow path via HEPA filters
- Protections in place to protect sensitive hardware from contamination
- Rover exposed to ambient flow at heatshield separation (bit carousel, corer)

**Launch**
- Transient event, depressurization
- ACA volume is closed out, preferred flow path via HEPA filters
- Protections in place to protect sensitive hardware from contamination

**Commissioning**
- ACA is opened up (belly pan dropped, carousel doors opened)
- Drive away from landing site
- Hardware checkouts

**Surface Operations**
- Non-sampling: tubes, seals, volume probe remain protected when not in use
- Sampling: up to 43 discrete sampling events, each 1 sol end-to-end

**Future Missions**
- Sealed samples retrieved by future rover, launched from Mars surface, and returned to Earth

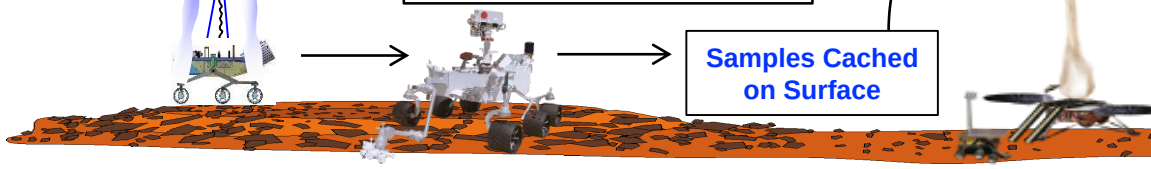

**Samples Cached on Surface**

**Assembly, Test, and Launch Operations (ATLO)**
- Precision cleaning & bakeouts
- Special cleaning and handling of sensitive hardware (350C bakeout, storage in clean environment, separate sterile and ATLO flight models)
- Protections in place to protect sensitive hardware from contamination post-cleaning
- T-0 purge of ACA (from final component installation through launch)

# FMPB Rationale and Use Cases



- Reason for not using a physical biobarrier is the need to meet Organic Contamination (OC) requirements in addition to Viable Organism (VO) requirements.

- FMPB use cases (operational scenarios) include:
  - Allow gas flow in and out during 200°C purge with N2/pull with vacuum prior to firing (When? ATLO?)
  - Allow gas flow out during 350°C firing in oxygen-containing atmosphere (When? ATLO?)
  - Prevent particle entry between firing and use on Mars (Elaborate)
  - Limit gas flow between firing and launch (for OC) (Elaborate)
  - Allow gas flow out during launch (Launch)
  - Limit gas flow during cruise (for OC)
  - Allow gas flow in during EDL
  - Limit gas flow on Mars surface until use (for OC) (Elaborate)
  - Maintain adequate mechanical clearances to allow extraction and re-insertion by Sample Handling Arm (SHA) on Mars

# Performance of FMPB During the Mission – ATLO & Cruise

Jet Propulsion Laboratory
California Institute of Technology

- Assembly, Test, and Launch Operations (ATLO) - Pre-launch
  - Pressure gradients in the vicinity of the FMPB are expected to be negligible since no direct flow or major pressurization events will occur.
  - Some small pressure fluctuations associated with personnel and/or equipment movements are expected in the assembly rooms but these have been estimated to be both of low intensity and short duration such that no particle penetration in the FMPBs is expected.

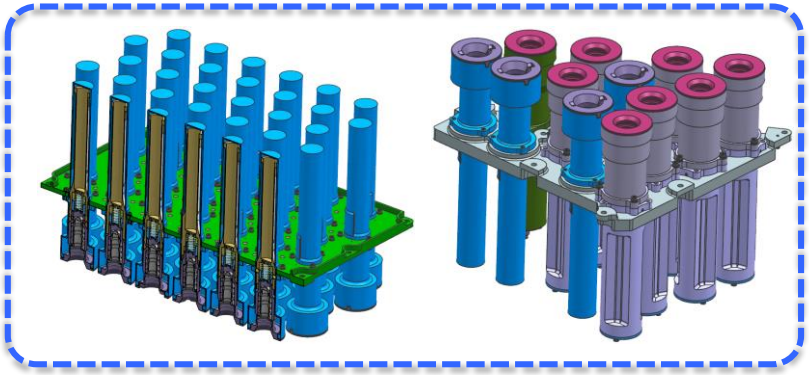

*Sample Tube Storage (sample tubes, sheaths, FMPB gloves)*
*Seal Dispensers (stack of 7 seals per dispenser, FMPB cover)*
*Volume Assessment Assembly (probe, housing, FMPB cover)*

- Separate ATLO Flight Model (AFM) and Sterile Flight Model (SFM) assemblies
- All are ultra-cleaned, undergo 350°C bake-out (1 hr, air)
- AFMs installed in rover for ATLO testing
- SFMs stored in clean environment, installed in rover at KSC

ATLO | Launch | Cruise | Mars EDL | Mars Surface: Commissioning | Mars Surface: Operations, Non-Sampling | Mars Surface: Operations, Sampling | Mars Surface: Future Missions

# Performance of FMPB During the Mission – Launch & Cruise

Jet Propulsion Laboratory
California Institute of Technology

- Launch
  - De-pressurization of the ACA as the vehicle ascends will occur but the flow field will be in a direction away from the FMPB. Therefore, any particles that are released during this phase of the mission will be directed away from the FMPBs.
- Cruise
  - The ACA will be in near-vacuum conditions so no flow that can carry particles to the FMPBs will exist.

- ACA is closed out, with preferred flow path via HEPA filters.
- Sample tubes FMPB-protected.
- Bit carousel doors are sealed, preventing particle transport into bit carousel interior volume.
- Corer is sealed with a launch bit, preventing particle transport into corer interior volume.
- Rover is stowed within aeroshell, until heatshield separation.

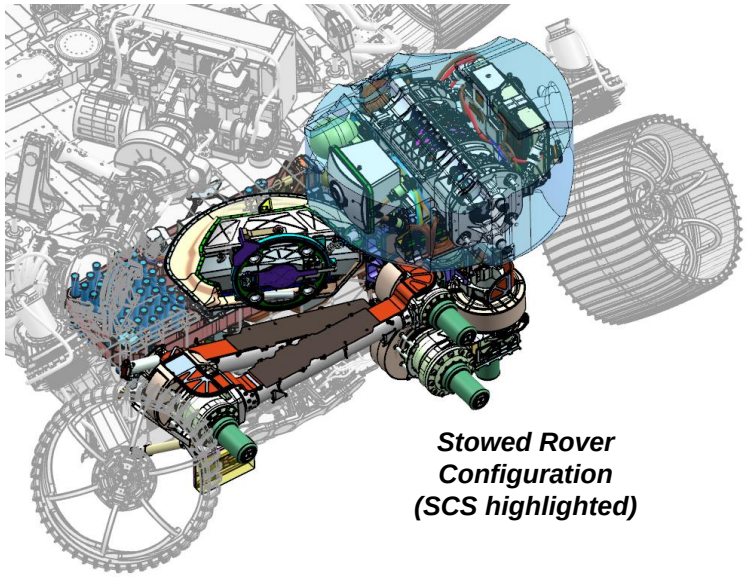

***Stowed Rover Configuration (SCS highlighted)***

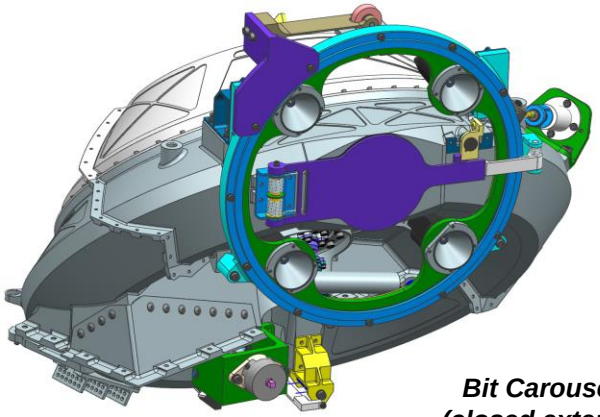

***Bit Carousel (closed exterior door shown)***

ATLO | Launch | Cruise | Mars EDL | Mars Surface: Commissioning | Mars Surface: Operations, Non-Sampling | Mars Surface: Operations, Sampling | Mars Surface: Future Missions

# Performance of FMPB During the Mission – Entry Descent & Landing (EDL)

Jet Propulsion Laboratory
California Institute of Technology

- EDL
  - Pressurization of the ACA as the vehicle descends will occur. Estimated flow fields allow assessments of particle penetration depths.
    - Pre-heat shield separation: pressure gradients very small
    - Highest pressure gradients at heat shield separation

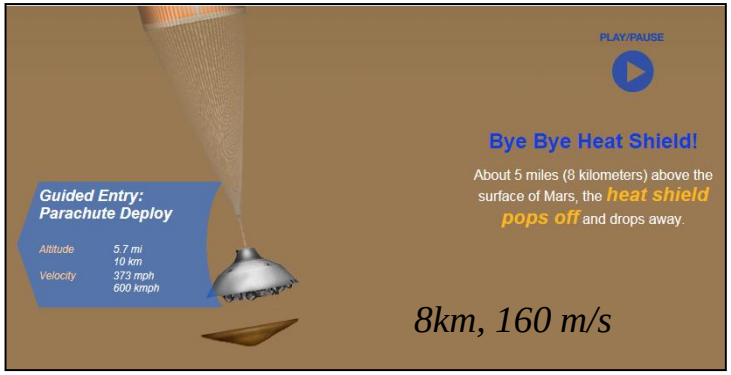


Flow speed into the ACA through HEPA (porous media) during EDL

$$u_p = -\frac{K}{\mu}\frac{p_\infty}{L_H}\left(\frac{p}{p_\infty}-1\right)-\frac{\lambda n\left(\frac{p}{p_\infty}\right)}{L_H}\left[\frac{4}{3}(1-\alpha)D_s+\alpha D_K\right]$$

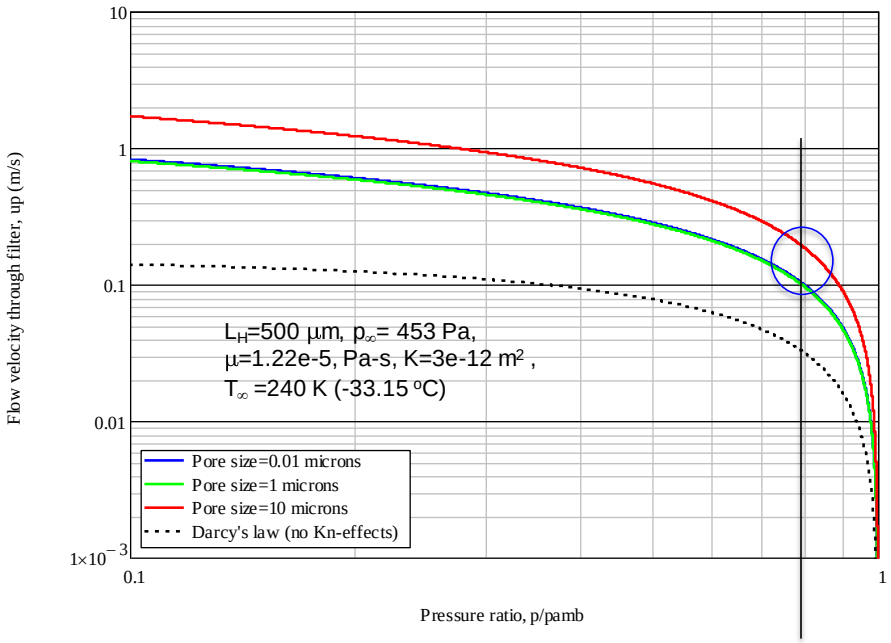


Range of flow speeds expected inside the ACA upon heat shield separation, induced by dynamic pressure of Δp(160m/s)=90 Pa outside of the ACA.
Note: 0.1-0.2 m/s at FMPB entrance (inside the ACA) is equivalent to $4.1\times10^{-4} > \Delta p > 14.5\times10^{-4}$ Pa across it.

$$\frac{p}{p_{amb}} \approx \frac{p_\infty}{p_\infty + \tfrac{1}{2}\rho u_M^2} \xrightarrow{u_M = 160 m/s} 0.78$$

$$\rightarrow 0.1 < u_H < 0.2 \ m/s$$

ATLO | Launch | Cruise | Mars EDL | Mars Surface: Commissioning | Mars Surface: Operations, Non-Sampling | Mars Surface: Operations, Sampling | Mars Surface: Future Missions

# Performance of FMPB During the Mission – Mars Surface Activities



- Commissioning
  - Belly panel released (to occur within first 30 sols). Induced flow field in vicinity of FMPB negligible. Ambient flow field into ACA computed via CFD; allows for particle penetration depths into FMPB.
  - Carousel inner and outer doors open. Induced flow negligible.
- Surface Operations
  - Ambient flow field into ACA computed via CFD; allows for particle penetration depths into FMPB.
  - Mechanical vibrations due to operation of interior components (e.g. SHA) induce negligible flows.

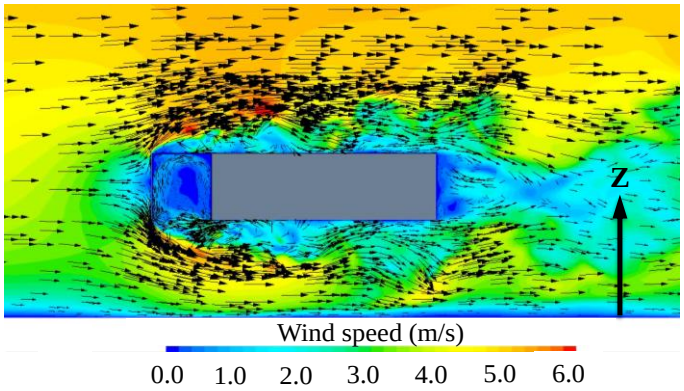


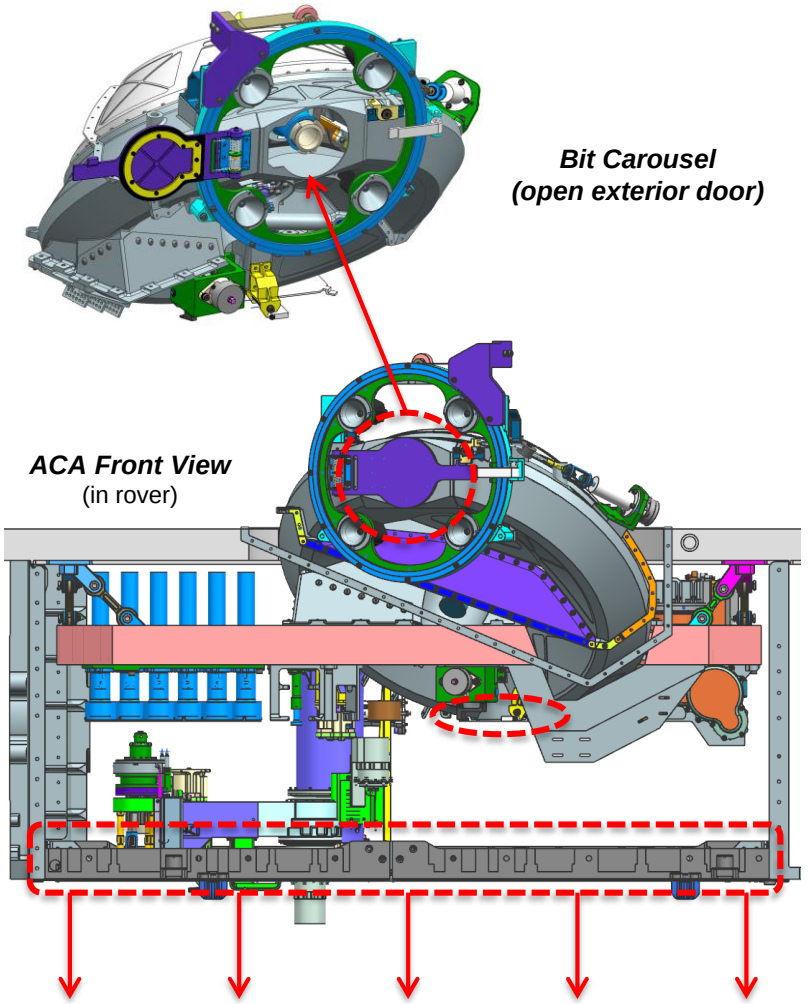


ATLO | Launch | Cruise | Mars EDL | Mars Surface: Commissioning | Mars Surface: Operations, Non-Sampling | Mars Surface: Operations, Sampling | Mars Surface: Future Missions

# Performance of FMPB During the Mission



- Maximum penetration of the smallest particle considered (0.15 μm) not expected to exceed 10% of the (first) FMPB orifice height ($H_{O1}$).

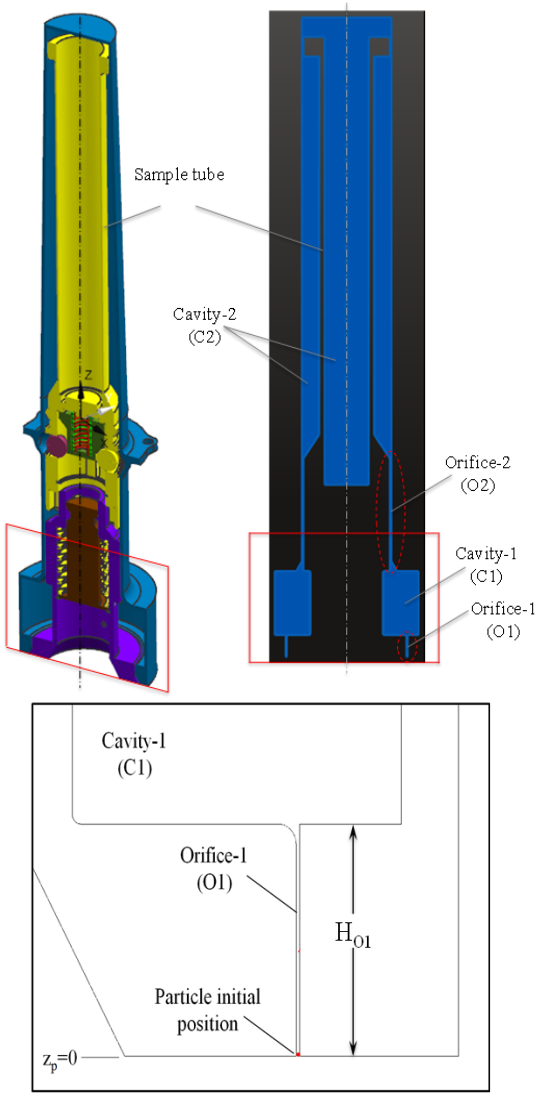


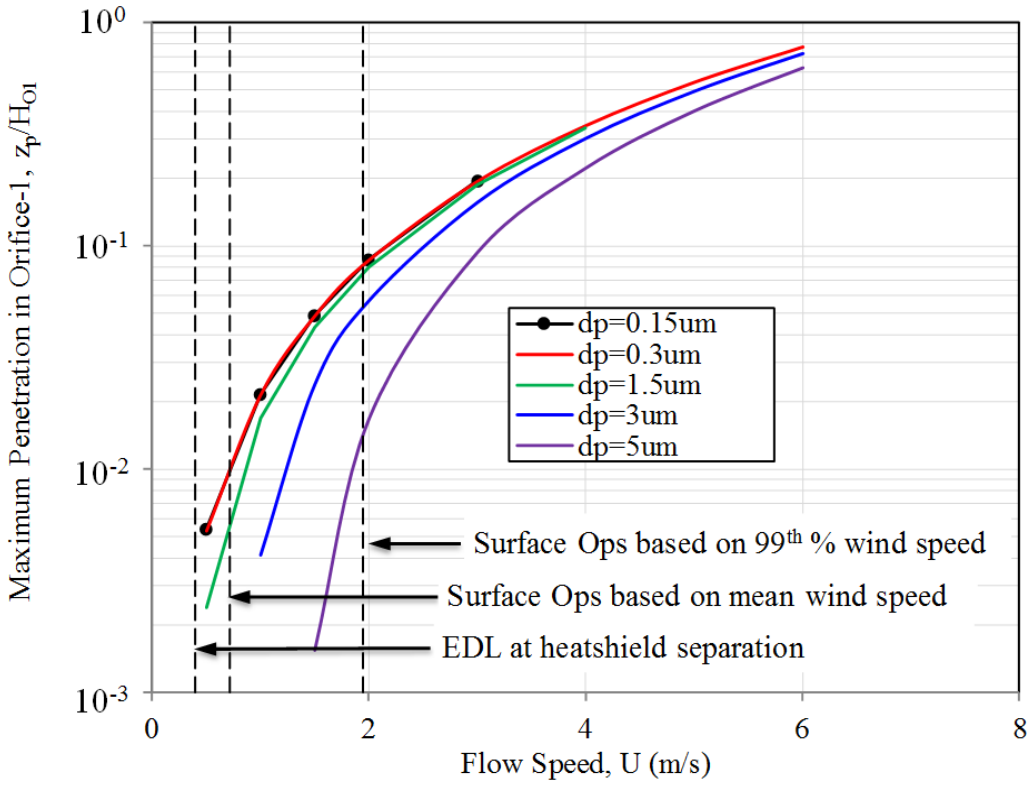

# 1:30-2:30 PM
# FMPB Verification by Analyses and Flow Tests

# Validation of the First-principles analytical model using CFD



- CFD simulations in 2-D and 3-D also have been performed [1]
  - Of Mars flow over the rover that have quantified expected speeds/pressure differentials to which the FMPB will be exposed
  - Of Mars flow and particle dynamics in the FMPB; simulation results validated the first-principles model

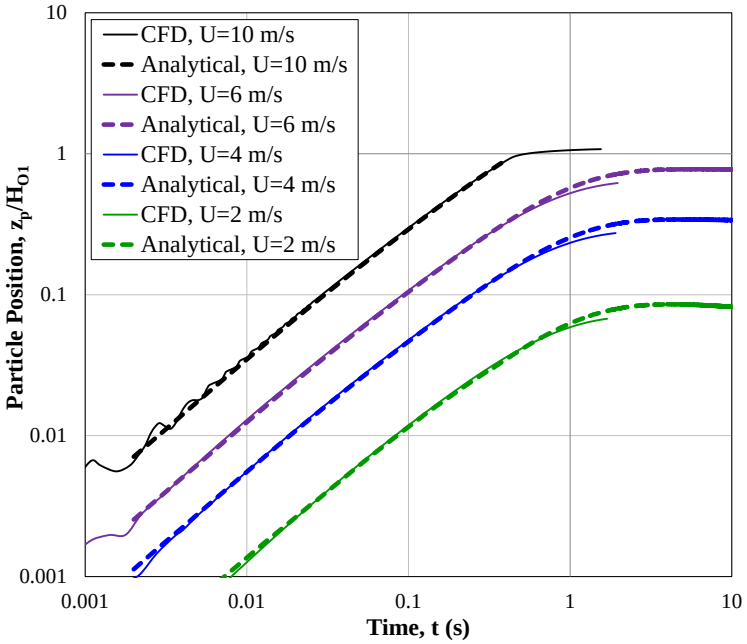


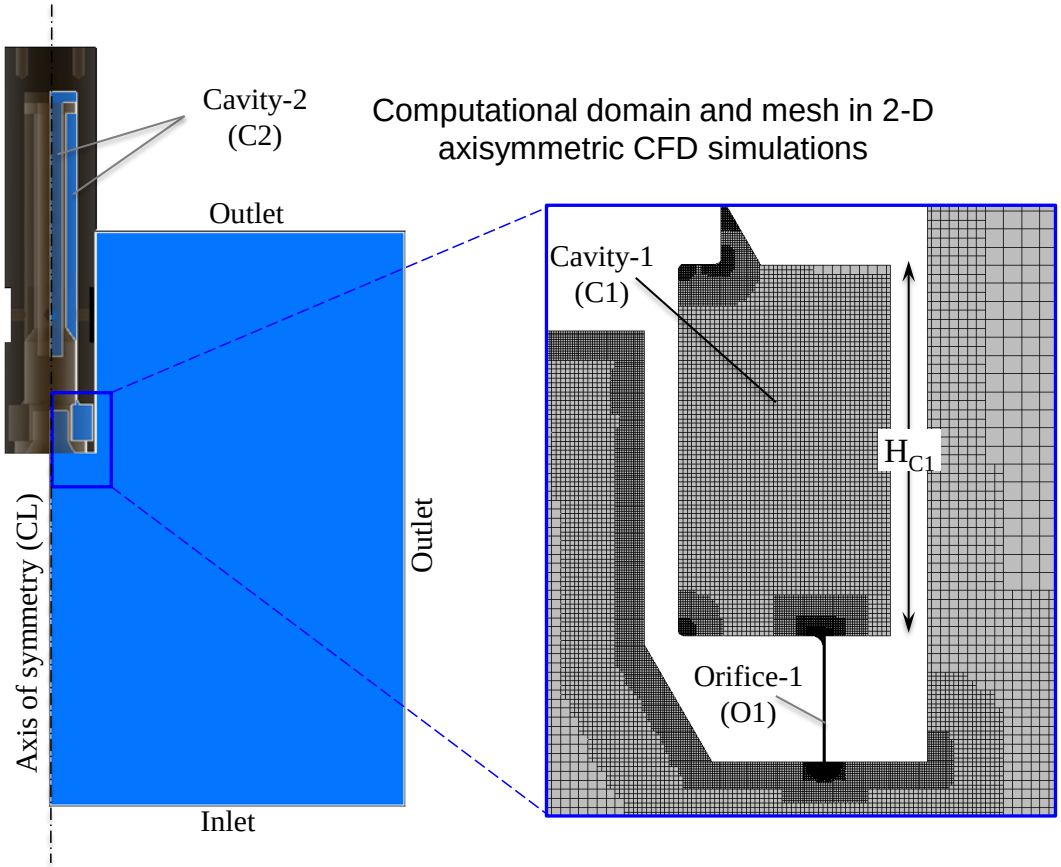

# A Closer Look at the CFD and Lagrangian Particle Simulations in Mars Environment

Jet Propulsion Laboratory
California Institute of Technology

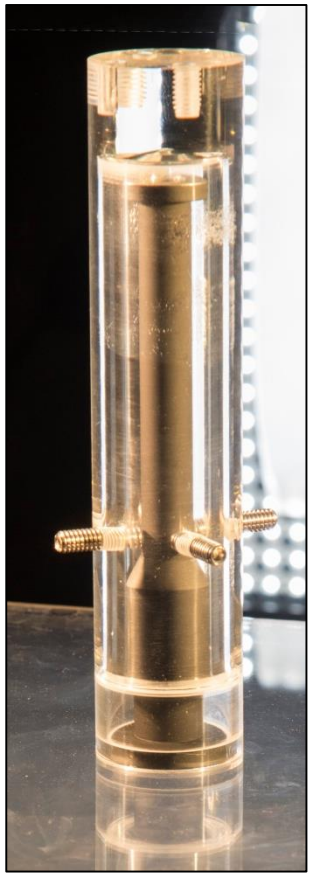

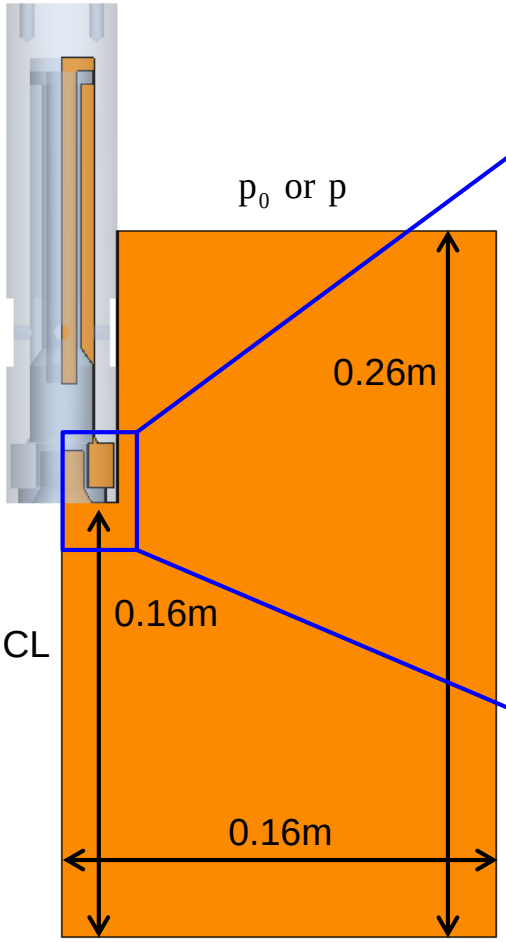


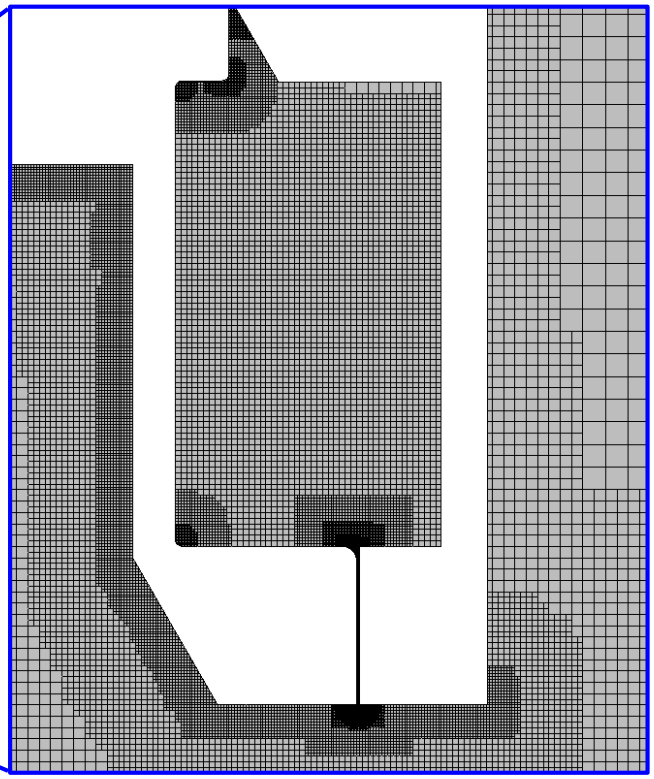

$$p_0 = p + \Delta p \quad (\Delta p = \tfrac{1}{2}\rho u^2)$$

--**Simulation series 1**: Pressurization event (all 3 pressure boundaries at $p_0$)
--**Simulation series 2**: Sustained winds (only inlet boundary at $p_0$, other two boundaries at p)

*Acknowledgment: All CFD simulations have been performed by Dr. Parthiv Shah and Mr. Albert Robinson of ATA Engineering, Inc., under the guidance of Dr. I.G. Mikellides.*

# Flow Field Solution in the FMPB Orifice for U=10 m/s During Pressurization Event

Jet Propulsion Laboratory
California Institute of Technology

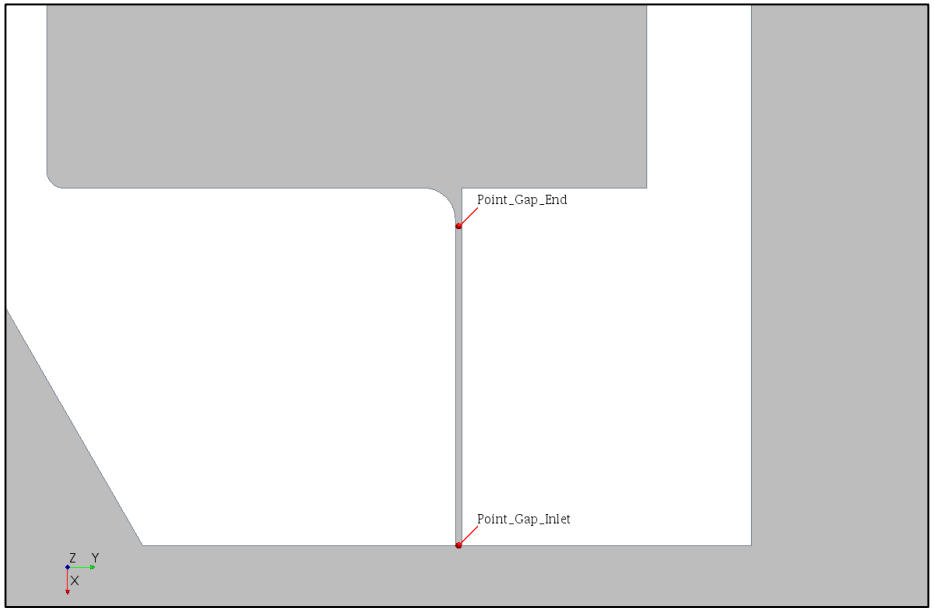


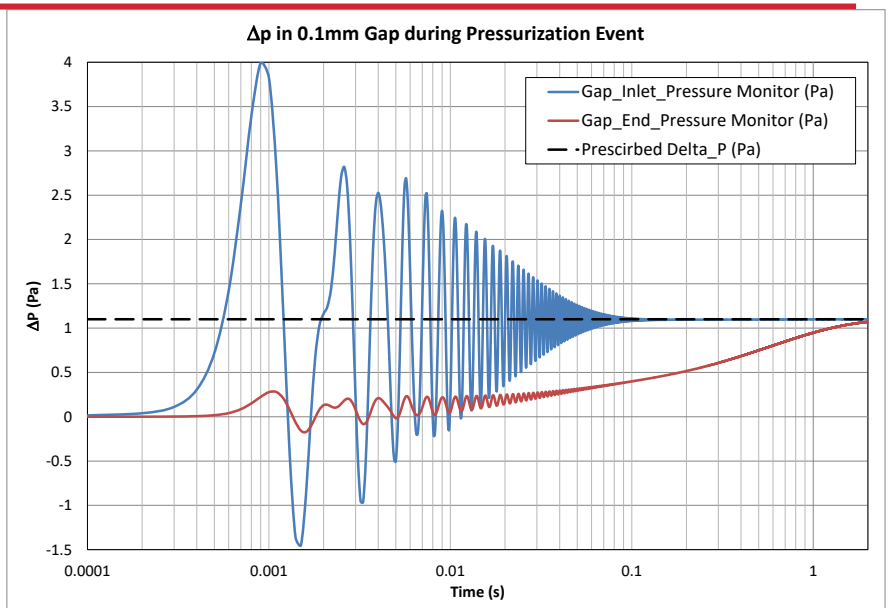


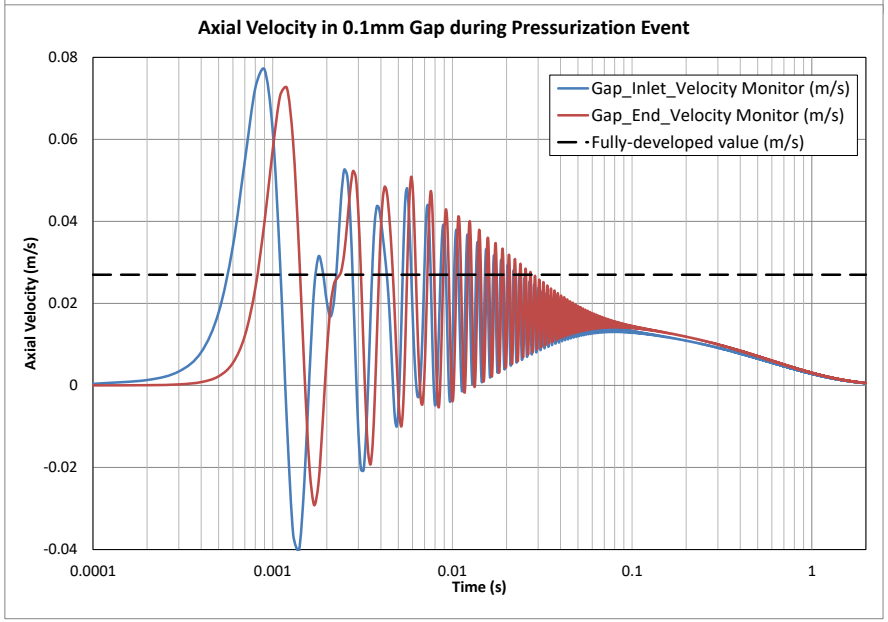


- Early acoustic oscillations due to pressure fluctuations over the outer boundaries (frequency ~600 Hz, sound speed~215 m/s → 2-way wave transit length: L=0.18 m
- Prescribed $\Delta p=\frac{1}{2}\rho U^2$
- Fully-developed value of velocity in gap determined from Poiseuille-flow solution at $\Delta p=\frac{1}{2}\rho U^2$

# Evolution of 5-μm Particles for U=10 m/s During Pressurization Event.

Jet Propulsion Laboratory
California Institute of Technology

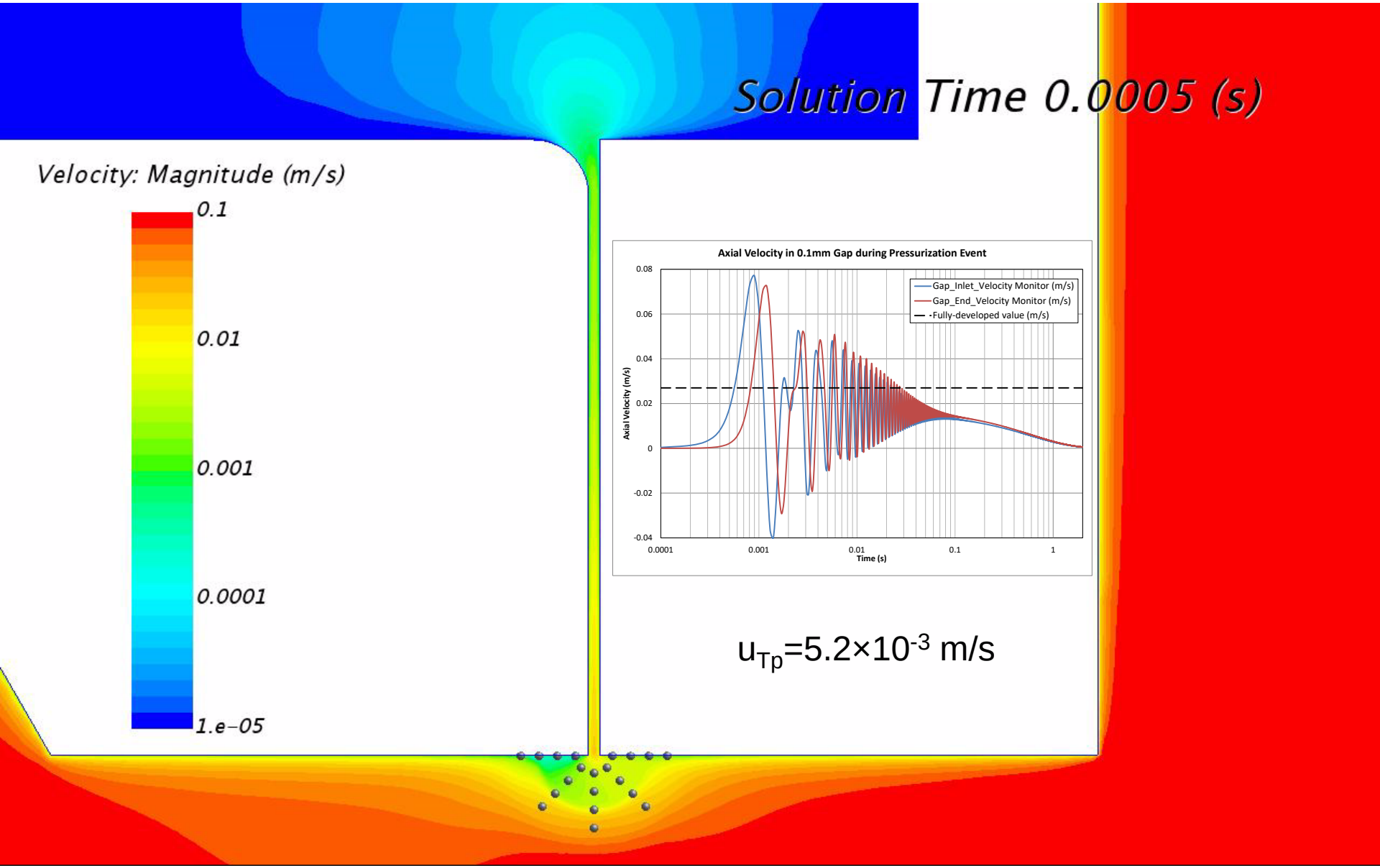


$u_{Tp}=5.2\times10^{-3}$ m/s

# Evolution of 0.3-μm Particles for U=10 m/s During Pressurization Event.

Jet Propulsion Laboratory
California Institute of Technology

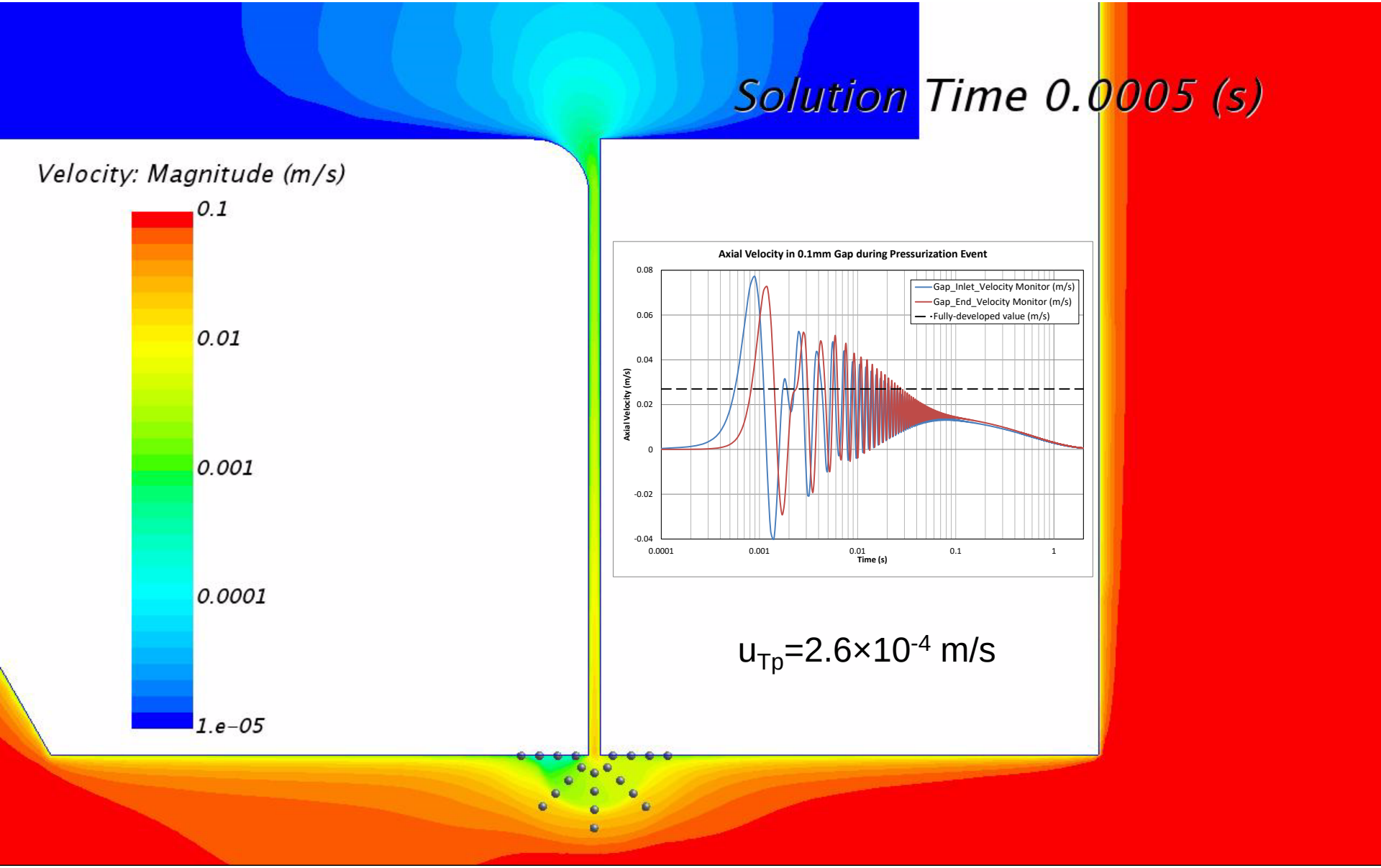


$u_{Tp}=2.6\times10^{-4}$ m/s

# Evolution of 0.3-μm Particles for U=10 m/s During Sustained Wind Event.

Jet Propulsion Laboratory
California Institute of Technology

Solution Time 0.0005 (s)

Velocity: Magnitude (m/s)

1.e+01
1.
0.1
0.01
0.001
0.0001
1.e-05

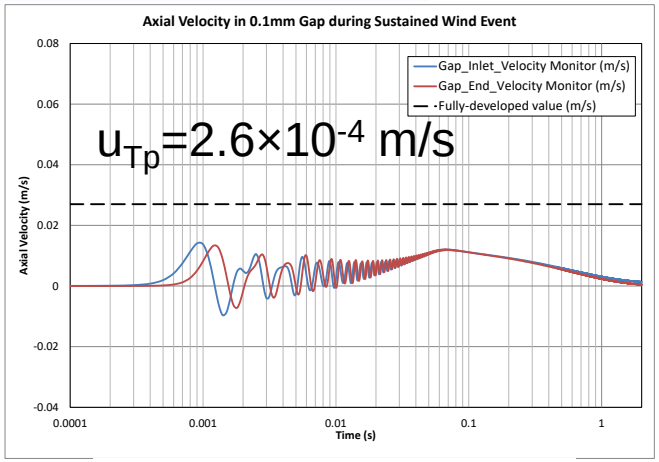


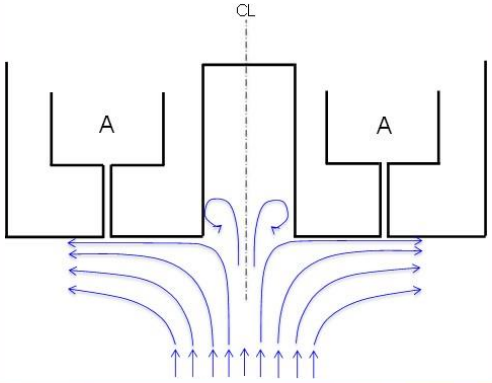

# Dimensional Analysis and Similarity Have been Used to Perform FMPB Flow Experiments in a Water Tunnel Under Mars-similar Conditions

Jet Propulsion Laboratory
California Institute of Technology

- Dimensional analysis reduces the number and complexity of (dimensional) variables that describe a given physical phenomena, by grouping them into non-dimensional parameters.
- Similarity in the physics of the phenomenon between prototype and a model is retained if the non-dimensional parameters are kept the same. Hence, it can be achieved even when the model fluid is different than the prototype fluid (e.g. water vs air).
  **So, YES! Sticking things in water actually DOES work!**

- Historical note: The subject received methodical attention toward the end of the 19th century, notably in the works of Lord Rayleigh, Reynolds, Maxwell, and Froude. By the 1920's the principles were essentially in place: Buckingham's now ubiquitous π−theorem had appeared (Buckingham, 1914), and Bridgman had published the monograph which still remains the classic in the field (Bridgman, 1922, 1931). Applications now include:
  - aerodynamics, hydraulics, ship design, propulsion, heat and mass transfer, combustion, mechanics of elastic and plastic structures, fluid-structure interactions, electromagnetic theory, radiation, astrophysics, underwater and underground explosions, nuclear blasts, impact dynamics, and chemical reactions and processing and also biology (McMahon & Bonner, 1983).

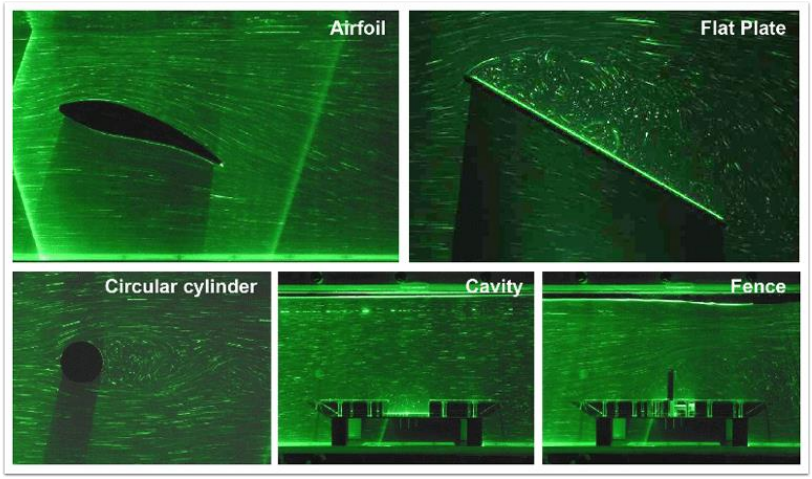


Flow visualization in water tunnels

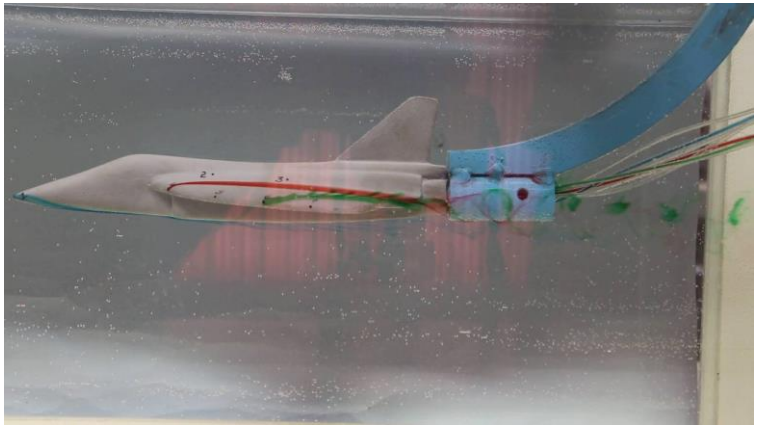

# Scaling Mars Conditions for Flow Visualization Tests in Water and Air Tunnels



- Present flow visualization tests intended to address sustained wind scenario only.
- Minimum water tunnel speed (0.1 m/s) corresponds to 62.5 m/s on Mars for full scale model.

$\rho_M=\rho_{Mars}=2.2\times10^{-2}$ kg/m$^3$
$\mu_M=1.222\times10^{-5}$ Pa-s
$\rho_E=\rho_{H2O}=1000$ kg/m$^3$ or $\rho_{air}=1.225$ kg/m$^3$
$\mu_E=\mu_{H2O}=8.9\times10^{-4}$ Pa-s (25 $^o$C) or $\mu_{air}=1.812\times10^{-5}$ Pa-s

$$Re_M = Re_E \rightarrow u_E = \frac{D_M \mu_E \rho_M}{D_E \mu_M \rho_E} u_M$$

**Full scale model**

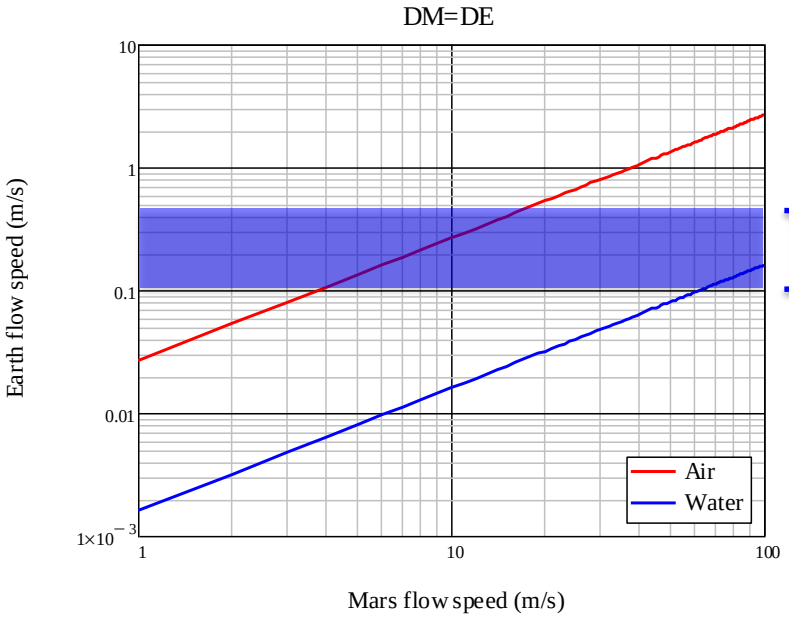


**Caltech water tunnel range**

# Flow Visualization from Water Tunnel Tests at Caltech

Jet Propulsion Laboratory
California Institute of Technology

- Water Tunnel at Caltech
  - Used for research on very slow flows, typically for requests outside of Caltech
  - Range of speeds: 0.1-0.5 m/s
- Tests have been performed at Mars-equivalent speeds >60 m/s and at varying angles of attack

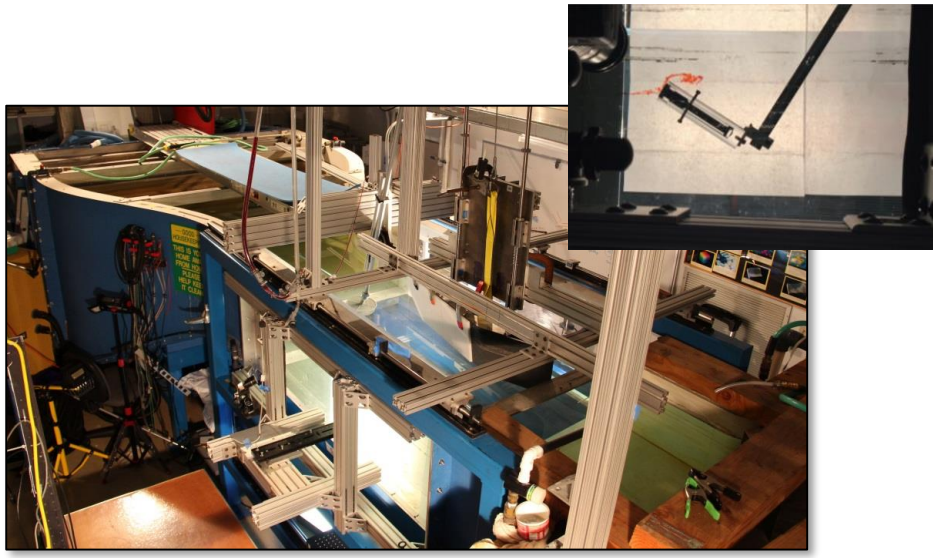

Test: 1/21/16, **4x the 3σ Mars wind speed** (62.5 m/s, θ=0 deg)

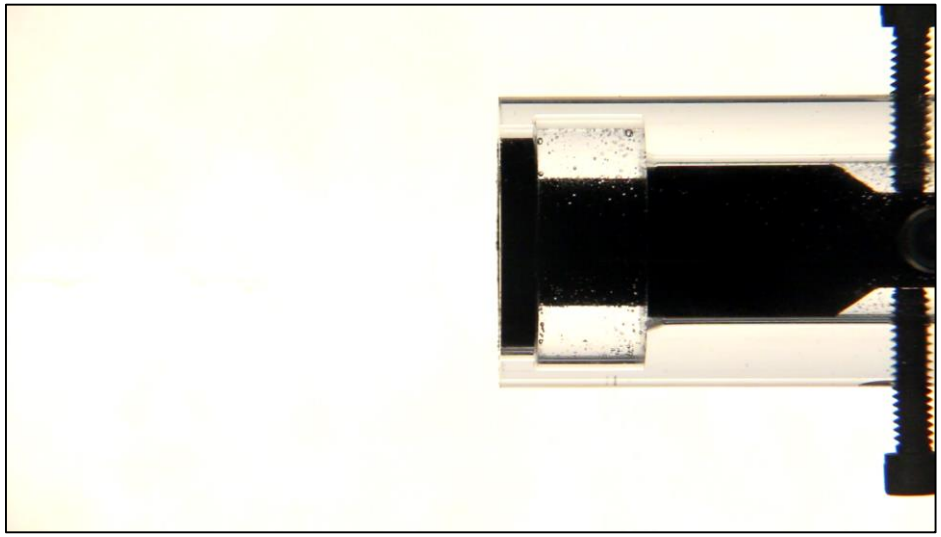

Test: 1/21/16, **10x the 3σ Mars wind speed** (162.5 m/s, θ=30 deg)

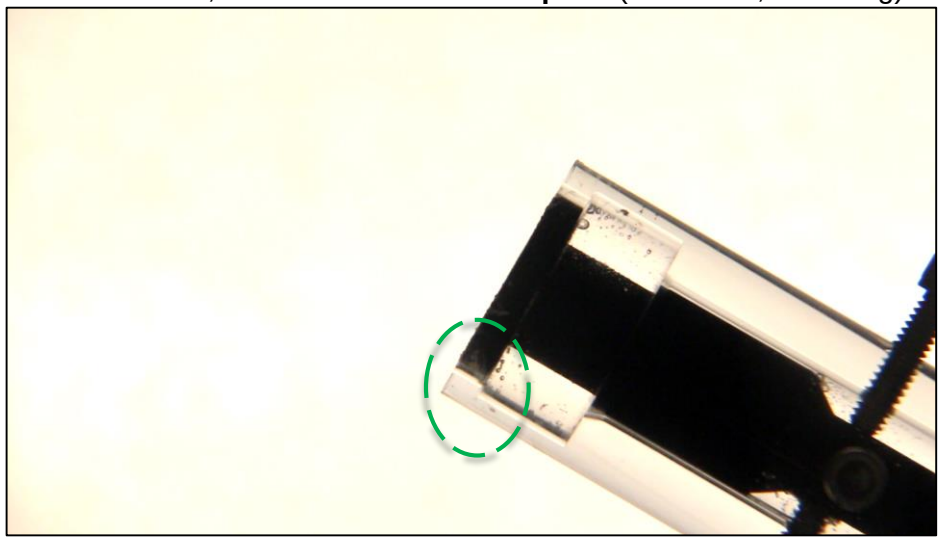

# Results from Water Tunnel Tests, Extrapolated based on First principles to Expected Wind Speeds on Mars Show Large Margins



- Both flow tests and CFD simulations were performed (over a period of ~18 months) to verify the predictions of our analyses on particle prevention by the FMPB. The results from the analyses, simulations and flow tests have been reported in [11]

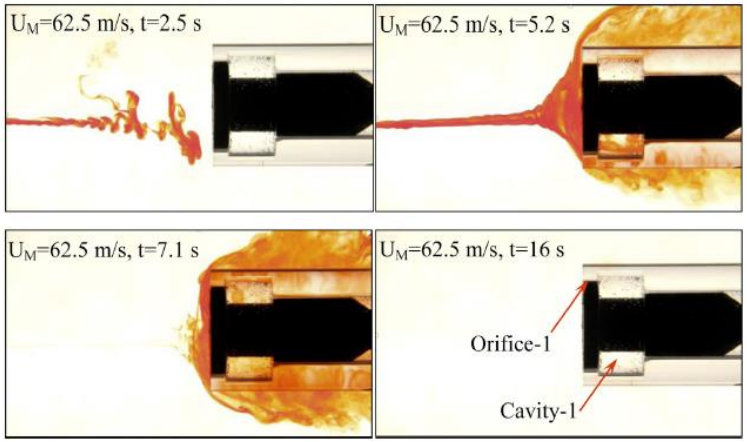


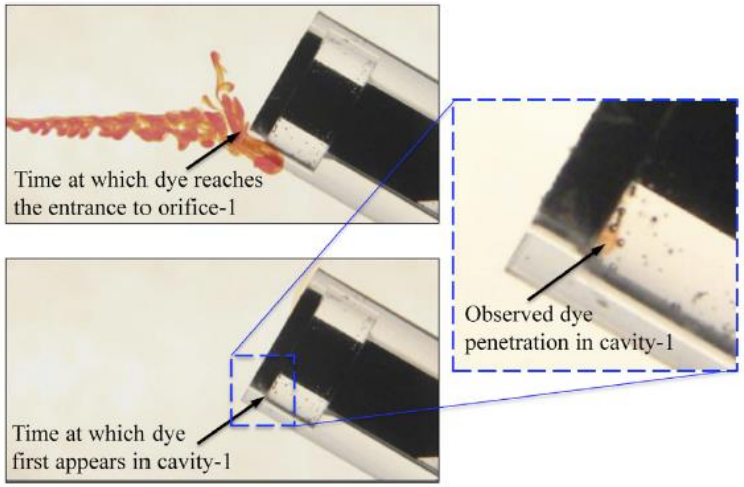


- The water tunnel tests were performed under Mars-similar conditions of >60-m/s flow over the FMPB, which is >10x the average wind speed on Mars (4.7 m/s)
- No flow penetration into Cavity-1 was observed at zero angle of attack, as expected.
- Flow penetration at non-zero angle of attack was expected and observed. But the flow speeds through Orifice-1 under Mars ambient wind conditions were found to be too small to allow particle penetration into Cavity-1.

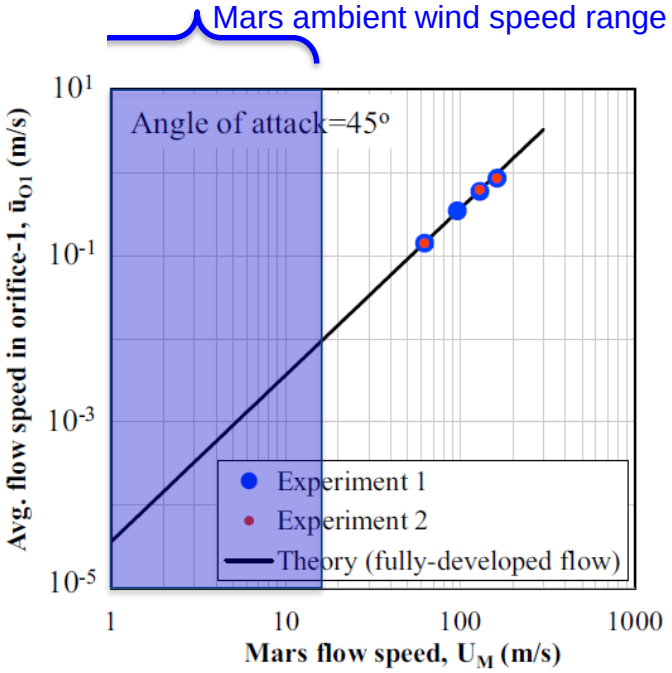

# Results from Water Tunnel Tests, Extrapolated based on First principles to Expected Wind Speeds on Mars Show Large Margins

Jet Propulsion Laboratory
California Institute of Technology

- Results below shown for **$u_M$=10 m/s**.
- Particle penetration height shows ~$10^4$ margin

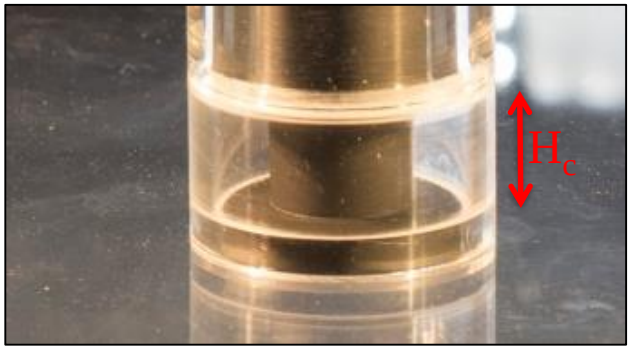


Compartment Height, $H_c$=16.4mm

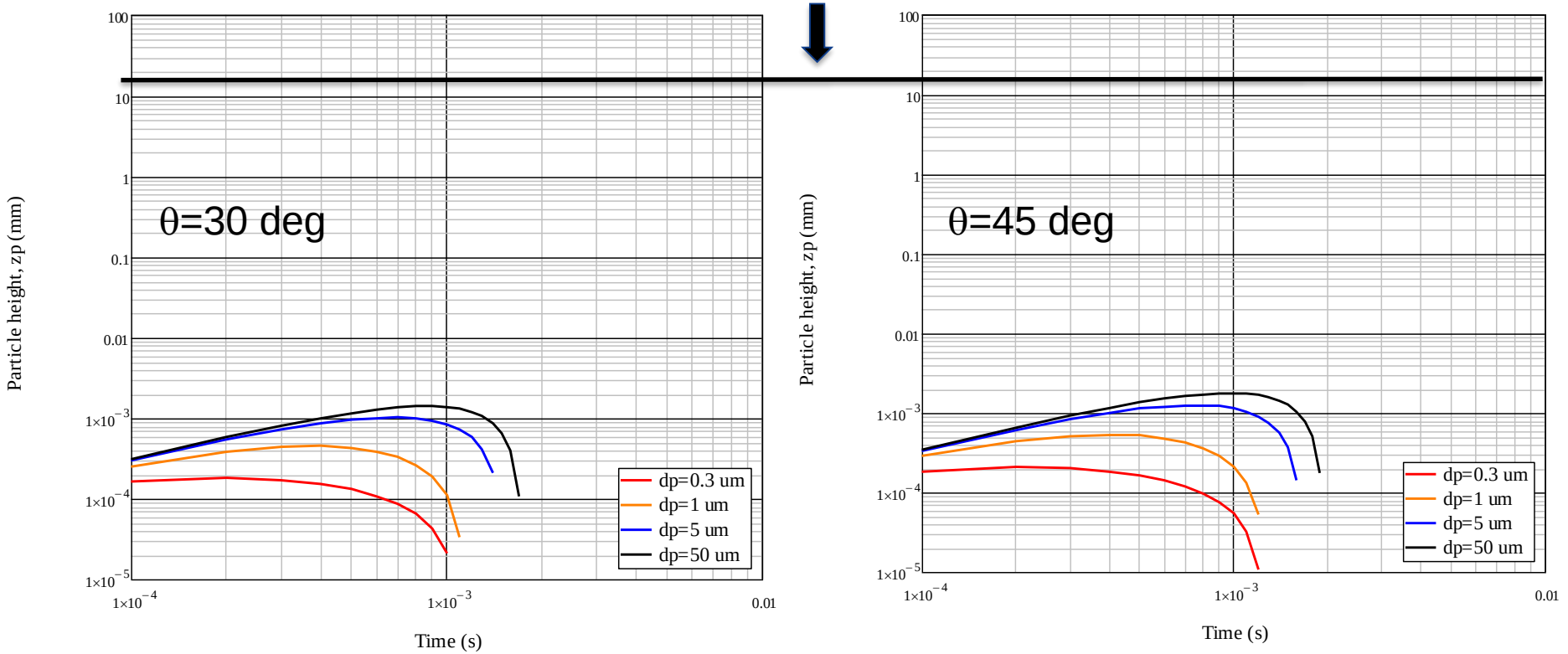

# Backup Charts

# First-principles particle dynamics
## — Re Corrections —

Jet Propulsion Laboratory
California Institute of Technology

- Re Corrections. When $Re_p$=1 the drag force predicted by Stokes is 13% lower due to neglect of inertia forces. To account for Re-effects over a large range of $Re_p$>1, the following (empirical) correction is made:

$$F_D = C_D S_p \rho_\infty V_\infty^2$$
$$= \frac{24 C_{Re}}{Re_p} \frac{\pi}{8} d_p^2 \rho_\infty V_\infty^2$$
$$= C_{Re} 3\pi \mu_\infty d_p V_\infty$$
$$= C_{Re} F_{D_S}$$

$$C_{Re} = 1 \qquad Re_p < 0.1$$

$$C_{Re} = 1 + 0.15 Re_p^{0.687} \qquad 0.1 < Re_p < 500$$

Clift & Gauvin, Proceedings of Chemeca, 70, Vol. 1, Butterworths, Melbourne, pp. 14-28.

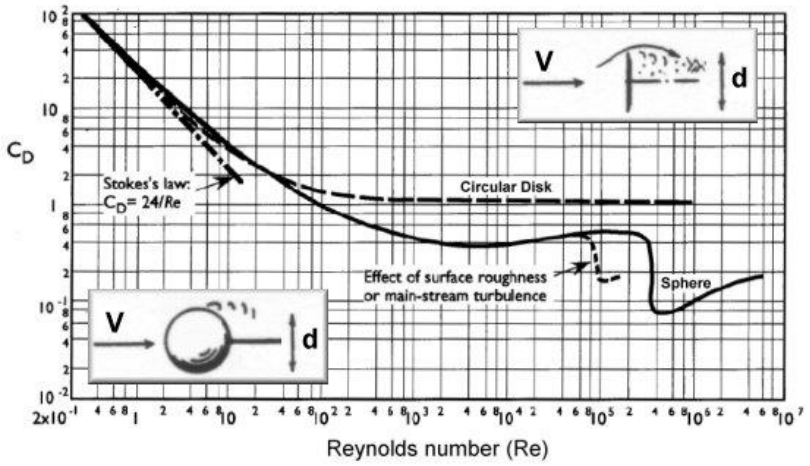


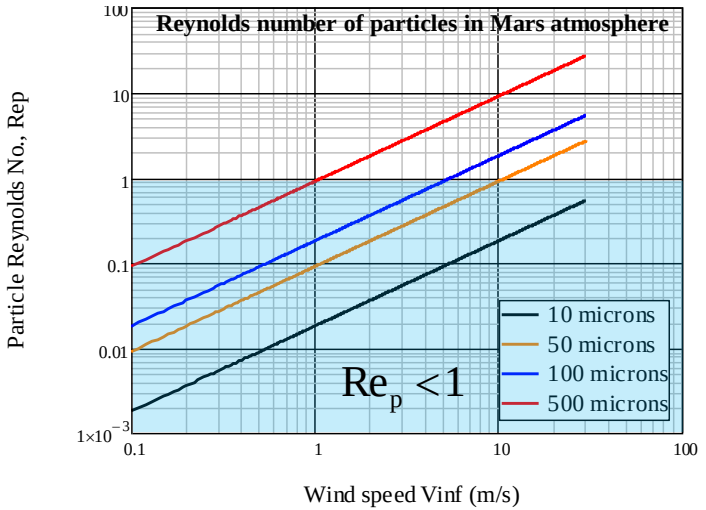

# First-principles particle dynamics
## — Kn Corrections —

Jet Propulsion Laboratory
California Institute of Technology

- Kn Corrections. When the particle diameter $d_p$ becomes comparable to the mean free path of particles making up the flow, the resisting force entered by the fluid is smaller that that predicted by Stokes' law. To account for non-continuum (slip) effects the following (empirical) correction factor is applied to Stokes drag force also known as the Cunningham correction factor:

$$F_D = \frac{3\pi\mu_\infty d_p V_\infty}{C_{Kn}} = \frac{F_{D_S}}{C_{Kn}}$$

$$\text{Fluid mfp } \lambda = \left(\pi\sqrt{2}n_\infty d_{CO_2}{}^2\right)^{-1}$$

$$\text{Knudsen No. } Kn_p = 2\lambda / d_p$$

$$C_{Kn} = 1 + Kn_p\left[\alpha + \beta\exp\left(-\frac{\gamma}{Kn_p}\right)\right]$$

$\alpha = 1.257, \quad \beta = 0.4, \quad \gamma = 1.1 \quad$ (air)

$\alpha = 1.210, \quad \beta = 0.44, \quad \gamma = 0.92 \quad (CO_2) \longleftarrow$ (Radar, 1990)

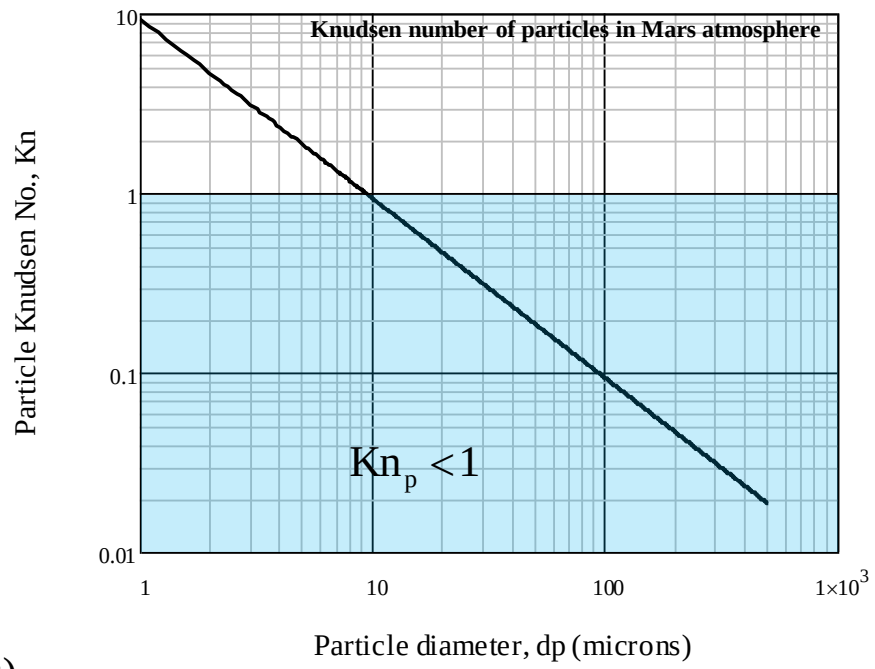

# Can We "Break" the FMPB?



- Yes!
  - In principle, non-uniform velocity (or pressure) field may lead to flow circulation inside the enclosure
- Preliminary CFD simulations (2014-105) illustrated the significance of taking advantage of viscosity in the FMBB and led to a design with a smaller gap thickness.

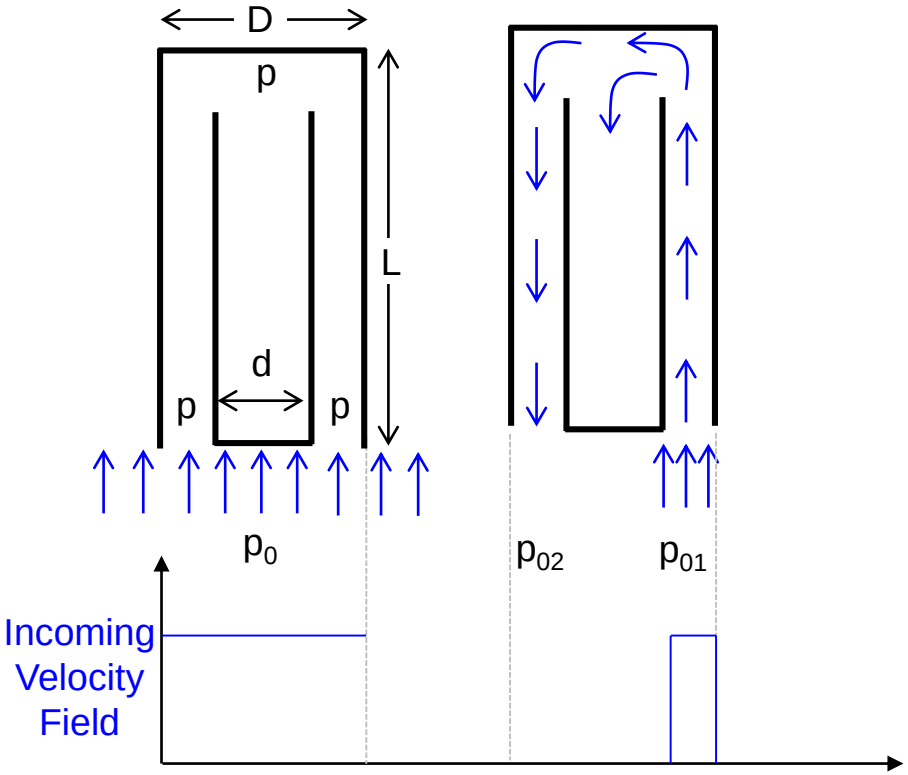


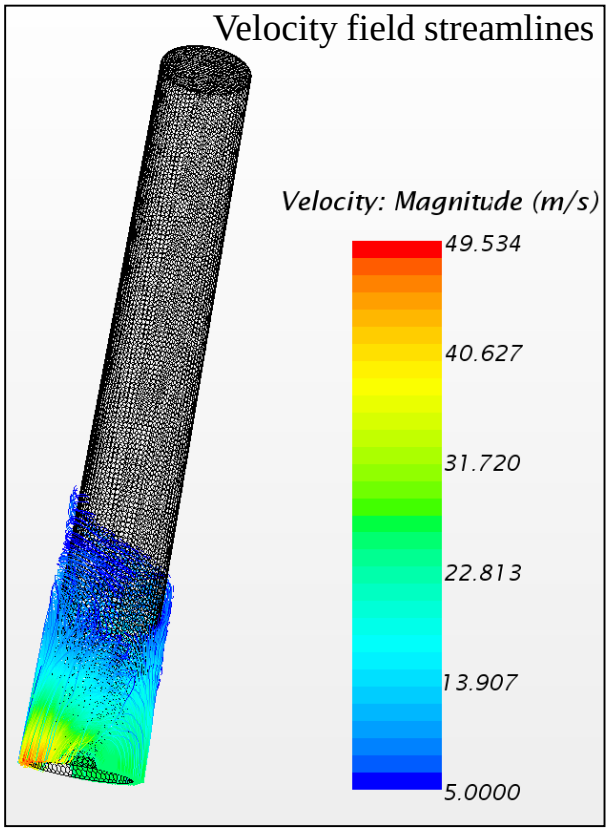


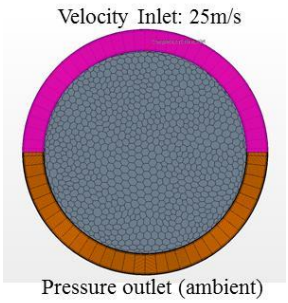


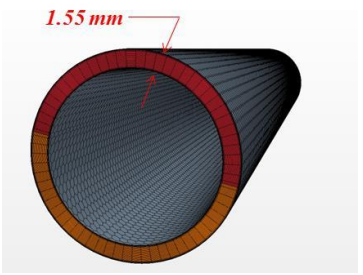

# Estimated Size and Velocity of Non-uniformities too Small to allow Asymmetric Flow into Cavity

Jet Propulsion Laboratory
California Institute of Technology

- Definitions
  - u=characteristic fluctuating velocity of largest eddies
  - v=characteristic fluctuating velocity of smallest eddies
  - L=characteristic size of largest eddies (integral scale)
  - $\ell_d$=characteristic size of smallest eddies (Kolmogorov scale)
  - μ=dynamic viscosity
  - Re=Reynolds number

$$\mathrm{Re} = \frac{\rho u L}{\mu} \qquad \frac{L}{\lambda} = \mathrm{Re}^{3/4} \qquad \frac{u}{v} = \mathrm{Re}^{1/4}$$

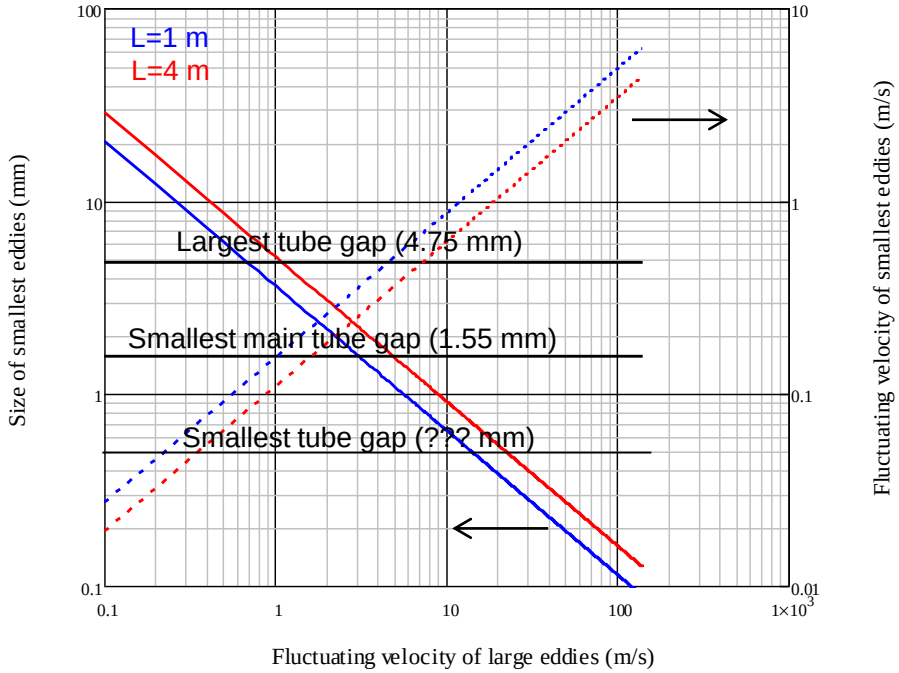


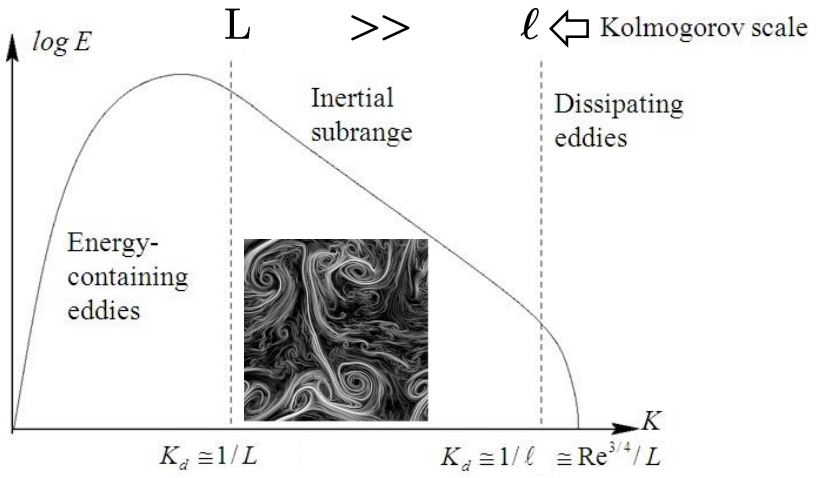


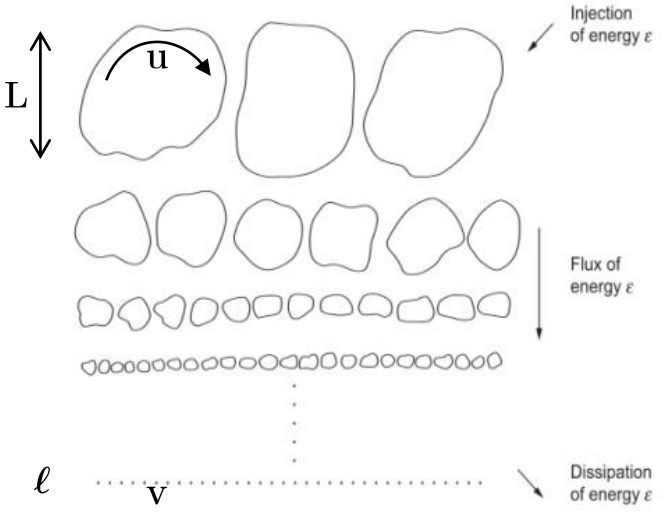

# Effects of size, shape and properties of biological particles.

Jet Propulsion Laboratory
California Institute of Technology

- **On particle size**: Analyses using validated first-principles analytical model with particles down to 0.15 microns show asymptotic penetration depth with decreasing particle size. This is because the particle speed adjusts almost instantaneously (compared to the characteristic filling time) to the flow velocity. Therefore, penetration of the smallest particles is driven by the evolution of the flow speed in O1 (which decreases in time as the FMPB is filled with ambient gas).

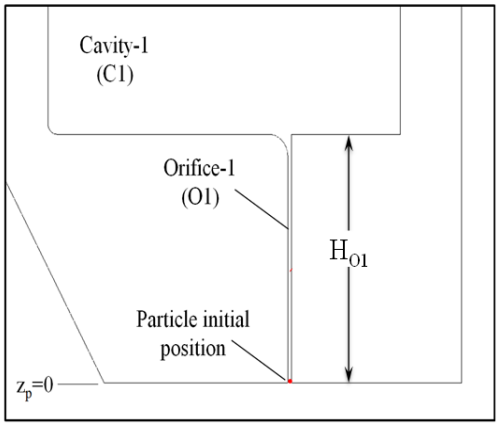


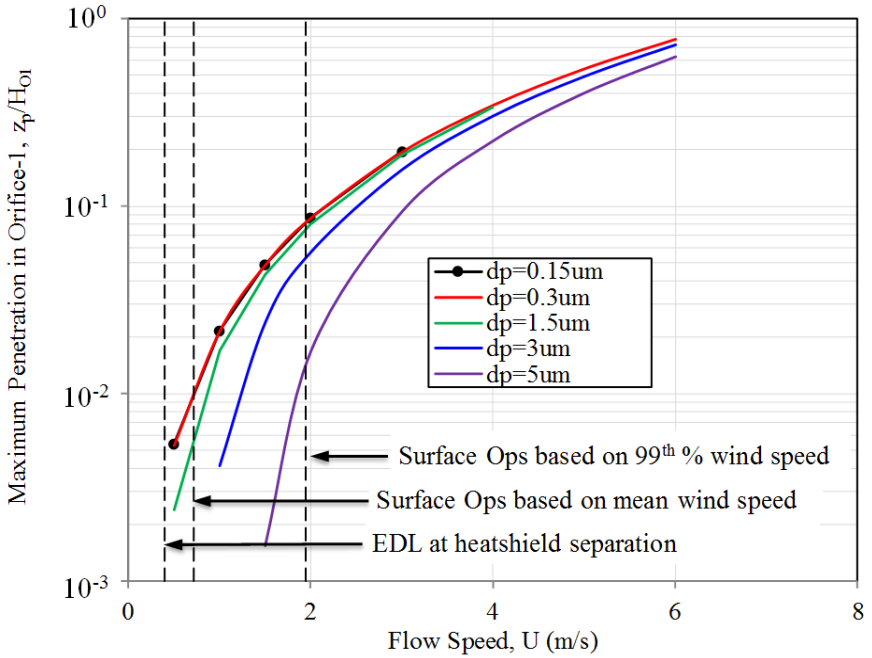


[1] I. G. Mikellides, A. D. Steltzner, B. K. Blakkolb, R. C. Matthews, K. A. Kipp, D. E. Bernard, M. Stricker, J. N. Bernardini, P. Shah and A. Robinson, "The Viscous Fluid Mechanical Particle Barrier for the Prevention of Sample Contamination on the Mars2020 Mission," Already Peer-Reviewed, to be accepted for publication in *Planetary and Space Sciences*, 4/2017.

# Effects of size, shape and properties of biological particles.



- **On particle size**: Analyses using validated first-principles analytical model with particles down to 0.15 microns show asymptotic penetration depth with decreasing particle size. This is because the particle speed adjusts almost instantaneously (compared to the characteristic filling time) to the flow velocity. Therefore, penetration of the smallest particles is driven by the evolution of the flow speed in O1 (which decreases in time as the FMPB is filled with ambient gas).

$$\frac{d\mathbf{u}_p}{dt} = \mathbf{F}'_D + \mathbf{g}$$ ← Equation of motion for particle under drag and grav. forces

$$\mathbf{F}'_D = k\left(\mathbf{V} - \mathbf{u}_p\right) \qquad k = \frac{g}{V_{Tp}}, \qquad V_{Tp} = \frac{\rho_p g d_p^2}{18\mu} C_{Kn}$$

Slip correction to Stokes law (a function of $d_p$)

Particle terminal velocity

$$z_p(t) = z_{p0} + \left(V_z - \frac{g}{k}\right)t + \left(\frac{\dot{z}_{p0} - V_z + \frac{g}{k}}{k}\right)\left(1 - e^{-kt}\right)$$

$$V_{Tp} \to 0: \qquad k \to \infty, \qquad z_p(t) \to V_z t$$

Solution of equation of motion in z for constant z-velocity flow field ($V_z$)

Note (1): $V_{Tp}(d_p=0.15\mu m)$=9.57e-9 m/s → k=39.7e7 /s, 1/k=2.5e-9 s
$V_{Tp}(d_p=0.30\mu m)$=76.0e-9 m/s → k=4.99e7 /s, 1/k=2.0e-8 s

Note (2): FMPB characteristic filling time ~ 0.01-0.1 s for $V_z$=2 m/s
Max characteristic flow speed in O1 ~ 0.001 m/s for $V_z$=2 m/s
Characteristic flow penetration depth based on max flow speed in O1: ~0.01-0.1 mm (HO1=5.6 mm)

# Effects of size, shape and properties of biological particles.

Jet Propulsion Laboratory
California Institute of Technology

- **On particle shape**: The drag coefficient for most irregularly shaped objects (bluff bodies) varies only by factors of 2-3 for subcritical flow at a fixed angle of attack. These factors are expected to be lower in our situation due to (1) slip effects (flow over these small particles is largely collision-less) and is already accounted for in our models, and (2) because particles also are rotating which tends to smooth out the details of shape irregularities. Regardless, the effects of these differences will be negligible for the FMPB since, per previous comment, particle penetration for these smaller particles is driven by how deep the flow itself penetrates.

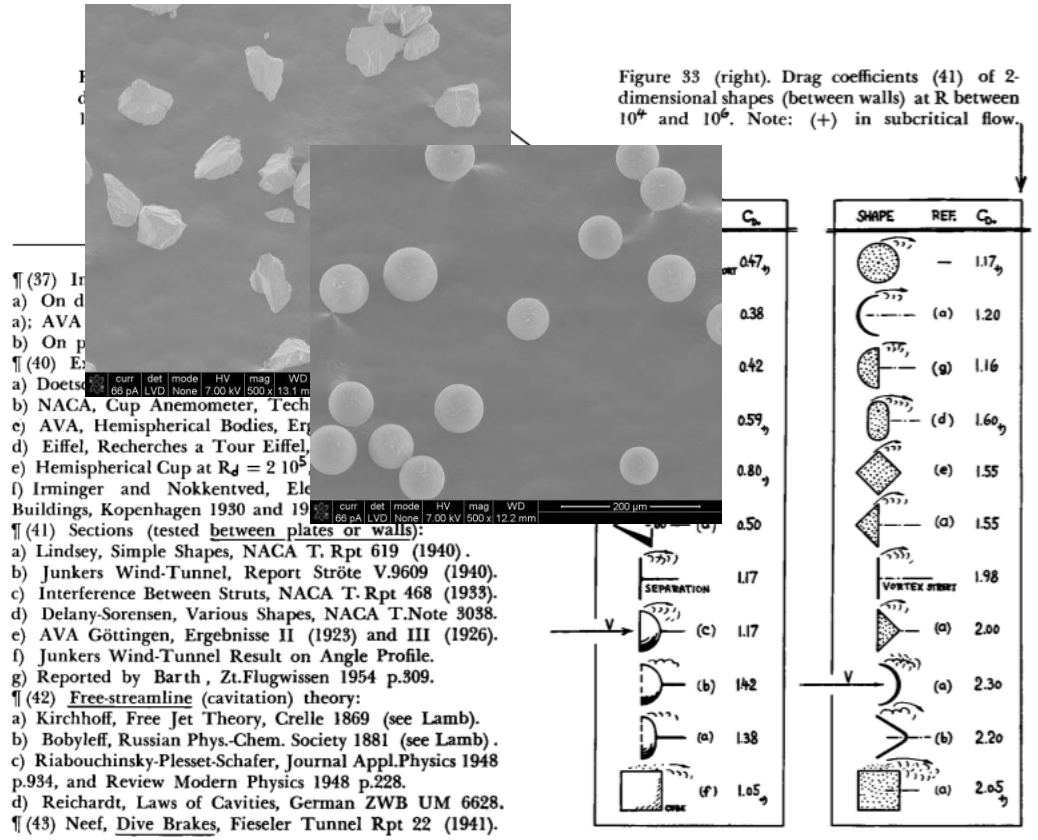

¶ (37) In
a) On d
a); AVA
b) On p
¶ (40) E
a) Doets
b) NACA, Cup Anemometer, Tech
c) AVA, Hemispherical Bodies, Er
d) Eiffel, Recherches a Tour Eiffel,
e) Hemispherical Cup at $R_d = 2\ 10^5$
f) Irminger and Nokkentved, Ele
Buildings, Kopenhagen 1930 and 19
¶ (41) Sections (tested between plates or walls):
a) Lindsey, Simple Shapes, NACA T. Rpt 619 (1940).
b) Junkers Wind-Tunnel, Report Ströte V.9609 (1940).
c) Interference Between Struts, NACA T. Rpt 468 (1933).
d) Delany-Sorensen, Various Shapes, NACA T.Note 3038.
e) AVA Göttingen, Ergebnisse II (1923) and III (1926).
f) Junkers Wind-Tunnel Result on Angle Profile.
g) Reported by Barth, Zt.Flugwissen 1954 p.309.
¶ (42) Free-streamline (cavitation) theory:
a) Kirchhoff, Free Jet Theory, Crelle 1869 (see Lamb).
b) Bobyleff, Russian Phys.-Chem. Society 1881 (see Lamb).
c) Riabouchinsky-Plesset-Schafer, Journal Appl.Physics 1948 p.934, and Review Modern Physics 1948 p.228.
d) Reichardt, Laws of Cavities, German ZWB UM 6628.
¶ (43) Neef, Dive Brakes, Fieseler Tunnel Rpt 22 (1941).

Figure 33 (right). Drag coefficients (41) of 2-dimensional shapes (between walls) at R between $10^4$ and $10^6$. Note: (+) in subcritical flow.




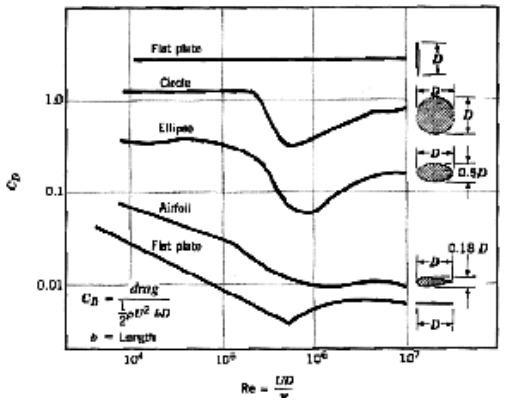


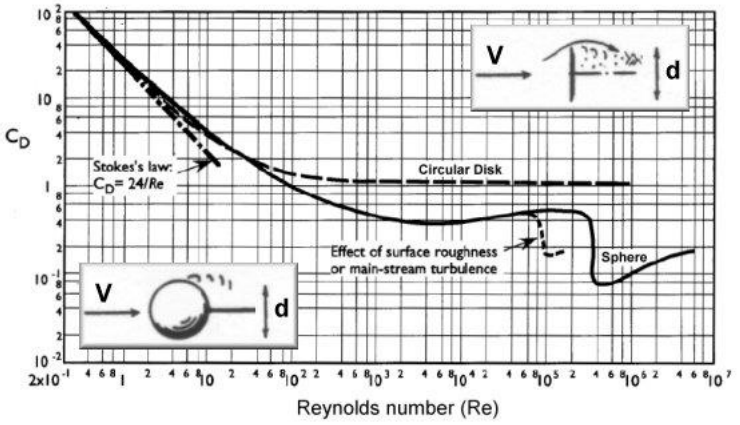

# Effects of size, shape and properties of biological particles.

Jet Propulsion Laboratory
California Institute of Technology

- **On particle properties**: A difference between inert (dust) and biological particles that may affect aerodynamic transport is mass density (dust particles ~ 2.5 g/cm3). Literature on mass density of spores (https://www.ncbi.nlm.nih.gov/pmc/articles/PMC244232/?page=3) indicates a representative range of 1.25-1.5 g/cm3. For penetration into the FMPB, the effect of these differences will be negligible for the smaller particles since particle penetration is driven by the flow penetration, per previous comment. We assume that biological particles are in a dry state upon arrival to Mars and therefore liquid layers around the microbe are not present.

APPLIED AND ENVIRONMENTAL MICROBIOLOGY, June 1982, p. 1307–1310 Vol. 43, No. 6
0099-2240/82/061307-04$02.00/0

## Wet and Dry Bacterial Spore Densities Determined by Buoyant Sedimentation†

L. S. TISA, T. KOSHIKAWA, AND PHILIPP GERHARDT*
*Department of Microbiology and Public Health, Michigan State University, East Lansing, Michigan 48824*

Received 24 August 1981/Accepted 14 March 1982

The wet densities of various types of dormant bacterial spores and reference particles were determined by centrifugal buoyant sedimentation in density gradient solutions of three commercial media of high chemical density. With Metrizamide or Renografin, the wet density values for the spores and permeable Sephadex beads were higher than those obtained by a reference direct mass method, and some spore populations were separated into several density bands. With Percoll, all of the wet density values were about the same as those obtained by the direct mass method, and only single density bands resulted. The differences were due to the partial permeation of Metrizamide and Renografin, but not Percoll, into the spores and the permeable Sephadex beads. Consequently, the wet density of the entire spore was accurately represented only by the values obtained with the Percoll gradient and the direct mass method. The dry densities of the spores and particles were determined by gravity buoyant sedimentation in a gradient of two organic solvents, one of high and the other of low chemical density. All of the dry density values obtained by this method were about the same as those obtained by the direct mass method.

# Effectives of FMPB During Diurnal Cycles on Mars

Jet Propulsion Laboratory
California Institute of Technology

- Diurnal temperature range: 184 K to 242 K (-89 to -31 C) (Viking 1 Lander site), but pressure variations small: $\Delta p < 30$ Pa

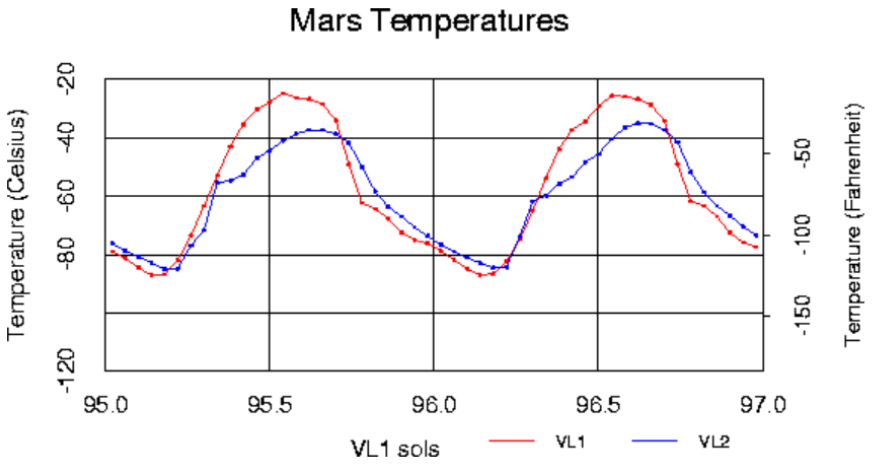


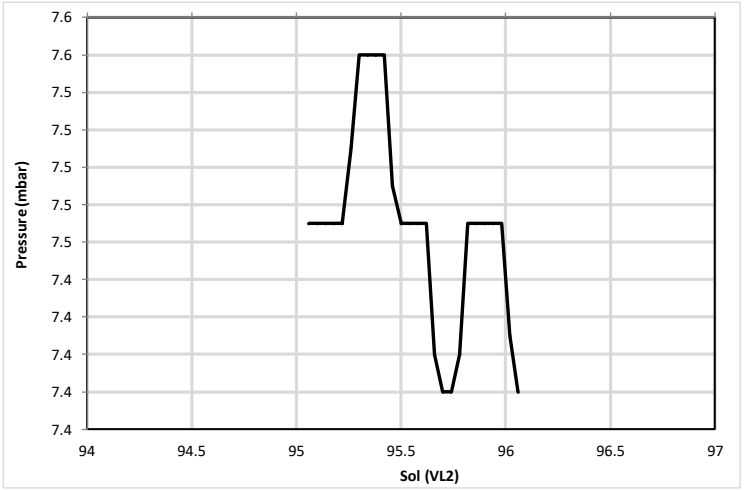


The Mars Pathfinder Atmospheric Structure Investigation/Meteorology (ASI/MET) Experiment

J. T. Schofield, J. R. Barnes, D. Crisp, R. M. Haberle, S. Larsen, J. A. Magalhães, J. R. Murphy, A. Seiff, G. Wilson

The Mars Pathfinder atmospheric structure investigation/meteorology (ASI/MET) experiment measured the vertical density, pressure, and temperature structure of the martian atmosphere from the surface to 160 km, and monitored surface meteorology and climate for 83 sols (1 sol = 1 martian day = 24.7 hours). The atmospheric structure and the weather record are similar to those observed by the Viking 1 lander (VL-1) at the same latitude, altitude, and season 21 years ago, but there are differences related to diurnal effects and the surface properties of the landing site. These include a cold nighttime upper atmosphere; atmospheric temperatures that are 10 to 12 degrees kelvin warmer near the surface; light slope-controlled winds; and dust devils, identified by their pressure, wind, and temperature signatures. The results are consistent with the warm, moderately dusty atmosphere seen by VL-1.

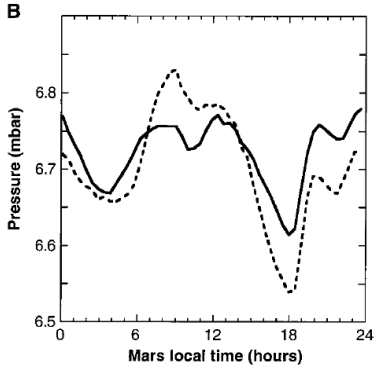


**Fig. 3.** (**A**) Time-averaged surface pressures measured by the MET instrument over the first 30 sols of the Pathfinder landed mission. The averages are primarily over the 3-min default measurement sessions, of which there are nominally 51 per sol; and the resulting points have been connected with straight lines, except for sols 12 through 15, where cubic spline interpolation has been used to fill data gaps of about 8 hours in length. MET operation was restricted to nighttime observations during this period to prevent spacecraft resets associated with MET data collection. The major gaps in the data set at sols 1, 8, 11, and 17 are caused by various spacecraft software reset and downlink problems. After sol 17, the reset problems associated with MET were corrected, and continuous sampling was resumed. The long-term trend in pressure is represented by a third-order polynomial fit to the data (solid curve). (**B**) Diurnal pressure cycles for sols 9 (solid line) and 19 (dashed line), illustrating the observed day-to-day changes in the diurnal pressure cycle and allowing details of the daily pressure variation to be seen more clearly.

# Effectives of FMPB During Diurnal Cycles on Mars, continued.

Jet Propulsion Laboratory
California Institute of Technology

- Typical diurnal cycle variations of pressure used to estimate range of time scales associated with pressure changes that could be relevant to the FMPB operation.
- Noted: Rate of pressure changes do not exceed 0.003 Pa/s. Assume 0.01 Pa/s to be conservative.

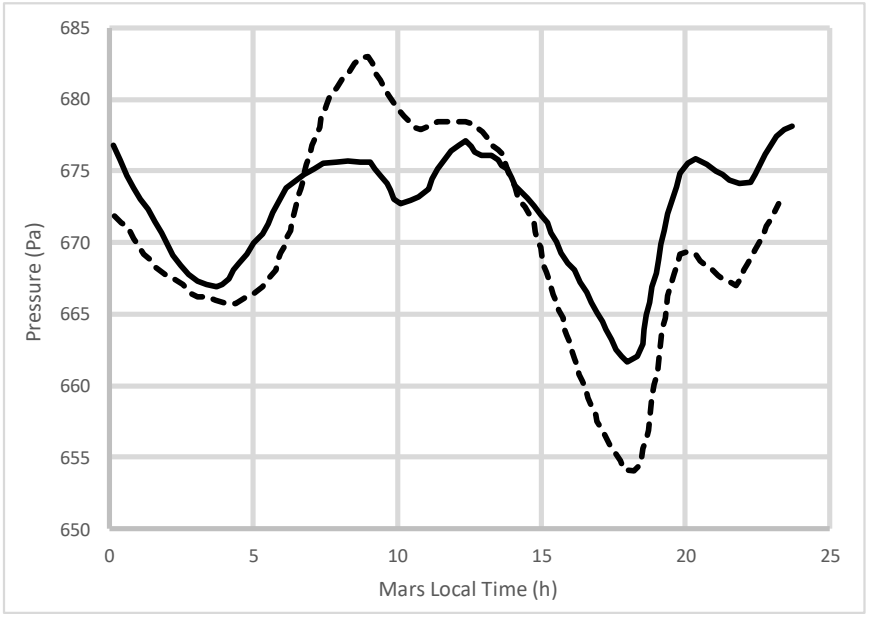


Data from Mars Pathfinder (Schofield, et al.) reproduced

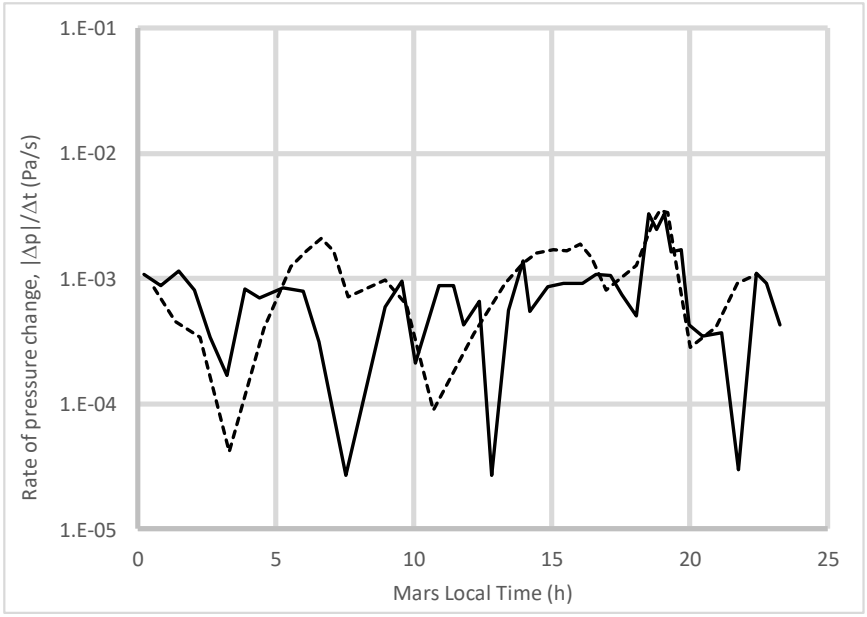


Data from Mars Pathfinder (Schofield, et al.) used to determine rate of change of pressure

# Effectives of FMPB During Diurnal Cycles on Mars, continued.



- Typical variations of pressure in the FMPB associated with its “filling time,” the characteristic time it takes the interior and exterior pressures to reach pressure equilibrium ($\Delta p=0$). Once in equilibrium, no flow (and therefore no particles) can be driven into the FMPB.
- Noted: Typical filling times in the order of a second for flow of 10 m/s, which corresponds to dynamic pressure of $\Delta p \sim 1.1$ Pa.

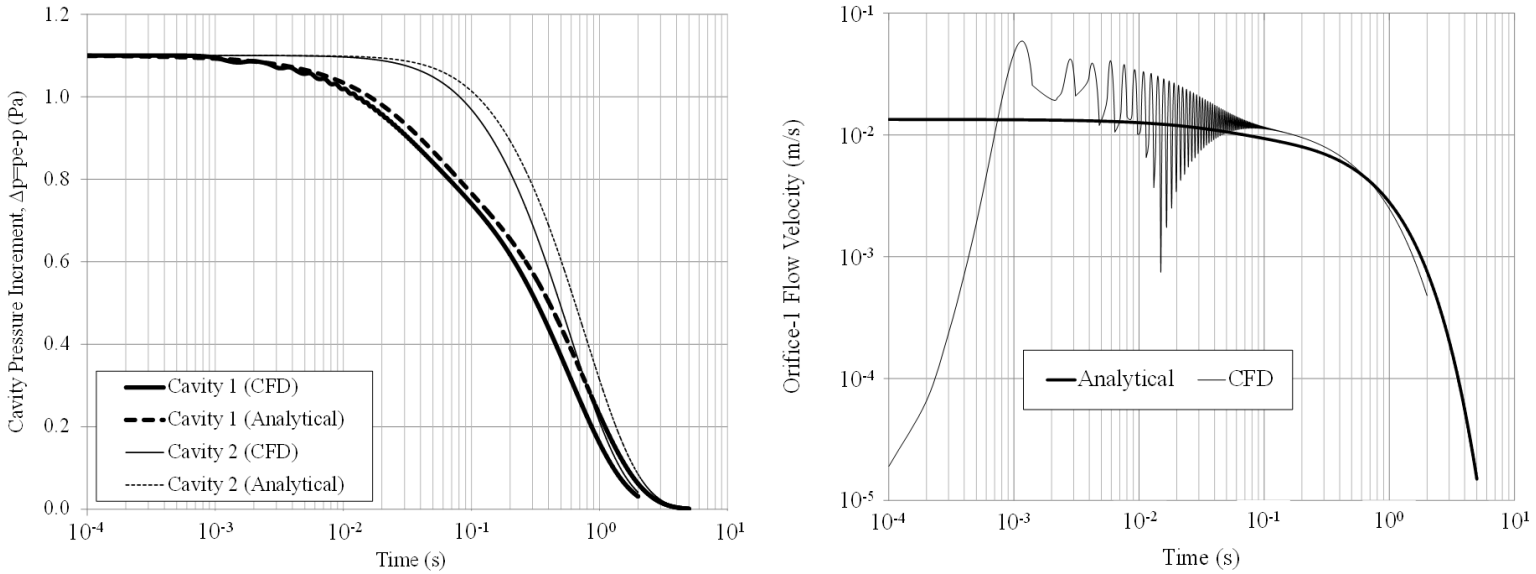


Fig. 6. Comparisons between the analytical solution (Sec.2.2) and the result from 2-D axisymmetric simulation (Sec.2.3) of the FMPB pressurization at U=10 m/s. Left: volume-averaged pressures midway through cavities 1 and 2. The analytical solution is given by Eq. (11). Right: mass-flow-averaged flow velocity at the exit of O1. The analytical solution is given by Eq. (12).

# Effectives of FMPB During Diurnal Cycles on Mars, continued.



- Particle penetration depth plotted as a function of pressure difference across FMPB (bottom right) to allow for estimates on the effect of the diurnal pressure changes.
- Conclusion: 0.15-micron particle penetration depth approximately 2% the height of O1 at Δp=0.01 Pa.

Δp associated with diurnal cycle fluctuations within FMPB filling times (<0.01 Pa)

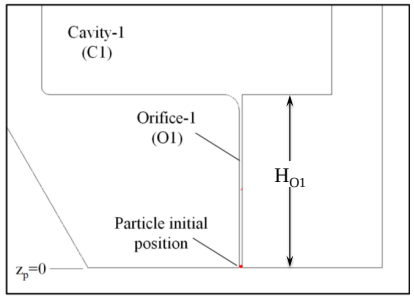


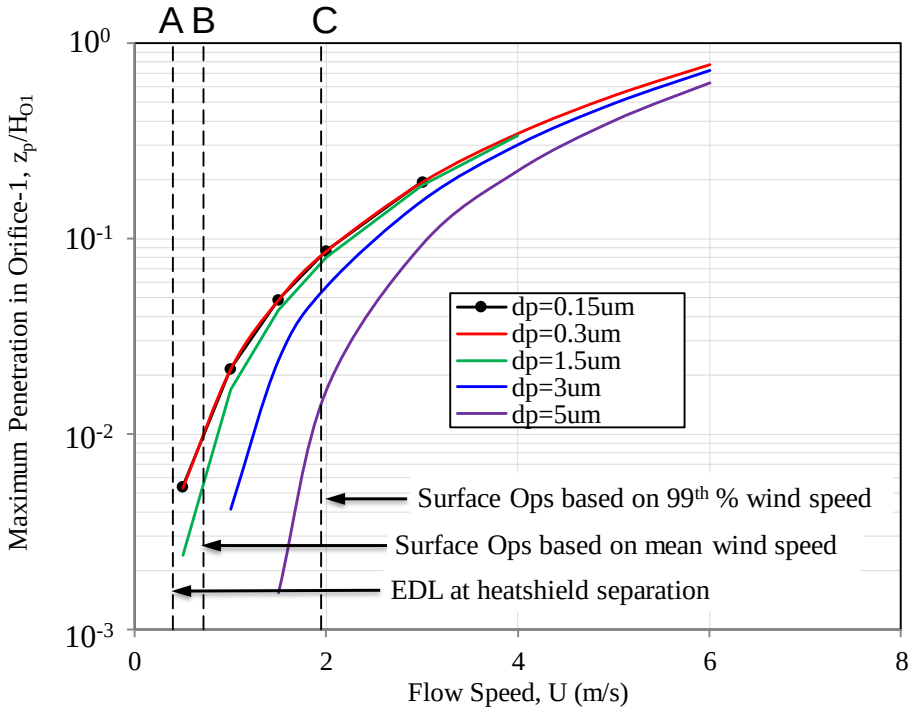


Particle penetration depth as a function of applied flow speed (from Mikellides, et al.).

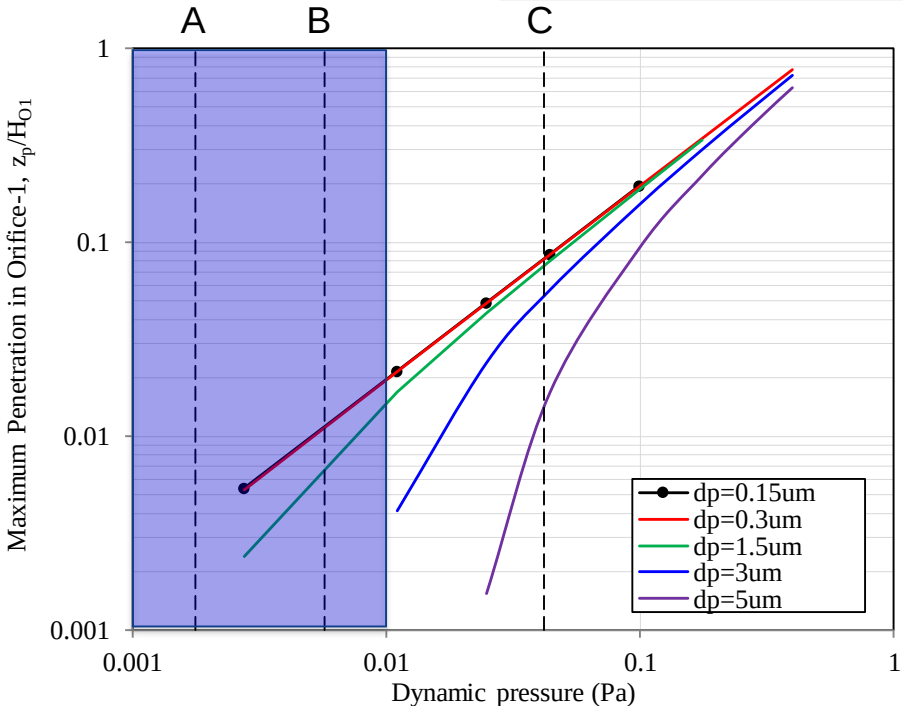


Particle penetration depth as a function of equivalent dynamic pressure (same result as in left figure but plotted against dynamic pressure)

# Flow through FMBB gap largely collision-less prior to heat shield separation.

Jet Propulsion Laboratory
California Institute of Technology

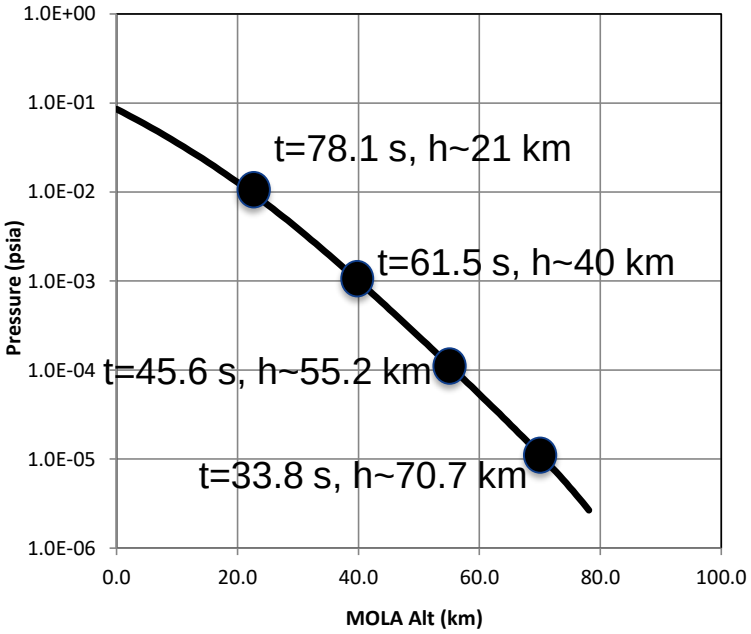


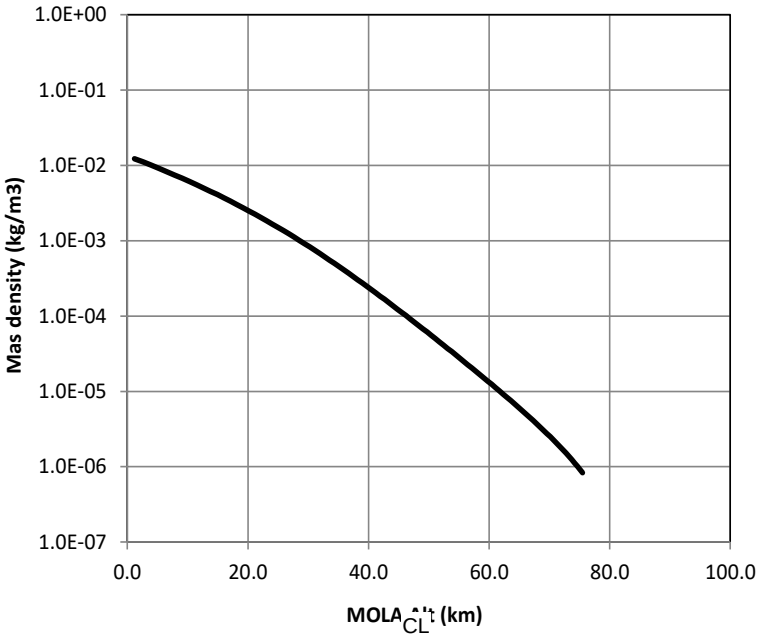


- Characteristic size:
  - FMBB gap thickness b=400 μm
- Knudsen Numbers
  - h~0 km (ρ=1.00e-2 kg/m3): Kn=0.02
  - h=21 km (ρ=2.20e-3 kg/m3): Kn=0.12
  - h=40 km (ρ=2.25e-5 kg/m3): Kn=11.4
  - h=55 km (ρ=2.75e-5 kg/m3): Kn>1
  - h=71 km (ρ=2.05e-6 kg/m3): Kn>>1

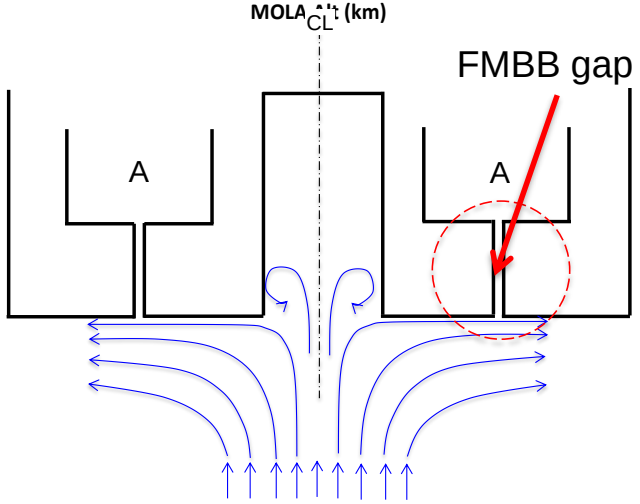

# Can speeds in FMBB gap be large enough to release particles from the gap surface?

Jet Propulsion Laboratory
California Institute of Technology

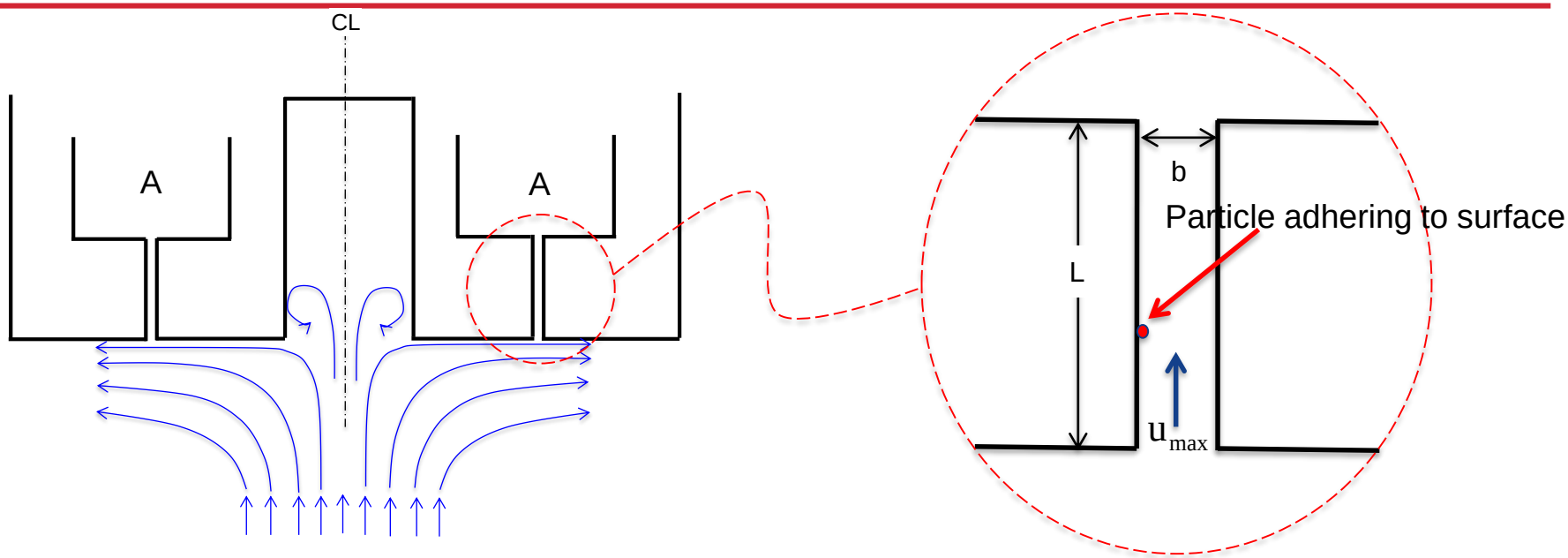


Flow through gap collision-less (no viscous reduction of gap speeds)

→Clausing factor K' for long short rectangular aperture (a>>b, a>>L, L>>b)

$$Q = uA = \frac{\dot{m}}{\rho} = \frac{K'}{\rho}\frac{A\Delta p}{\sqrt{2\pi RT}}, \quad A = ab$$

$$\rightarrow u = \frac{K'}{\rho}\frac{\Delta p}{\sqrt{2\pi RT}}, \quad K' = \frac{b}{L}\lambda n\left(\frac{L}{b}\right) = 0.19$$

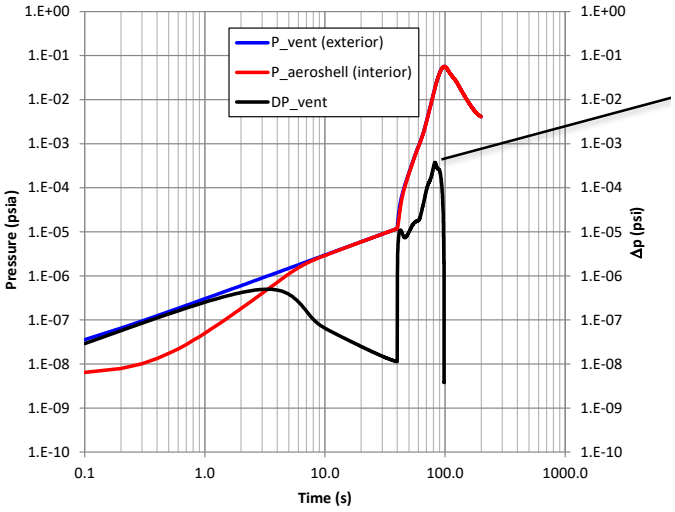


Max Δp~5e-4 psi
=3.45 Pa
at ~ 80 s (h=21 km)

$$u_{max} \approx 0.4 \text{ m/s}$$

# Stokes drag force on particles significantly diminished in collision-less flow over them.

Jet Propulsion Laboratory
California Institute of Technology

- Kn Corrections. When the particle diameter $d_p$ becomes comparable to the mean free path of particles making up the flow, the resisting force entered by the fluid is smaller that that predicted by Stokes' law. To account for non-continuum (slip) effects the following (empirical) correction factor is applied to Stokes drag force also known as the Cunningham correction factor:

Stokes drag force

$$F_D = \frac{3\pi\mu_\infty d_p V_\infty}{C_{Kn}} = \frac{F_{D_S}}{C_{Kn}}$$

$$\text{Fluid mfp } \lambda = \left(\pi\sqrt{2} n_\infty d_{CO_2}{}^2\right)^{-1}$$

$$\text{Knudsen No. } Kn_p = 2\lambda / d_p$$

$$C_{Kn} = 1 + Kn_p\left[\alpha + \beta \exp\left(-\frac{\gamma}{Kn_p}\right)\right]$$

$\alpha = 1.257, \quad \beta = 0.4, \quad \gamma = 1.1 \quad$ (air)

$\alpha = 1.210, \quad \beta = 0.44, \quad \gamma = 0.92 \quad (CO_2)$ ← (Radar, 1990)

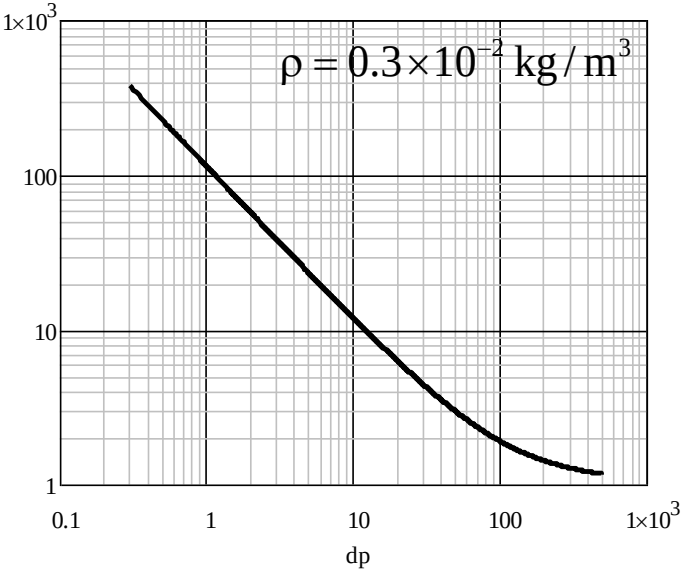

# Resuspension of particles from the FMBB surface



- Particles overcome adhesion to surface when hydrodynamic moment exceeds moment of adhesion
- At u=0.4 m/s, particles >100 μm may be released from interior gap surface. Smaller particles will continue to adhere to surface
- But terminal velocity of >100 μm particles is >0.8 m/s, so these particles will fall under gravity.
- Moreover, collision less flow velocity significantly diminishes once flow enters FMBB reservoir (see below), so even some particles make it through the gap they will fall once in the reservoir.

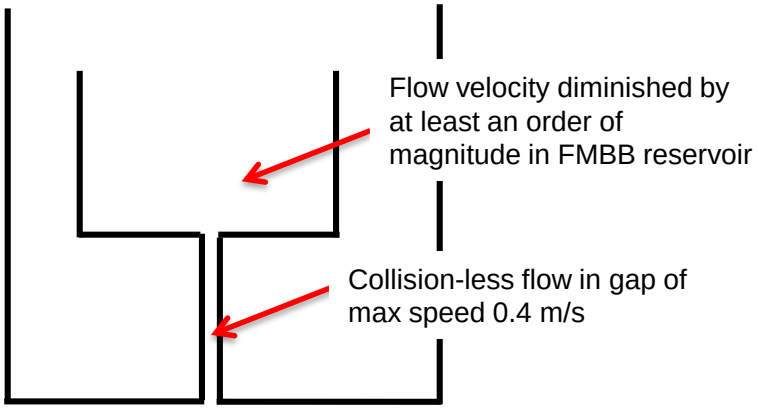


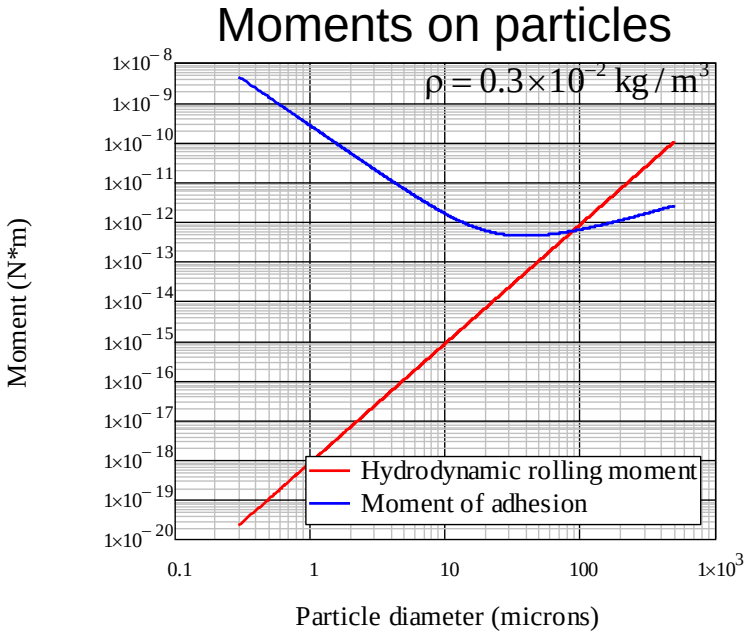


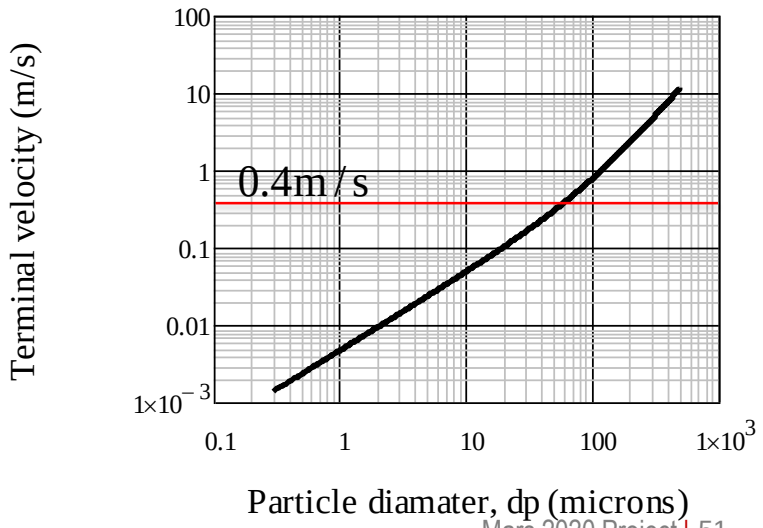

# Summary remarks



- Question: Can particles on the FMBB gap surface be released and propagate into the sample tubes during EDL, prior to heat shield separation?

- Comments:
- Based on pressurization history from entry interface to parachute release, the maximum $\Delta p$ in the aeroshell does not exceed 3.45 Pa. In the ACA, where the FMBBs reside, this will be even less, so choice of 3.45 Pa is conservative.
- Based on ambient conditions when $\Delta p$=3.45 Pa, flow through the gap is collision-less, thus viscosity does not diminish flow speeds. Estimated maximum flow velocity is 0.4 m/s.
- At this speed, the moment of adhesion is smaller than the hydrodynamic moment of particles for particles larger than ~100 $\mu$m; these particles then in principle can come off the surface. But they will immediately fall since their terminal velocity is larger than 0.4 m/s.
- Even if some particles make it to the top of the gap they will fall since the velocity diminishes rapidly (~open area ratio) once flow enters the FMBB reservoir.

- Answer: No.

# Response to Q6 (b)

## On planned tests with FMPB in vacuum chamber, with particles.



- Q6: …*(b) Is the project planning to take a cleaned engineering model FMPB, place it into a vacuum chamber with dust and microbes, and run several cycles of evacuation and re-pressurization of the chamber before checking the cleanliness of the interior of the FMPB?*

- Response: NO.
- Justification:
  - As is the case for many engineering problems, an FMPB test with particles in Mars atmosphere belongs to the category of full-scale tests in a relevant environment that, though preferred, are both challenging and unnecessary. Flight qualification of commercial and military aircraft, certification of nuclear weapons, and Mars EDL are a few large-scale examples in this category for which the combination of only limited testing, typically with scaled-down engineering models, and physics-based modeling and simulations carries sufficiently low risk.
  - Why unnecessary?
    - The prediction of particle penetration into the FMPB requires (1) prediction of the flow-field around and inside the FMPB under nominal conditions and (2) prediction of the forces on the particles, both of which are amenable to predictive physics-based analyses. In [11] we demonstrated both (1) and (2).
    - For off-nominal scenarios that are not easily amenable to analyses, such as flow instabilities and turbulence around the FMPB opening on Mars, a flow test is indeed necessary. It is well-known (for over a century) that if flow similarity can be established, the physics of such flows in the non-terrestrial environment can be exactly replicated in a terrestrial-flow tunnel. The results from a Mars-similar water tunnel test, aimed at demonstrating the feasibility of the FMPB to prevent particle penetration under such off-nominal scenarios, also were reported in [11].

# Flow Through Porous Media



- Volumetric rate (or velocity) of viscous flow though porous media determined by Darcy's law, when Re<10 and Kn<<1
- When Re>10, correction leads to the Darcy-Forchheimer Law to account for inertia effects
- When Kn$\gtrsim$0.1, a correction must be made (per below) according to Cunningham and Williams, 1980, p. 51
  - $u_p$=flow velocity through porous media (m/s)
  - K=permeability ($m^2$)
  - $\mu$=dynamic viscosity (Pa-s)
  - $D_s$=Slip diffusion coefficient ($m^2$/s)
  - $D_K$=Knudsen diffusivity ($m^2$/s)
  - Kn=Knudsen number
  - C_bar=average thermal speed of gas (m/s)

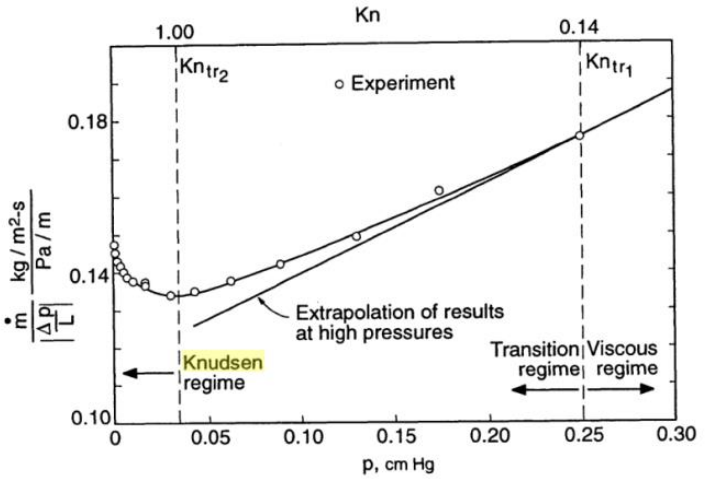


**Figure 6.1** The results of Knudsen experiment showing the mass flow rate through a bundle of capillary tubes at various absolute pressures. (From Cunningham and Williams, reproduced by permission ©1980 Plenum.)

Viscous flow (Darcy's Law (Kn<<1)) | Slip flow (Kn~1) | Knudsen flow (Kn>>1)

$$u_p = -\frac{K}{\mu}\frac{dp}{dx} - \frac{4}{3}(1-\alpha)D_s\frac{1}{p}\frac{dp}{dx} - \alpha D_K\frac{1}{p}\frac{dp}{dx}$$

$$= -\frac{dp}{dx}\left[\frac{K}{\mu} + \frac{4}{3}(1-\alpha)\frac{D_s}{p} + \alpha\frac{D_K}{p}\right]$$

$$\alpha \equiv \frac{Kn}{1+Kn}, \qquad D_s = \pi R_p\frac{\bar{c}}{8}, \qquad D_K = C_K\sqrt{p/\rho}\ \left(C_K \approx 7\times10^{-7}\,m\right)$$

Measured by Gunn & King for a fritted-glass filter

55 The technical data in this document are controlled under the U.S. Export Regulations. Rele

# Average Velocity in FMBB Gap at Mars Conditions Relevant to Mars2020 ($\lesssim$10 m/s)



- Extrapolate from high-speed measurements to low speeds using scaled Poiseuille law

$$u(R) = \frac{\alpha}{4\mu}\frac{\Delta p}{H}\left[\frac{\ln\left(\frac{R}{r_1}\right)}{\ln\left(\frac{r_2}{r_1}\right)}\left(r_2^2 - r_1^2\right) - \left(R^2 - r_1^2\right)\right] = \alpha C u_M^2$$

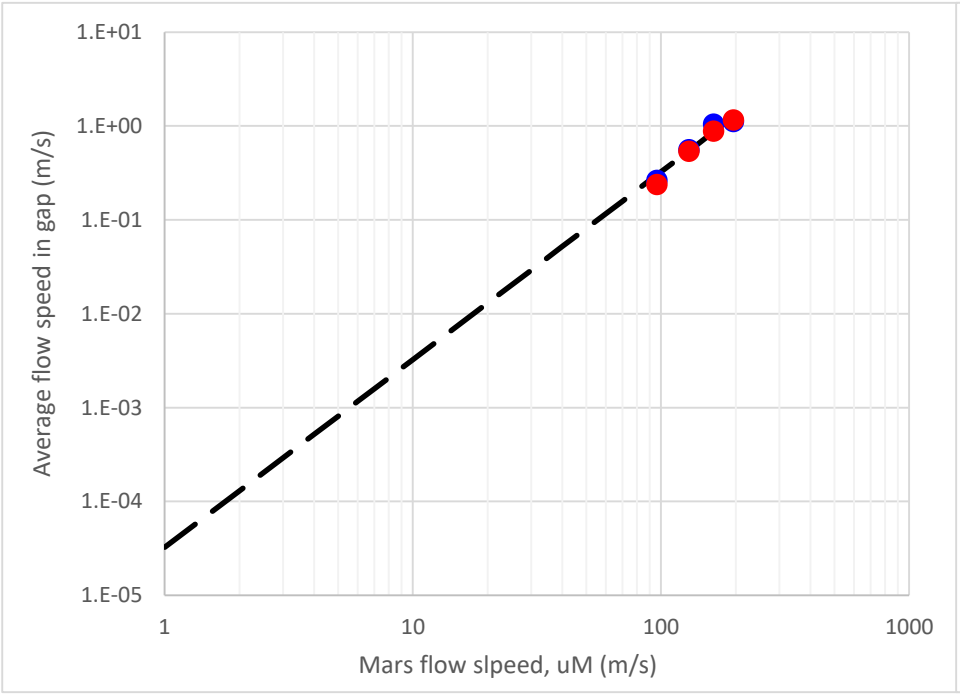


θ=30 deg

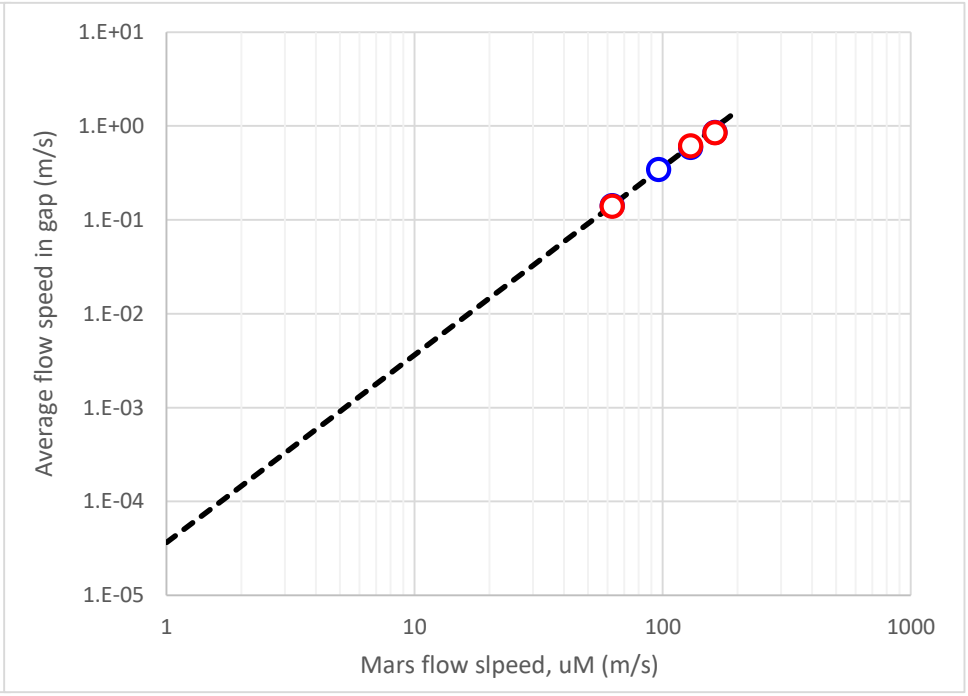


θ=45 deg

# Introductory Information

## — Particle Transport Analysis for Contamination Assessments on Mars Requires Knowledge of the Aerodynamic Loads —

Jet Propulsion Laboratory
California Institute of Technology

- Natural wind conditions during surface operations
  - Nominal
    - 99%-wind speed = 15.3 m/s
    - 70%-wind speed = 5.7 m/s
  - Off-nominal (momentary events)
    - Wind speed during dust storms: up to 40 m/s
    - Rotational speed of dust devils: up to 60 m/s
- Induced flow speeds over rover during EDL
  - Up to 170 m/s at bottom and sides of rover at high altitudes
  - Excess of 60 m/s on top of rover during MLE interactions with ground (courtesy of CFD sims by NASA Langley)

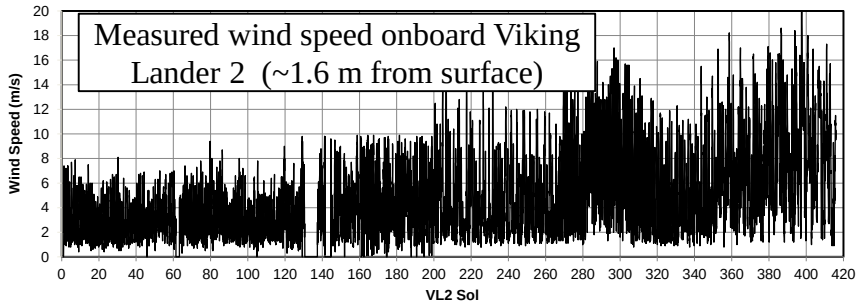


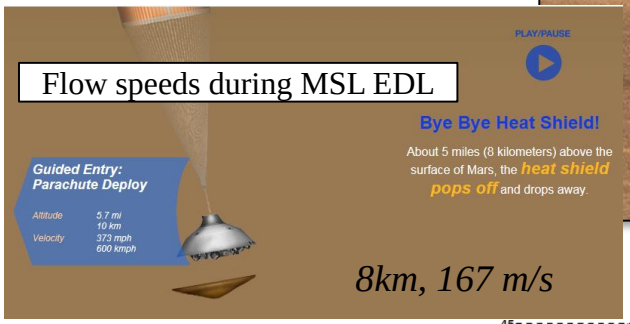

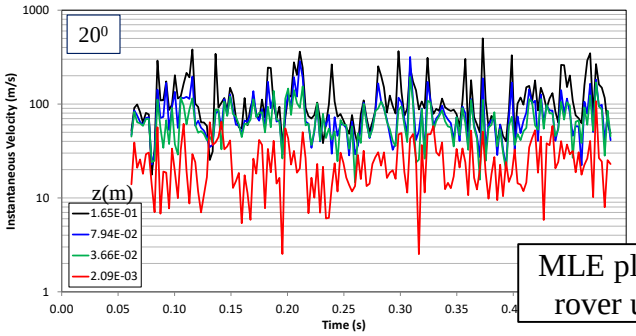


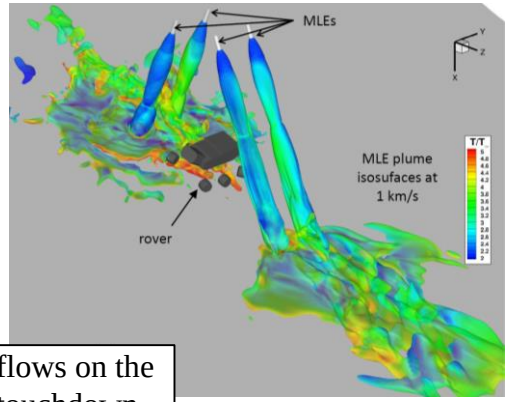


MLE plume flows on the rover upon touchdown

Ambient winds as a function of altitude at Site 1

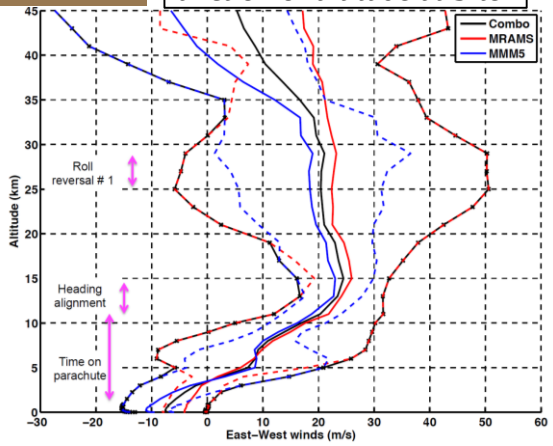

# Introductory Information

## — Particle Transport Analysis for Contamination Assessments Requires environments —



- Consider adding chart here about low density, low humidiy and other rekevant Mars conditons that affect the biology (dry, dead)

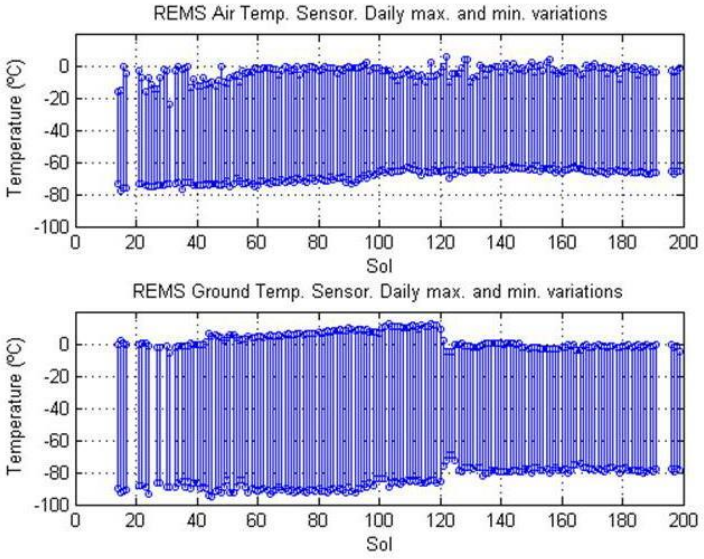


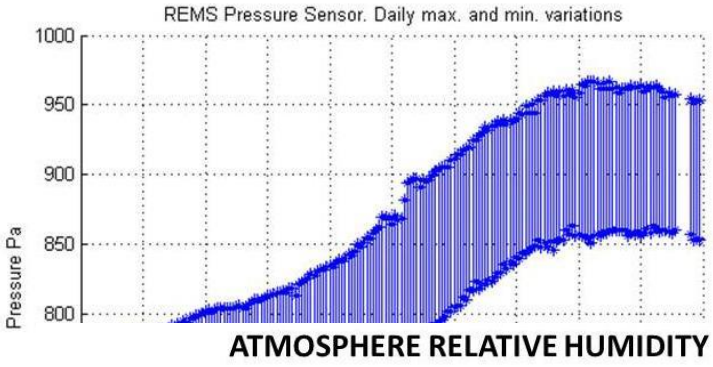


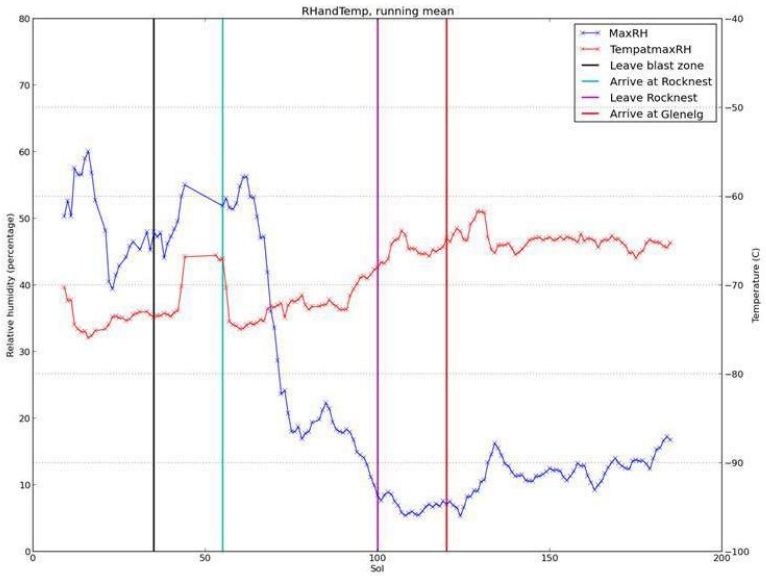


**Curiosity rover – Temperature, Pressure, Humidity at Gale Crater on Mars (August 2012 – February 2013)**

NASA/JPL-Caltech/CAB(CSIC-INTA)/FMI/Ashima Research

# Flow into a Large Cavity Closed at One End: Operational Principle of the Inviscid FMBB

Jet Propulsion Laboratory
California Institute of Technology

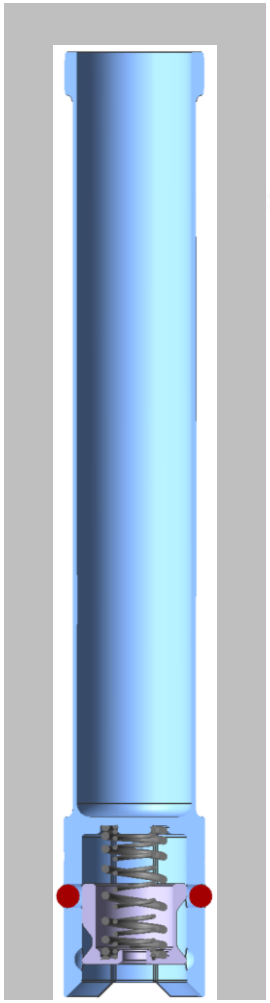

**"Sustained Wind" Scenario:**
**Tubes in the Mars atmosphere exposed to direct winds**

$$p_0 = p + \Delta p \quad (\Delta p = \tfrac{1}{2}\rho u^2)$$

$$u_{70\%} = 5.7 m/s,\ u_{99\%} = 15.3 m/s$$

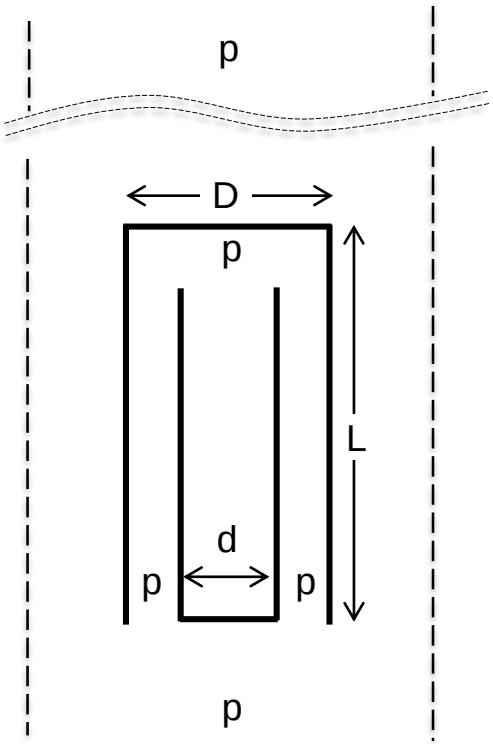


Initial State

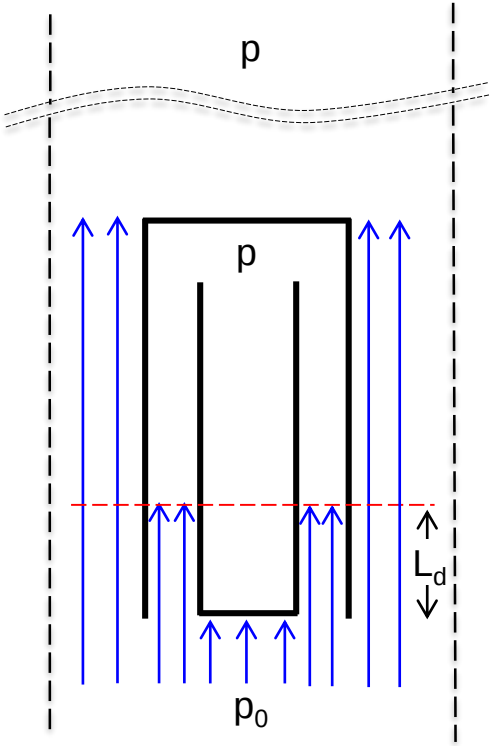


Transient State

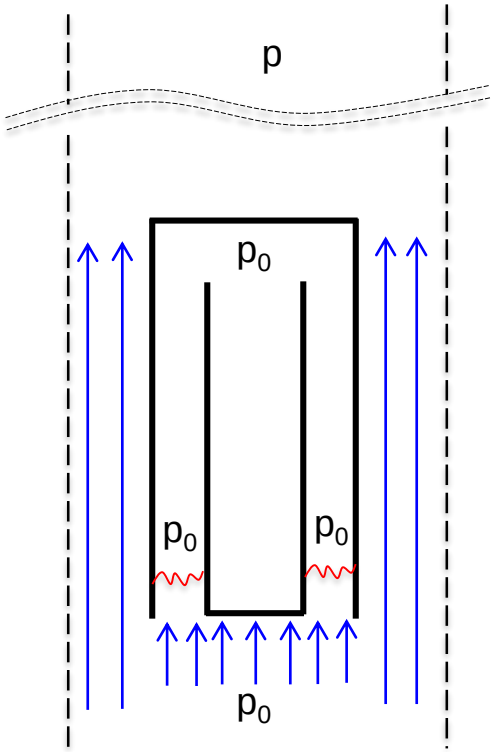


Steady State

The technical data in this

# Flow into a Large Cavity Closed at One End: Operational Principle of the Inviscid FMBB

Jet Propulsion Laboratory
California Institute of Technology

**"Pressurization" Scenario:**
**Tubes in an enclosure suddenly opened/exposed to a higher-pressure environment**

$$p_0 = p + \Delta p \quad (\Delta p = \tfrac{1}{2}\rho u^2)$$
$$(0.17 < u < 0.29\ m/s)$$

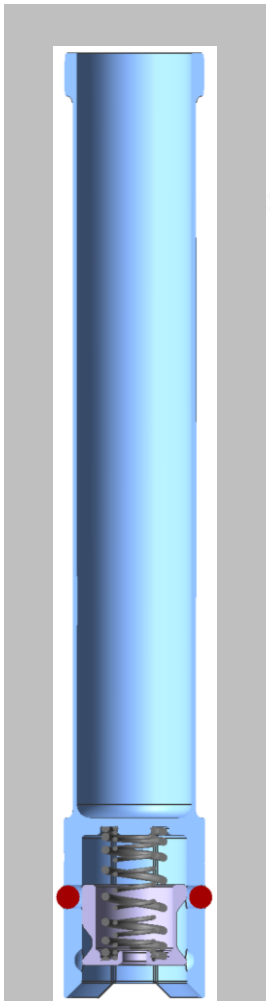

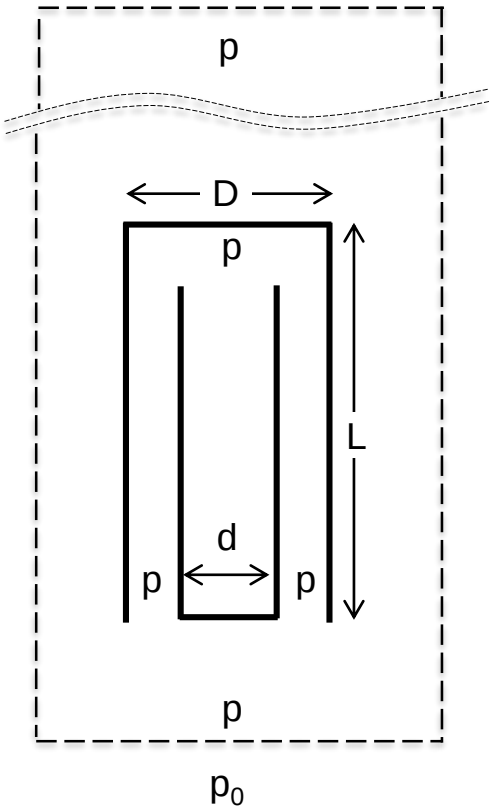


**Initial State**

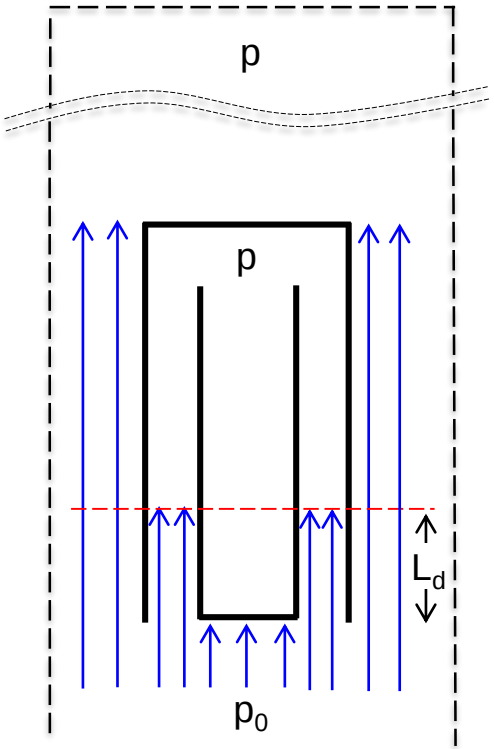


**Transient State**

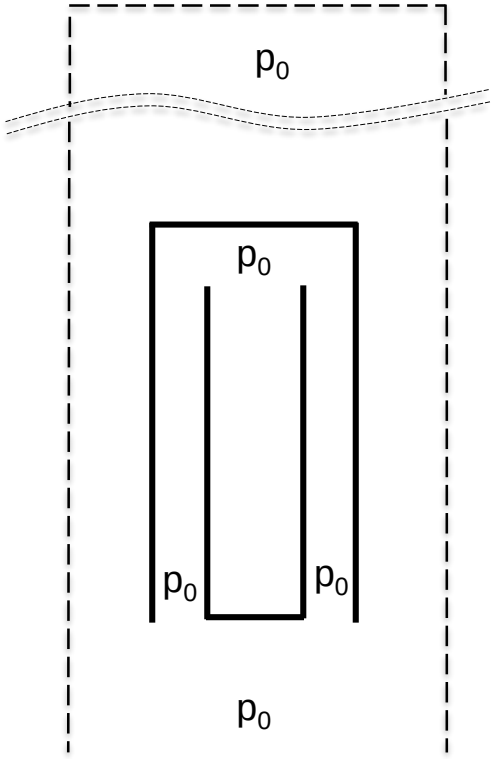


**Steady State**

# Introductory Information
## —The Mars 2020 Mission—

Jet Propulsion Laboratory
California Institute of Technology

- The Mars 2020 mission is part of NASA's Mars Exploration Program, a long-term effort of robotic exploration of the Red Planet.
  - Will leverage the proven design and technology developed for the 2011 Mars Science Laboratory (MSL) mission and rover (Curiosity) that arrived at Mars in August 2012.
  - Will fly with new payload elements to meet described science objectives and human exploration measurement goals, within agency and flight system resource constraints.
  - Will be launched sometime between 16 July and 4 August 2020.
- The Mars 2020 mission will deliver a rover to the surface of Mars
  - Will be designed to take scientific *in situ* measurements on Mars
  - Will acquire, encapsulate, and cache individual scientifically selected samples of martian material for possible return to Earth by a subsequent mission.

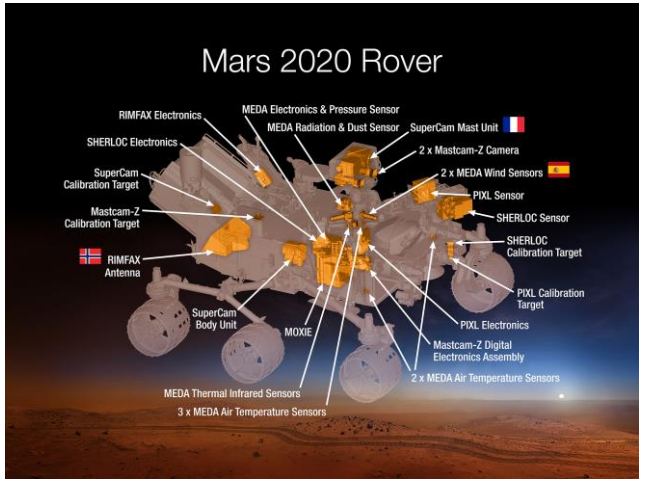

# Sample Tubes, Seals, Coring Bits

Jet Propulsion Laboratory
California Institute of Technology

***Tube Exterior***
*(unsealed)*

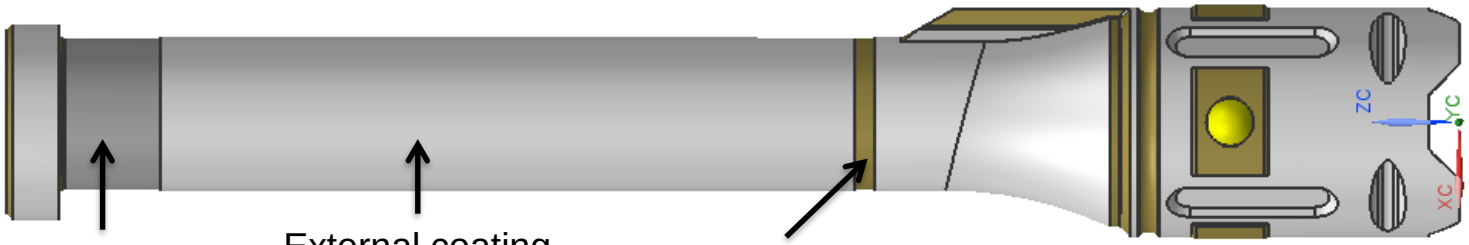


Bare Titanium

External coating
*(Alumina)*

Tube Body
*(Nitrided Ti-6Al-4V)*

***Tube Interior***
*(sealed)*

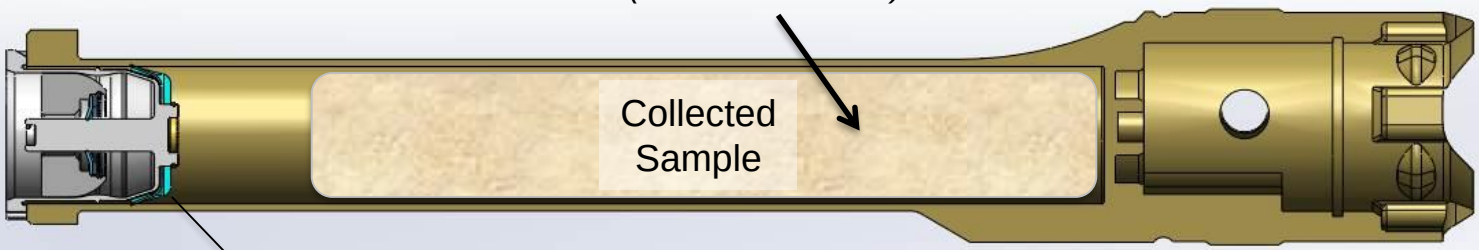


**Hermetic Seal**

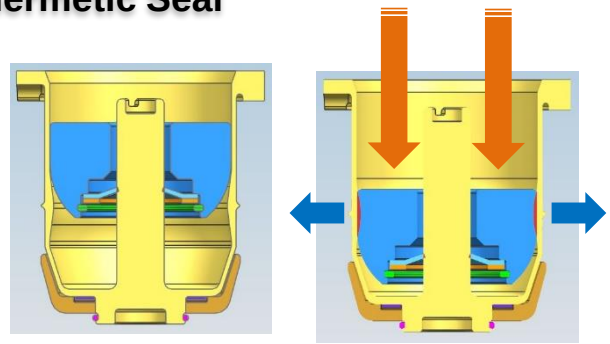

Pre-Activation

Post-Activation

***Sample Tube in Coring Bit***

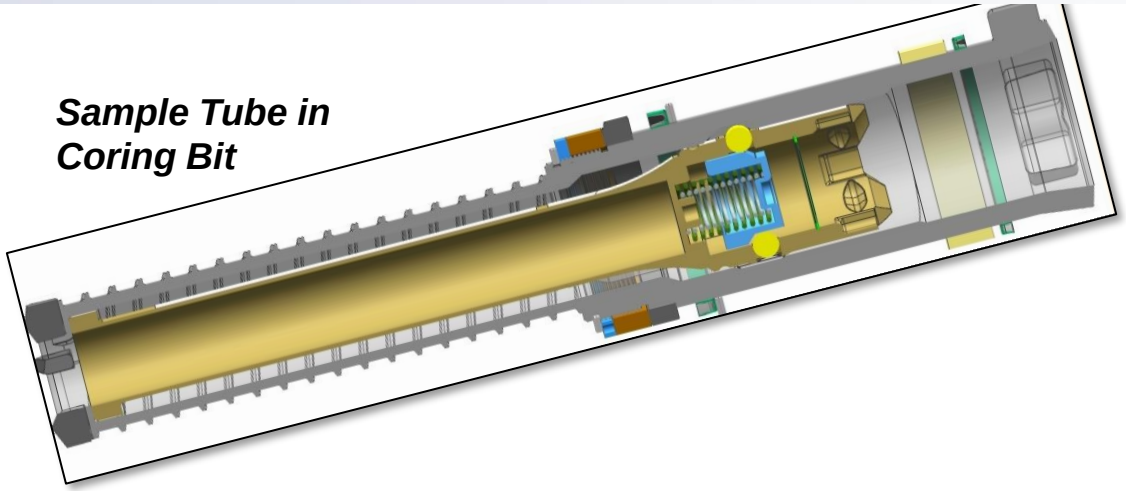

# SCS Features for RSCC: Fluid Mechanical Particle Barriers

Jet Propulsion Laboratory
California Institute of Technology

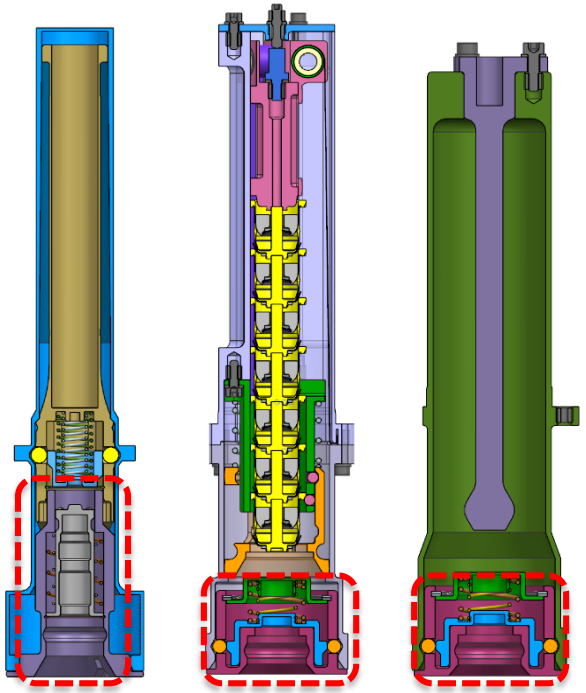

*Sample Tube Storage* | *Seal Dispenser* | *Volume Probe*

***Fluid Mechanical Particle Barriers (FMPBs)***

- *Installed at stations from final cleaning through landing on Mars surface; only removed when stations are actively in use for sample acquisition*

Fluid Mechanical Particle Barriers (FMPBs)

- Biological contamination of sensitive hardware is prevented by two main processes:
  - Reduction of the aerodynamic drag on particles due to the (viscous) flow resistance in the orifice and the large expansion ratio into the first cavity, and
  - By a geometrical design that ensures short filling times compared to particle transit times across the orifice.
- Also slows molecular diffusion into protected volumes

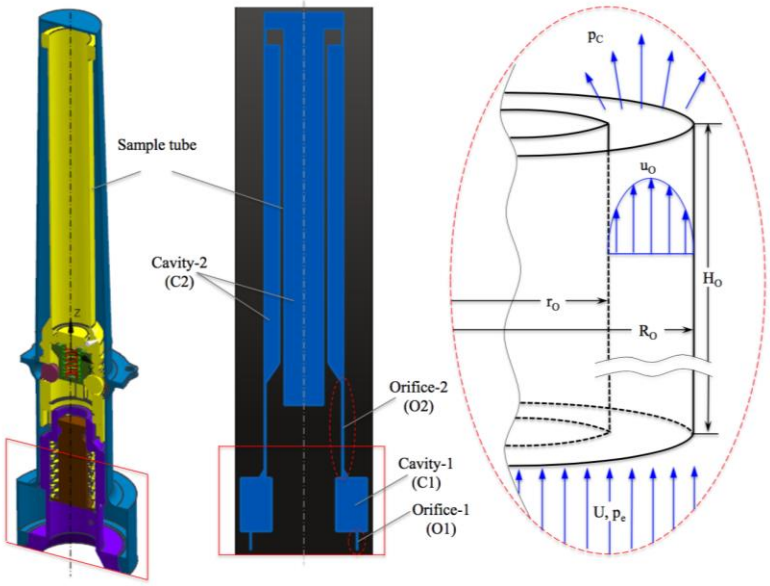

# Introductory Information

## ─ Approach to Meeting Level-1 Requirement Must Account for all Possible Contamination Vectors During all Mission Phases ─

Jet Propulsion Laboratory
California Institute of Technology

- What are the contamination levels of the rover at launch?
  - Inert particle concentrations? Microbial particle concentrations (Standalone? On inert particles?)
- What are the adhesion and re-suspension physics of the particles on the rover surfaces?
- Where do particles go?
  - What are the relevant environments?
  - What are the transport physics?

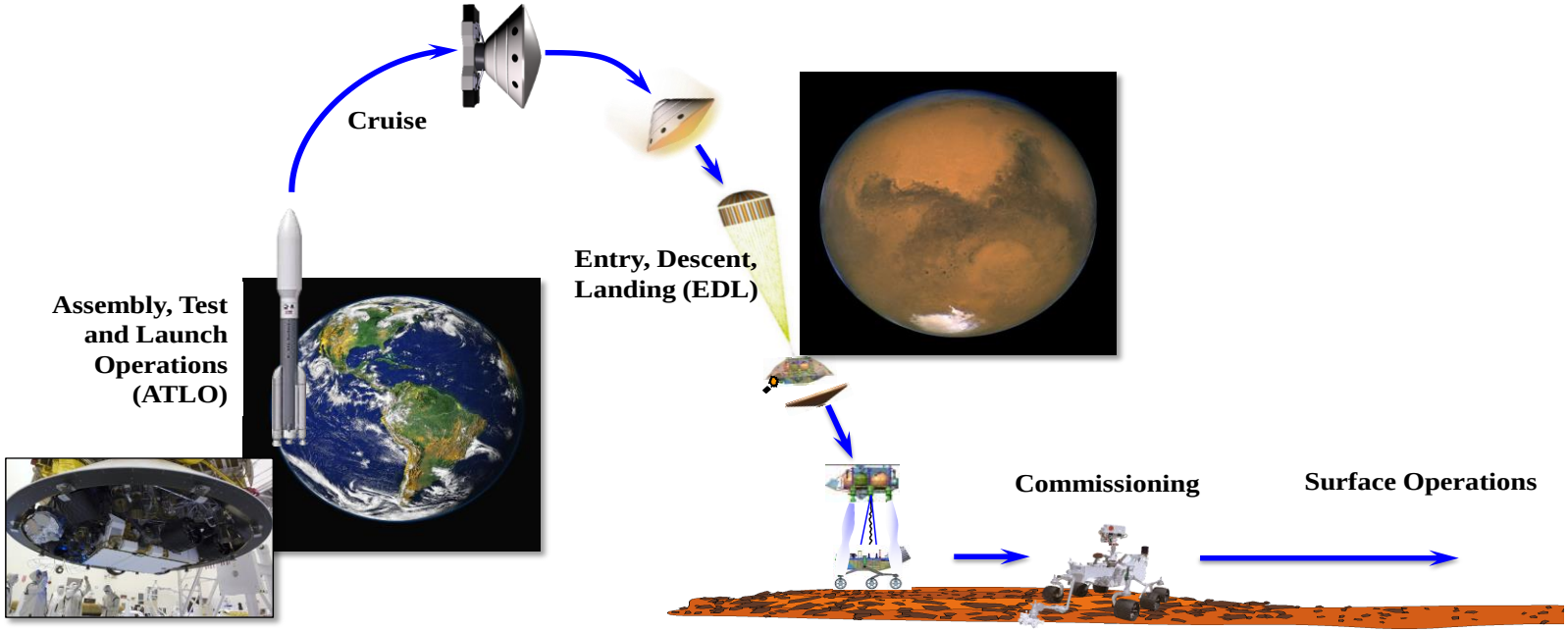

# A 3-D Particle and Biological Transport Computational Model Has Been Developed that Incorporates all the Particle Resuspension and Transport Physics Models

Jet Propulsion Laboratory
California Institute of Technology

## Cleanliness, bio and non-biological particle initial distributions on s/c

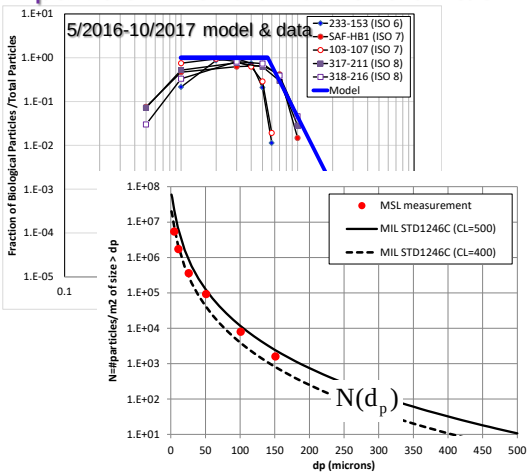


## Ambient and induced environments

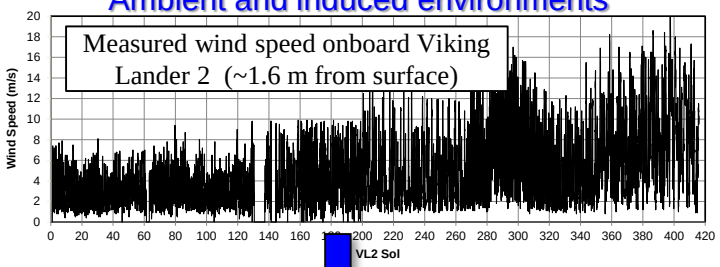


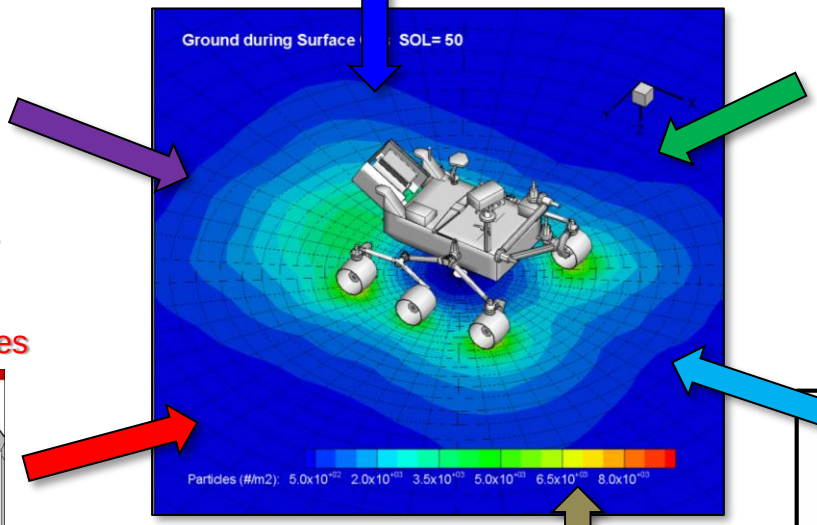


## Particle adhesion and resuspension physics

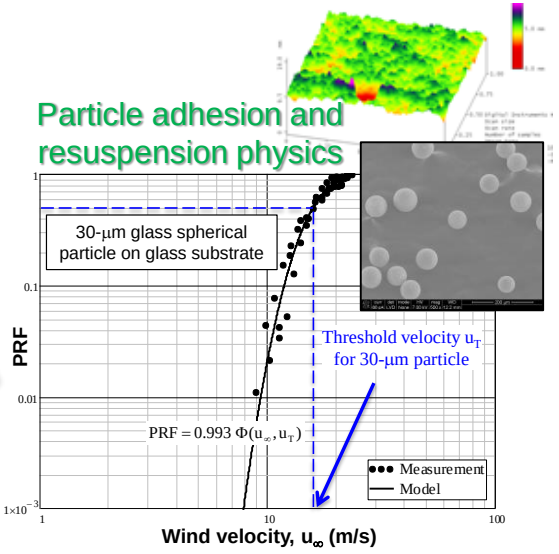


## Cruise and UV lethality of microbes

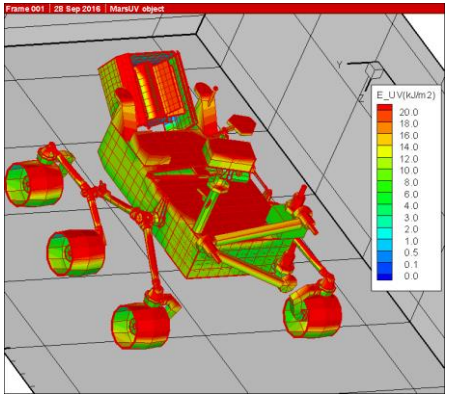


## Particle transport physics

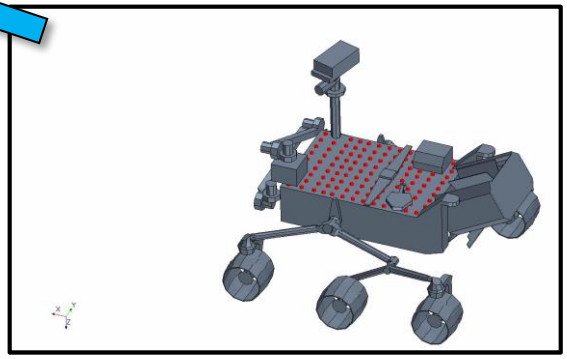

## Fluid dynamics over the rover

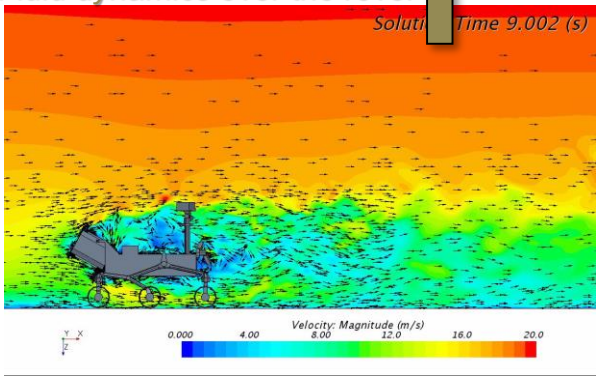

# Where Are We Going?



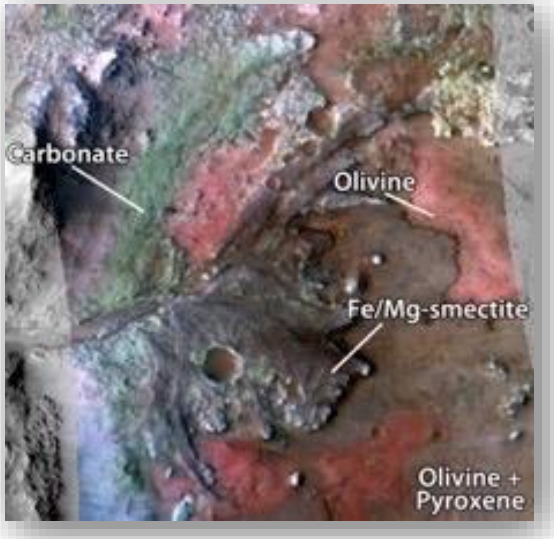


## JEZERO CRATER

- Deltaic/lacustrine deposition with possible igneous unit and hydrous alteration
- Mineralogic diversity including clays and carbonates
- Shallow water carbonates?

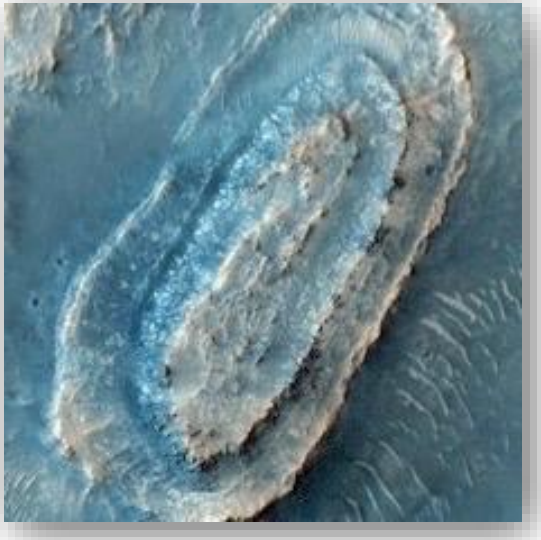

## NORTHEAST SYRTIS

- Extremely ancient igneous, hydrothermal, and sedimentary environments
- High mineralogic diversity with phyllosilicates, sulfates, carbonates, olivine
- Possible serpentinization and subsurface habitability.

## COLUMBIA HILLS

- Carbonate, sulfate, and silica-rich outcrops of possible hydrothermal origin and Hesperian volcanics
- Potential biosignatures identified
- Previously explored by MER

Final Landing Site Workshop scheduled for October 2018.

# 3-D CFD Simulations



- Why 3-D? To show that particle penetration is only negligibly affected by non-uniformities in the global flow field. Such features can be induced by the inherent 3-D nature of the ACA pressurization event and/or by turbulence at high Re.
  - At high speeds (>15 m/s), Reynolds number of flow over FMPB no longer in laminar regime (turbulence inherently 3-D)
  - ACA pressurization case is in most cases not 2-D axisymmetric

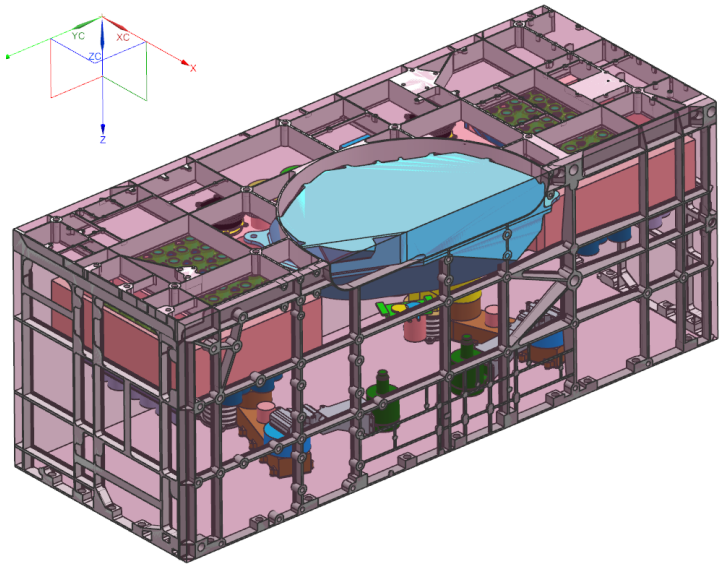

Re=ρuD/μ, D=FMPB diameter (~4.5 cm)

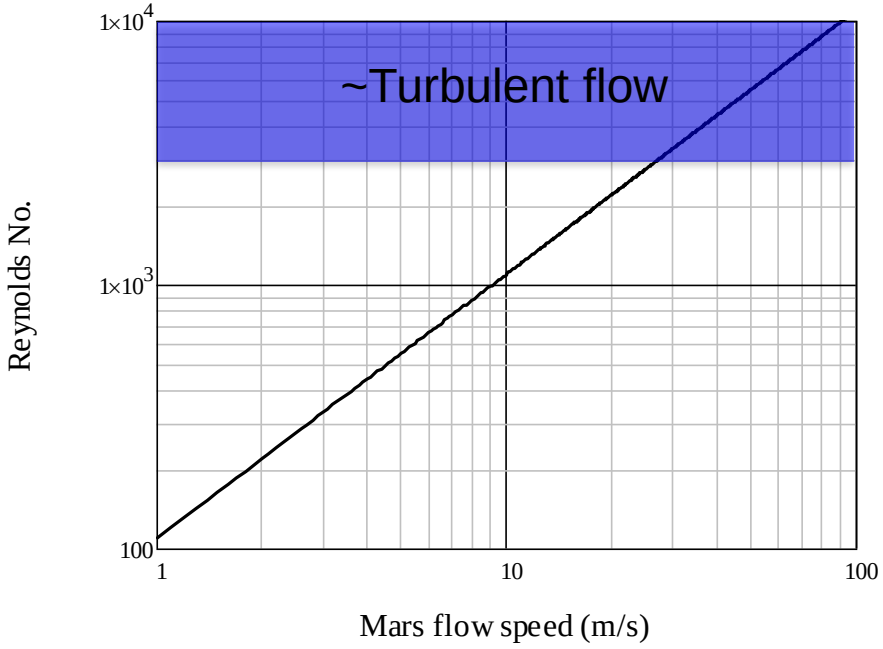

# Computational Domain for 3-D Simulations



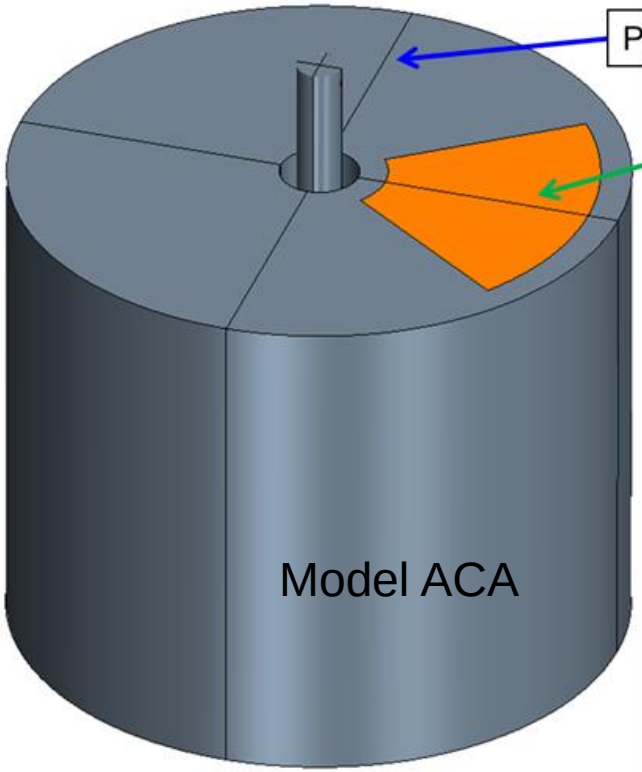


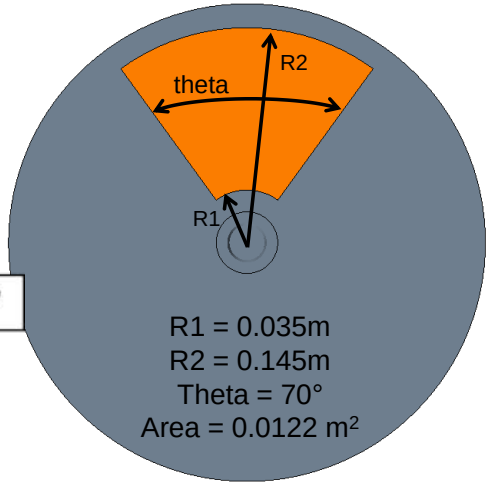


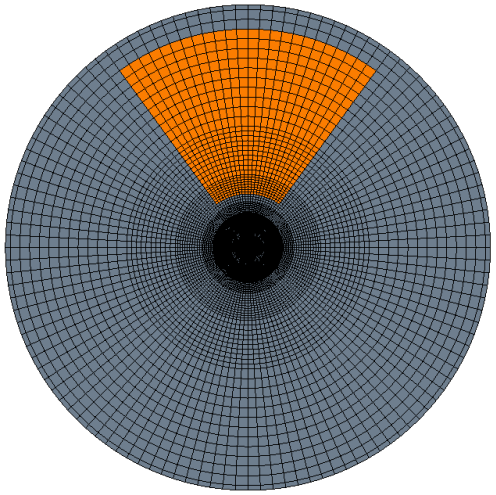

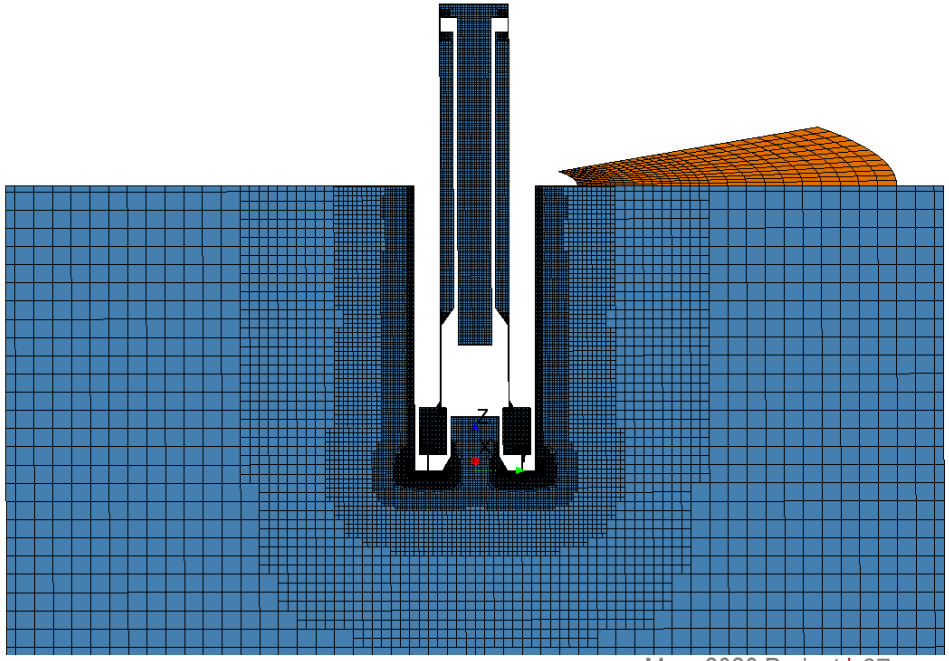

HEPA Filter is the only region with a pressure boundary condition. All other boundaries are walls.

# Asymmetric Pressurization Case at 15.3 m/s, 0.1-mm Gap

Jet Propulsion Laboratory
California Institute of Technology

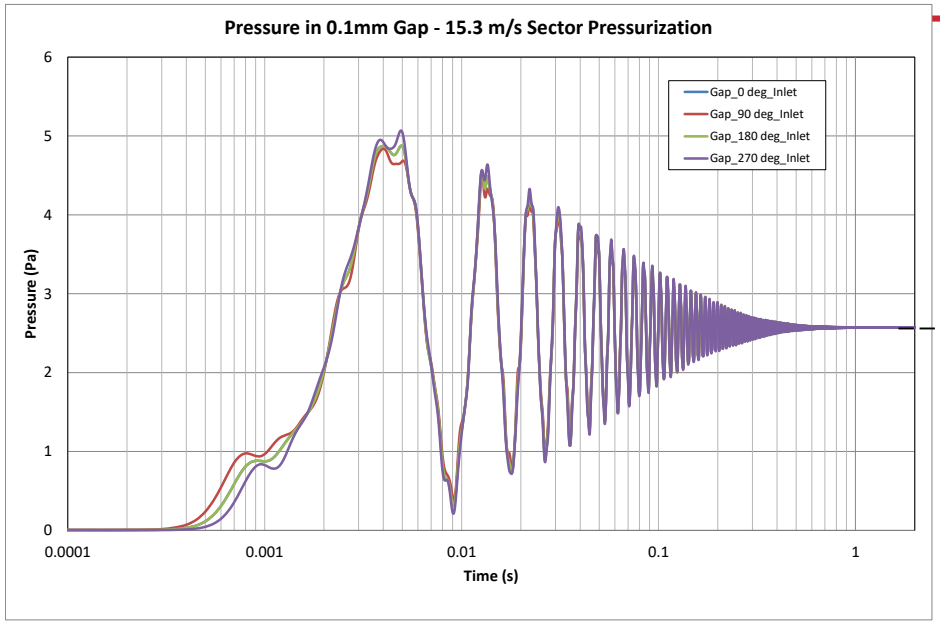


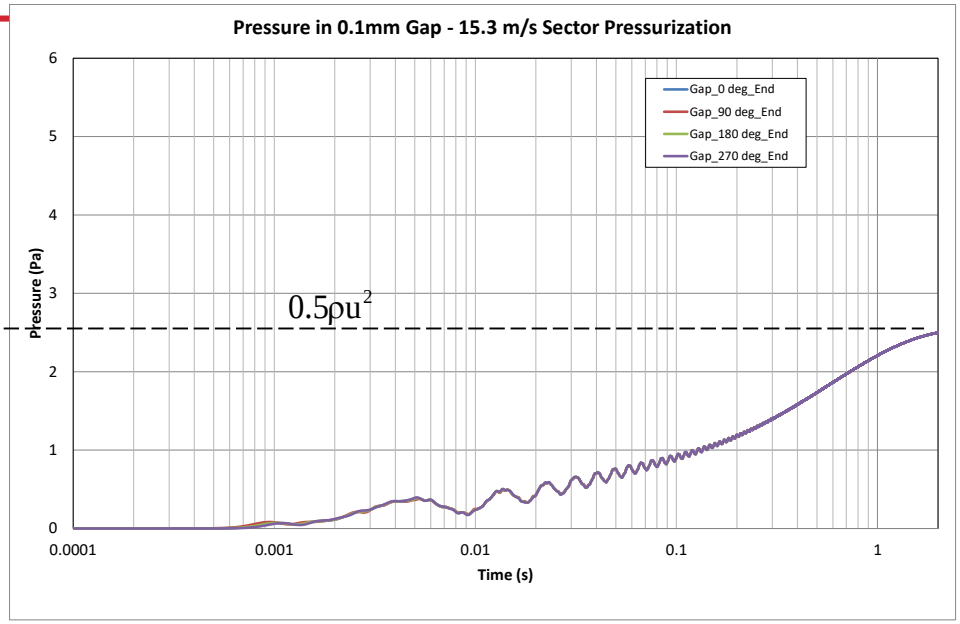


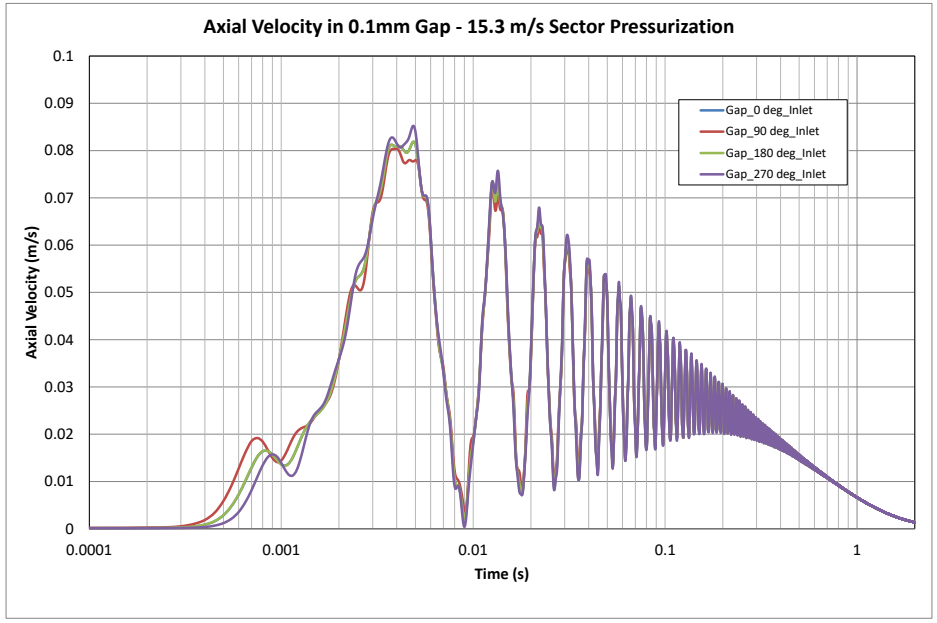


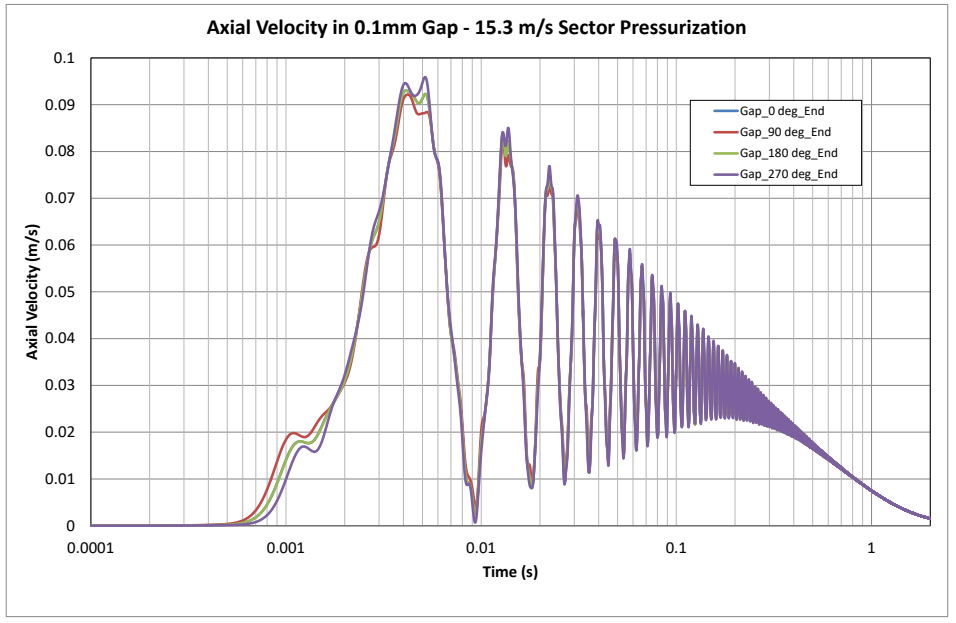

# Animation
# Particle diameter: 0.3 μm
# Asymmetric Pressurization Case at 15.3 m/s, 0.1-mm Gap

Jet Propulsion Laboratory
California Institute of Technology

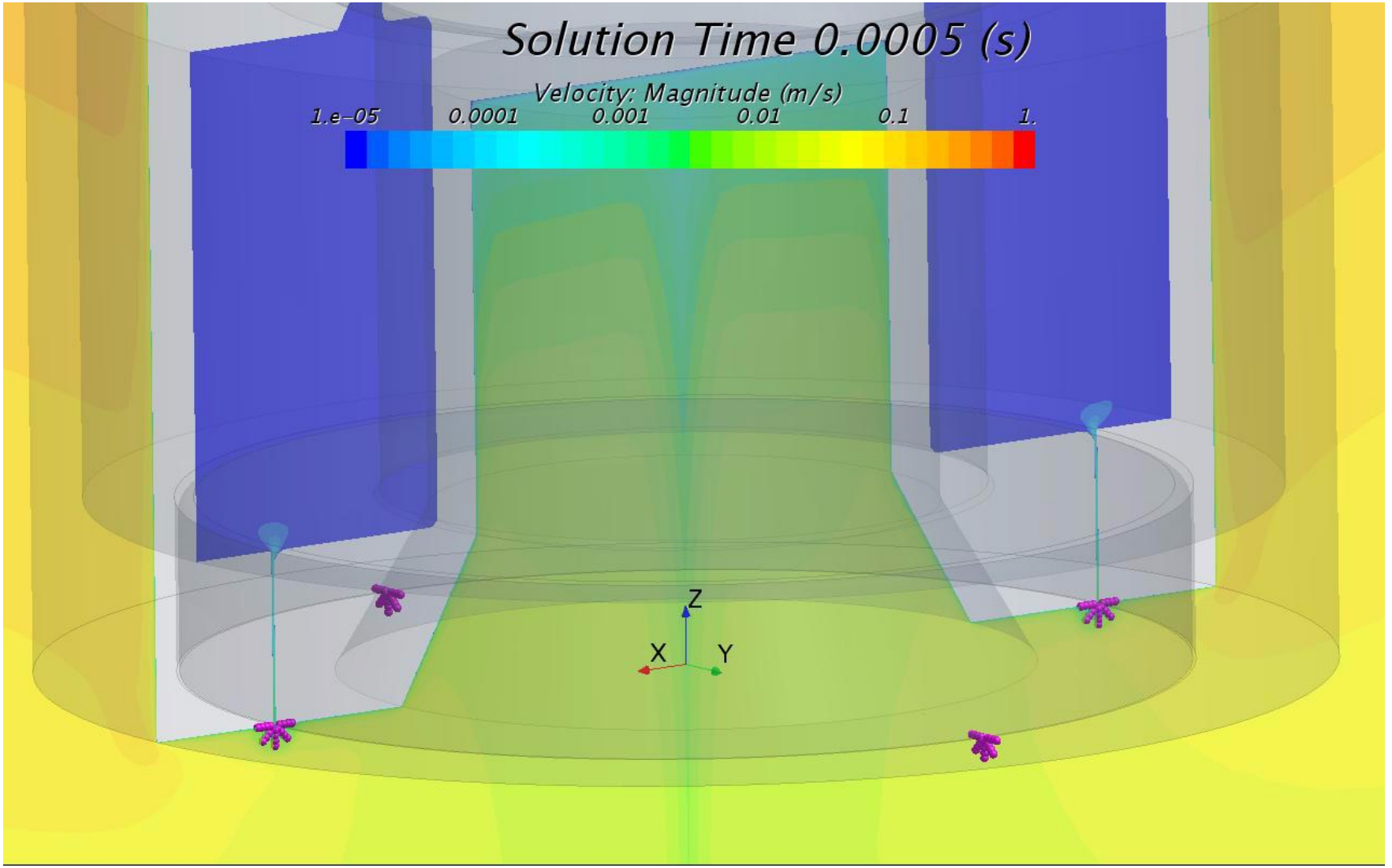


Plane a

# Animation
# Particle diameter: 0.3 μm
# Asymmetric Pressurization Case at 15.3 m/s, 0.1-mm Gap

Jet Propulsion Laboratory
California Institute of Technology

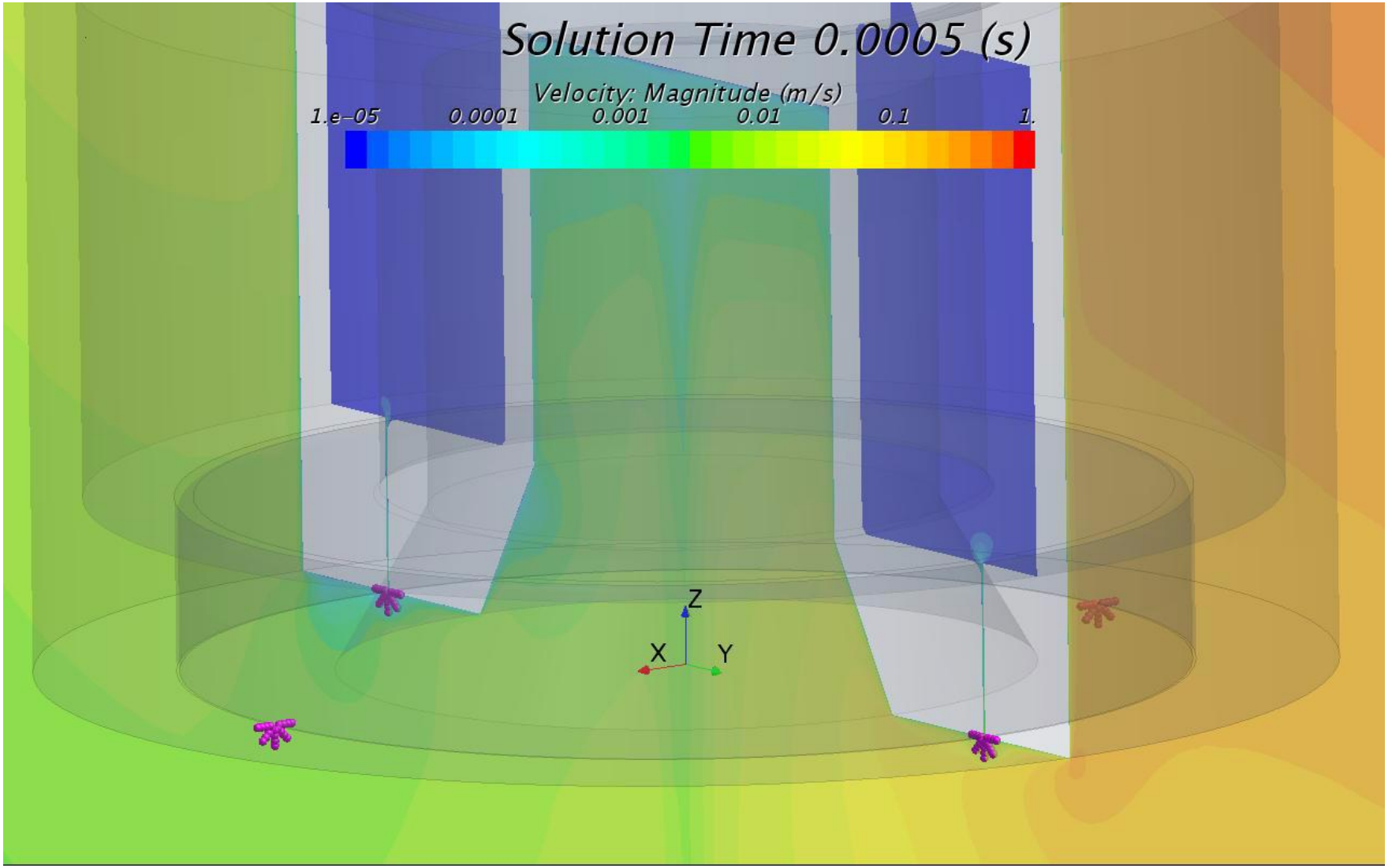


Plane b

# Animation
# Velocity Field – Large Scale
# Sustained Wind Case at 60 m/s, 0.1-mm Gap

Jet Propulsion Laboratory
California Institute of Technology

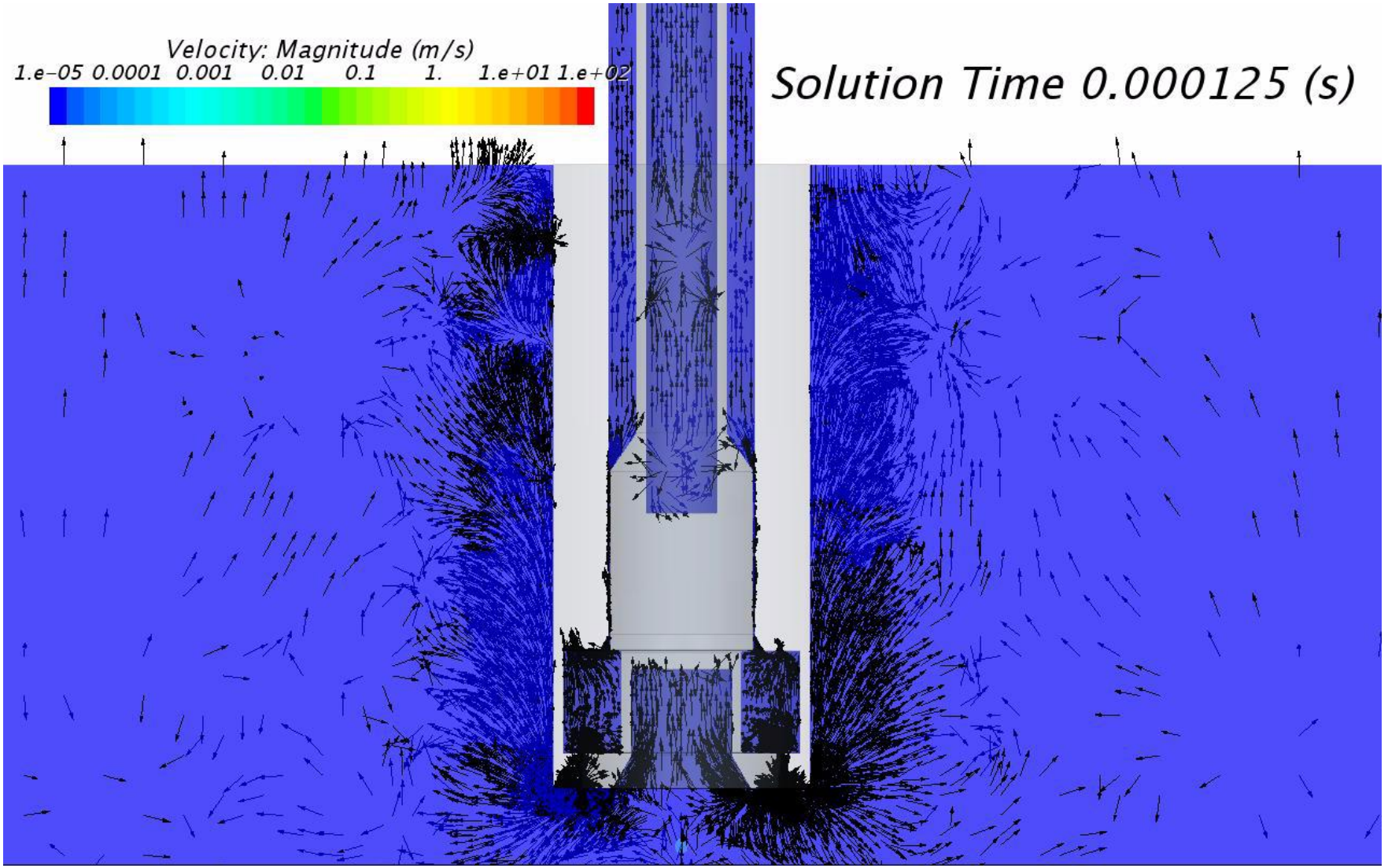

# Animation
# Particle diameter: 0.3 μm
# Sustained Wind Case at 60 m/s, 0.1-mm Gap

Jet Propulsion Laboratory
California Institute of Technology

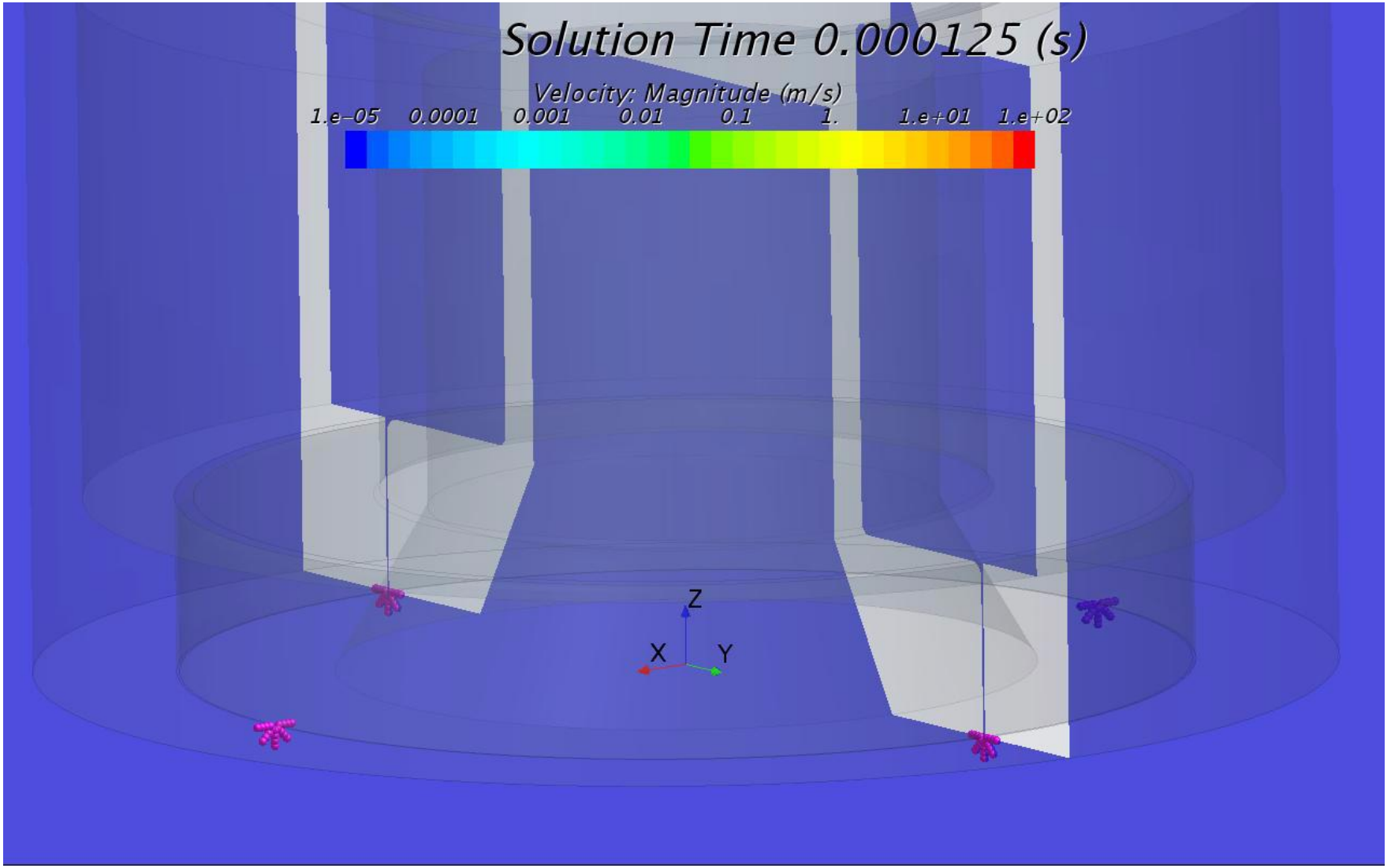


Plane b

# Why not an FMPB flow test with particles under Mars conditions?



- As is the case for many engineering problems, an FMPB test with particles in Mars atmosphere belongs to the category of full-scale tests in a relevant environment that, though preferred, are both challenging and unnecessary. Flight qualification of commercial and military aircraft, certification of nuclear weapons, and Mars EDL are a few large-scale examples in this category for which the combination of only limited testing, typically with scaled-down engineering models, and physics-based modeling and simulations carries sufficiently low risk.
- Why unnecessary?
  - The prediction of particle penetration into the FMPB requires (1) prediction of the flow-field around and inside the FMPB under nominal conditions and (2) prediction of the forces on the particles, both of which are amenable to predictive physics-based analyses.
  - For off-nominal scenarios that are not easily amenable to analyses, such as flow instabilities and turbulence around the FMPB opening on Mars, a flow test is indeed necessary. It is well-known (for over a century) that if flow similarity can be established, the physics of such flows in the non-terrestrial environment can be exactly replicated in a terrestrial-flow tunnel. The results from a Mars-similar water tunnel test, aimed at demonstrating the feasibility of the FMPB to prevent particle penetration under such off-nominal scenarios were reported in [1].

# Challenge With Performing Terrestrial Particle-flow Tests While Retaining Mars Similarity

Jet Propulsion Laboratory
California Institute of Technology

$$Re \equiv \frac{\rho_\infty U_\infty D}{\mu_\infty} \sim \frac{\text{fluid inertia force}}{\text{fluid viscous force}}$$

**:Reynolds number → similarity of flow over object**

$$St \equiv \frac{u_{Tp}/g}{D/U_\infty} \sim \frac{\text{particle response time}}{\text{fluid response time}}$$

**:Stokes number → similarity of particle in flow over object**

- **St >> 1 (Inertia-flow regime)**: particle trajectories do not follow flow streamlines and will likely strike stationary object of size D.
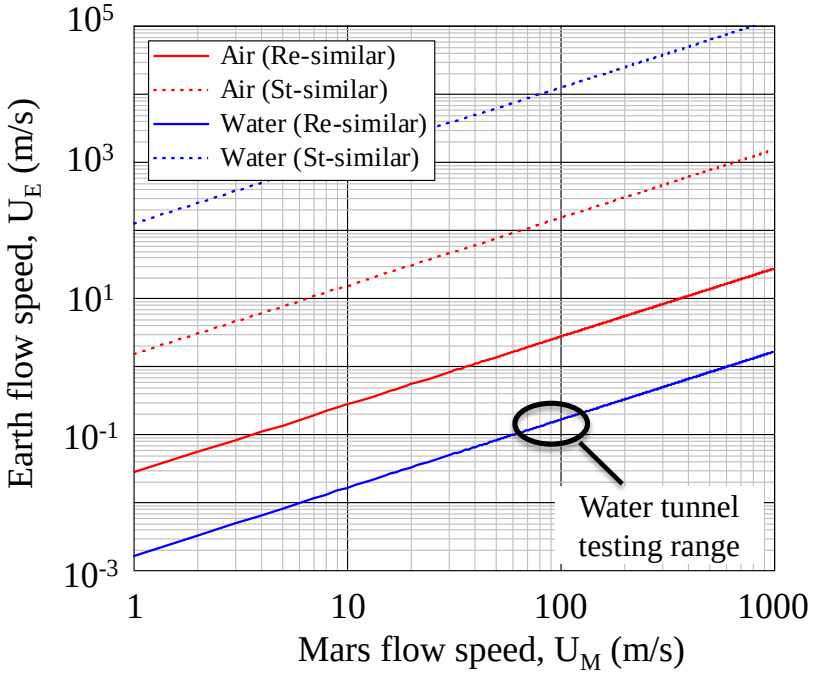
- **St << 1 (Viscous-flow regime)**: particle trajectories follow flow streamlines and will likely not strike stationary object of size D.